THE RESIDUAL STRENGTH DETERMINATION DUE TO FATIGUE LOADING BY FRACTURE MECHANICS IN NOTCHED COMPOSITE MATERIALS

by

Ming-Hwa Robert Jen

Dissertation submitted to the Faculty of the
Virginia Polytechnic Institute and State University
in partial fulfillment of the requirements for the degree of
DOCTOR OF PHILOSOPHY
in
Engineering Mechanics

APPROVED:

K. L. Reifsnider, Chairman

C. W. Smith

J. N. Reddy

D. P. Telionis

R. H. Plaut

January, 1985

Blacksburg, Virginia

THE RESIDUAL STRENGTH DETERMINATION DUE TO FATIGUE LOADING BY FRACTURE MECHANICS IN NOTCHED COMPOSITE MATERIALS

by

Ming-Hwa Robert Jen

(ABSTRACT)

The objective of this investigation is to predict the residual strength of notched composite laminates with various layups, subjected to low frequency fatigue loading with constant amplitude at room temperature, by using a material modeling approach, fracture and fatigue mechanics and the finite element method (FEM).

For simplicity, after thousands of cycles, the geometry of a circular hole of the deformed laminate was categorized as (1) uniformly expanded hole into elliptic shape, (2) crack propagation around the hole transversely. Both types were studied for 12 cases of layups with various proportions of 0, 45, -45 and 90 degree plies. The effect of geometry change during fatigue on residual strength was attributed to the elliptical hole, longitudinal splitting, matrix cracking (reduction moduli of plies), crack propagation and local delamination. Due to the thin through-the-thickness notched laminate, two-dimensional FEM was used and interlaminar stresses were not considered.

Reduction of stress concentration is a reason for the increase of the residual strength of the notched laminate. The stress concentration

factor decreases while the elliptic hole becomes more slender; that was examined by the FEM. The residual strength and stiffness were determined by the material modeling with moduli reduction and damaged zone, and the numerical result was obtained by FEM. Laminate theory, point stress criterion, polynomial failure criterion, ply discount method, and fatigue and fracture mechanics (Paris' Power Law) were also included in this research.

Geometry change and moduli reduction are two major effects that are considered to predict the notched strength. The WN point stress fracture model is adopted for simplicity, instead of the average stress criterion. K_{tg} that corresponds to the unnotched strength in the normalized stress base curve is used to obtain the characteristic length (d_o). We find that K_{tg} decreases when the elliptic hole becomes more slender and more moduli are reduced (more plies crack). At the time d_o that is determined from K_{tg} in the base curve is not necessarily a fixed material constant.

The correlation between the fatigue life and the residual strength as predicted by the model and those determined numerically is found within acceptable errors in comparison with the experimental data.

ACKNOWLEDGEMENTS

I am deeply indebted to Professor Reifsnider for the many opportunities and guidance in the course of my graduate education. His assistance and continued encouragement is deeply appreciated.

I am grateful to Professors C. W. Smith, J. N. Reddy, D. P. Telionis and R. H. Plaut for serving as members of my examining committee and for their review of this dissertation. Also I would like to thank Professor W. W. Stinchcomb for his kind suggestions in my dissertation.

Finally, and most importantly, I am forever indebted to my parents who instilled the value of an education in their son, and to my wife, , for her moral support and unselfish sacrifices throughout this research.

TABLE OF CONTENTS

LIST OF FIGURES

LIST OF TABLES

Chapter I

LITERATURE REVIEW

In recent years, composite materials have replaced metals in many applications because of their light weight, high strength and low cost. Composites also provide improved fatigue capability, good damage tolerance and the ability to be molded in complex aerodynamic configurations.

In many structural applications, notched composite material components can not be avoided. However, the effects on the component itself and the whole structure caused by notches are very complex. The problem and the influence of a notched component can be found in the literature in the recent ten years. For simplicity, in this work we are only concerned with the change of residual strength of a composite laminate with a central hole subjected to two types of fatigue loadings, tension-tension and tension-compression, (T-T and T-C), with constant amplitude at room temperature and low frequency.

A few investigators have reported the increase of residual strength after fatigue loading for certain composite material laminates. Most of these observations can not be used as clearcut evidence, because of the experimental complexity involved. It is felt that comparing the residual mean strength with the mean of the top percent of the static strength leads to fairer conclusion [1]. Now let us summarize a few of the experimental works that involve an increase of residual strength. Reifs-

nider et al [2] measured residual strength of boron/epoxy laminates with layup of $[0/\pm45/0]_s$, and with a central hole. After cyclic loading, static residual strength was measured. Their results show that specimens with higher applied cycles had higher residual strength. They concluded that fatigue loading may increase the residual strength. Kulkarni et al [3] also observed an increase in residual strength after tension-tension fatigue in notched boron/epoxy laminates. Their results for notched (circular hole) coupons of $[0_2/\pm45]_s$ layup with maximum fatigue stress equal to 80% of the static strength, and R=0.1, show an increase of residual strength of 10% after 50000 cycles. The increase was 15% after 500000 cycles, and 16% after 1.5 million cycles.

Waddoups et al [4] observed an increase in residual strength in $[0/90]_s$ graphite/epoxy composite laminate with circular notch, subjected to fatigue loading. Chang et al [5] observed approximately 30% increase of residual strength in $[0/\pm45]_s$ graphite/epoxy coupons with a center slit under fatigue loading to 0.2 million cycles without failure. Their results were described by the nonlinear damage growth rate rule quite well. Chang et al [6] also found an increase in residual strength in $[0/\pm45/90]_s$ graphite/epoxy notched specimens.

To explain the increase of residual strength, a few investigators have attempted to use fracture mechanics. Zweben [7] offered an explanation for notched composite specimens. He studied the 0 deg layer of a composite laminate subjected to an axial loading. The notch is perpendicular to axial direction and cuts n fibers. In a fatigue loading

situation the fiber at the root of the notch might not fail but the length of the matrix failed region might continue to grow. Thus the stress concentration might decrease with applied fatigue cycles. In such a case it is not unexpected to find the residual tensile strength to be higher than the static tensile strength for some composites and layups. Sendeckyj [8] also cited the decrease in stress concentration as the reason for increase of residual strength. He discussed the fatigue failure of $[0/45/90]_s$ graphite/epoxy laminates with a central hole. Under fatigue loading, matrix cracks will occur in various laminates which eventually lead to a decrease in the stress concentration caused by the hole. As a result, the residual tensile strength could increase.

The test data of Chou [9], Awerbuch and Hahn [10], indicate an increase in fatigue residual strength in unidirectional graphite/epoxy composites. There are also other test data of different composites and layups which have an increase in residual strength in graphite/epoxy specimens with a central hole after fatigue loading, see reference [11] for T-T test and [12] for T-C test. It is also reported in [1] that graphite/epoxy (AS-3501-05) $[0_6]$ specimens without notches also show an increase in residual (tension and compression) strength after T-T test. That behavior might be due to micro-damage of the coupon.

Some investigators [3]-[4], [7]-[8], [13]-[20], analyzed the problem theoretically by fracture mechanics and found good agreement with experimental data. They considered the cumulative damage, crack growth rate and fracture toughness at the notch, and attributed the

increase of residual tensile strength to the reduction of stress concentration. Chou and Croman [9], [21] used the "strength-life equal rank assumption" and " degradation and sudden-death models" to predict the residual strength and life. However, there is no satisfactorily complete theoretical or analytical way to predict the residual strength after cyclic loading due to the complexity of the notched composite specimen, especially since the micro-mechanical properties and micro-damage development details around the notch are still unknown.

To date there exist only a few attempts to consider the specific effects of the complexity of damage around notches in composite materials, and to derive a theoretical or analytical method to predict the residual strength and life. The importance of understanding fracture behavior is intensified because of the characteristic statistical variability in material strength and the observation of fracture phenomena that are significantly different from those of metals.

There are two common approaches to describe the notched strength phenomena; the first is by statistics using the strength-life equal rank assumption, and the second is to use fracture and fatigue mechanics. In this work the latter approach is used in combination with the stress analysis theorem and finite element method (FEM). Our goal is to work out an analytical method that closely correlates with experimental data.

The objective of this research is to model the stress redistribution caused by damage development around a hole in a composite coupon, and to estimate the residual strength as a function of cycles of loading

using those stress states and an appropriate failure theory. The present approach is the first reported attempt to account for both the relaxation of the stress concentration around the hole and the change in stiffness due to matrix cracking throughout the laminate. A normal feature of the approach is the representation of the stress concentration change by an effective change in the hole from circular to elliptical.

Chapter II

INTRODUCTION

The analysis of crack problems in plane elasticity has intrigued mathematicians for nearly sixty years. Inglis [22] found the solution for a single crack in an infinite sheet with the use of elliptical coordinates. Muskhelishvili's work on the complex form of the two-dimensional equations due to Kolosoff [23] has undoubtedly been the major development and influence on analytical techniques for solving plane crack problems during this era. Several results of the complex variable formulation of two-dimensional elasticity for both isotropic and orthotropic materials will be summarized briefly. For complete accounts of the isotropic and anisotropic theories, the reader is referred to the classical treatments of Muskhelishvili [24] and Lekhnitskii [25-26], respectively. A brief introduction to the respective theories may be found in Timoshenko and Goodier [27], and Savin [28].

In reference [27] is found the solution for the stress distribution around an elliptic hole in homogeneous isotropic infinite plate due to uniaxial tension. The solution for tension or compression in two perpendicular directions can easily be obtained by superposition. The case of a circular hole near a straight boundary of a semi-infinite plate under tension parallel to this boundary was analyzed by Jeffery [29]. A corrected result and a comparison with photoelastic tests were given later by Mindlin [30]. The stress at the hole, at the point nearest the

edge, becomes a very large multiple of the remote tensile stress when the distance from the circle to edge is small [31] compared with the diameter. The case of a plate of finite width with a circular hole on the axis of symmetry was discussed by Howland [32]. The method used in [27] for analyzing stress around a small circular hole can be applied when the plate is subjected to pure bending. Many specific cases for both tension and bending have been worked out. These include one hole or a row of holes in a strip and in a semi-infinite plate, circular arrays of holes, and semicircular notches in a strip. Most different geometries of notches and notches with inclusions are not considered here.

The circular hole can be thought of as the special case of an elliptic hole with both semiaxes equal to the radius. The problem of a plate with an elliptic hole is more complicated than the circular hole. For an infinite isotropic plate loaded in tension with an elliptic hole, the stress distribution can be found in [27] by complex variables in elliptic coordinates which is a type of curvilinear coordinates. Solutions for the plate with an elliptic hole were first given by Kolosoff and Inglis. The method employed in [27] is that of Kolosoff. The same method was applied to several two-dimensional problems of elasticity by Stevenson [33]. Also many further solutions for elliptic and other noncircular holes, or inclusions, with various loadings, have been worked out in detail but are not of interest here. Other stress distribution information for elliptic holes under axial loading were given in [34-39].

In general, we can not employ the above solutions of stress distributions directly to the finite width composite laminate with an elliptic hole, because we have to modify infinite to finite width and isotropic and anisotropic plate to orthotropic layered plate. The exact solution for the stress distribution for an isotropic infinite plate with an elliptic hole due to axial tension is shown in Eq. (1), see Appendix II. The exact solution for finite width composite laminate is not available. Actually, there exists a general polynomial and series equation approximate solution to this complex problem. Cracks in plates of finite size are of great practical interest, but for these cases no closed form solutions are available. The problems are difficult because of the presence of complex boundary conditions [40]. An approximate solution can be obtained for a strip of finite width loaded in tension and containing a central crack.

There exist several possible methods to obtain approximate solutions of the stress fields for a finite composite laminate with an elliptic hole. One is to revise the solutions for an anisotropic infinite plate with an elliptic hole by coefficients of a function of (d/w). Others are the finite difference method, finite element method and approximate theoretical series solutions (Exponential power series, Hyperbolic trigonometric series, etc). For simplicity we could use the method of modifying the exact solutions with finite-width coefficients. For more complete considerations of the influence of all factors associated with damage we chose to use the FEM. Finite element methods have difficul-

ties in regions with rapidly varying stress gradients such as notches. Such devices as building in specialized local displacement fields into the elements are often awkward and imprecise. In fact, as we have already remarked, in the case of notches the singular nature of the solution is usually not sufficiently understood to estimate the local character of the displacement fields. These difficulties can be removed by utilizing a continuous representation of the solution locally and a finite element representation elsewhere. In FEM the concept of isoparametric elements for inclusion of irregular boundaries in a finite element formulation poses no great difficulty. Also moving the central nodal points to the quarter point on the sides near singularities for triangle and quadrilateral elements can achieve better accuracy close to the singular points of notches.

Implicit to the classical technique of conformal mapping is the global representation of the solution. When a closed-form solution for the stress function can be found, this solution is ideal. Usually, however, this is not posiible and a series or integral representation of the solution must be considered. Owing to rapidly varying stress gradients in the notch vicinity as contrasted to the more remote stress distribution, it is evident that numerical convergence can become a factor in a global representation of the stress functions. When a series representation is taken, it is usually necessary to retain a large number of terms to ensure notch stress accuracy. The classical approach lacks the flexibility to provide effective localized expressions, and, at the same time, a less

demanding representation of the more uniform portions of the solution. Effective local expressions are clearly desirable to document numerical solutions for general use.

Chapter III

ANALYSIS AND FORMULATION

Actually, some factors are neglected such as frequency, temperature and moisture. Also, the interlaminar stresses which we do not consider in the process may be the controlling stress for residual tensile strength. Zweben [7] suggested three main approaches to analyze the present problem. The first applies classical fracture mechanics (CFM) on a macro-scopic level, treating composites as homogeneous, anisotropic materials. The second recognizes material heterogeneity and applies CFM to the problems of crack propagation in the matrix and fiber phases and interfaces separately. The third method, which might be called the material modeling approach, uses approximate models in order to represent the major effects of heterogeneity and to simplify the analysis.

After the advantages and limitations of the three approaches are compared, the emphasis will be placed on material modeling for simple analysis. Waddoups et al [4] reported the fracture model by the application of CFM to laminated composites with a central hole. That approach will be tested here. Also, we will use a crack growth rate theorem and stress analysis theorem in the process to solve the problem. The stress analysis is based on treating the laminate as a homogeneous plate using a finite element technique. The strength analysis is based on the tensor polynomial failure criterion applied to each ply.

The ultimate laminate failure strength is based on the last ply failure stress [41]. After the simulation of material modeling, we can find the residual tensile strength after the specific cycles of loading and see the change of residual tensile strength and a function of the increase of cycles.

Consider a composite laminate with a central hole shown in Fig. 1. Our aim is to determine the residual strength of this notched laminate subjected to fatigue loadings. For simplicity, we neglect the parameters that are not important, such as environmental effects. First, the aspect ratio of l and w should not be large in order to avoid the buckling by compressive loading. The test environment is assumed to be room temperature and dry, with no temperature and moisture changes. The test frequency quency is taken to be constant at some normal frequency. The stress amplitude is constant and the stress ratio is a fixed value. The geometries of the through-the-thickness notches will be of two types, circular hole, ellipse, slit, etc. First, we consider a graphite/epoxy composite laminate with a central hole, subjected to T-T test. Other types of notches, fatigue loadings, and the parameters will be considered later.

After several thousand cycles, the geometry of a circular hole of the deformed laminate is categorized as (1) uniformly expanded hole into an elliptic shape, (2) symmetric crack propagation at the hole edge transversely, (3) irregularly deformed shape. However, the case of irregularly deformed shape is omitted here, because it is very difficult to

model. The case of transverse crack propagation is expressed in a compact form shown in the last section of this chapter, because some damage properties are still unknown.

First, let us consider the case of a circular hole deformed into an elliptic hole. For a homogeneous isotropic plate with a central circular hole due to uniaxial tension, see Fig.1. We know that a circular hole is the special case of an elliptical hole, so we directly consider an elliptical hole. There are several ways to derive stress and strain fields for a notched plate with an elliptical hole subjected to uniaxial loadings, such as classical complex potential methods and finite element methods. The classical method is suitable for only special cases. Muskhelishvili [42] worked on the complex form of two-dimensional elasticity to solve plane crack problems. Timoshenko et al [43] derived the stress distribution for a homogeneous, isotropic, infinite plate with a centered elliptical hole due to uniaxial tension. In elliptical coordinates ξ and η shown in Fig. 2 instead of x and y, we obtain the stress distribution along ξ-axis expressed in Eq. (1), see Appendix II. At $\beta=0$, $\eta=\pi/2$, $\xi=\xi_o$, Eq. (1) reduces to

$$\sigma_\eta = S(1+2b/a) \qquad (2)$$

That is the stress concentration. For a circular hole a=b=radius, $\sigma_\eta=3S$, i.e., the SCF=3. Similarly, we can derive σ_ξ, $\sigma_{\xi\eta}$ and strain field. In fact, the stresses σ_ξ and $\sigma_{\xi\eta}$ are not important in the consideration of SCF. To apply Eq. (1) for rectangular coordinates, we set

$$c\text{Cosh}\xi_o=a,\quad c\text{Sinh}\xi_o=b,\quad c^2=a^2-b^2$$
$$\text{Sinh}2\xi_o=2ab/c^2,\quad \text{Cosh}2\xi_o=(a^2+b^2)/c^2$$
$$e^{2\xi_o}=(a+b)^2/c^2,\quad e^{-2\xi_o}=(a-b)^2/c^2 \qquad (3)$$

where 2c=length of the foci. If a and b are known, we can determine c and ξ_o. Then setting $\eta=\pi/2$ and $\xi=\xi_o$, $1.1\xi_o$.., we have the stress distribution σ_η along the ξ-axis. For special cases, $\xi_o=0\rightarrow b=0$ and $a=\pm c$, that is a crack of length 2c. And if $\xi_o=\infty\rightarrow a=\infty$ and $b=\infty$, that is an infinite hole.

However, for composite laminates we have to modify isotropic plate to make it anisotropic, see Ref. [44]. The orthotropic stress concentration factor K_t^∞ for an infinite width plate with a circular hole, Lekhnitskii [45] expressed it as

$$K_t^\infty=1+\sqrt{2[\sqrt{A_{11}A_{22}}-A_{12}+(A_{11}A_{22}-A_{12}^2)/2A_{66}]/A_{22}} \qquad (4)$$

In order to obtain SCF for an elliptical hole, Eq. (4) is not applicable. For the real finite width plate, we also need to modify Eq. (1) from infinite width to finite and isotropic to anisotropic. That is a very complicated problem. In addition, the resulting complex expressions are not well suited to be adopted to practical applications. So the approximate numerical methods are the direct and applicable way to solve the problems. The finite element method and the numerical results will be discussed later.

Now consider the failure criteria suggested by Whitney and Nuismer [46] and [47], such as the point stress and the average stress criteria. The first failure criterion referred to as the "point stress criterion"; it assumes failure to occur when σ_y at some distance, d_o, ahead of the hole first reaches the unnotched tensile strength of the material. The relation of notched and unnotched strength of the infinite width laminate is

$$\frac{\sigma_N^{\infty}}{\sigma_o}=\frac{2}{\{2+\xi_1^2+3\xi_1^4-(K_t^{\infty}-3)(5\xi_1^6-7\xi_1^8)\}} \tag{5}$$

where $\xi_1=R/(R+d_o)$, d_o is characteristic distance and a material property, σ_o=unnotched strength, σ_N^{∞}=notched strength.

The details of the numerical results will be included in the following chapters for the case of an elliptic hole. Now we try to formulate the transverse crack propagation in the last part of this chapter.

We describe the transverse crack propagation problem in Fig. 3 by using linear elastic fracture mechanics, we obtain the Stress Intensity Factor (SIF) at the crack tip. That is

$$K_I=\sigma\sqrt{\pi a}f(a/r) \tag{6}$$

where a is characteristic dimension of the intense energy region. The energy available for crack extension in isotropic materials is

$$G_I=(1-\nu^2)\pi K_I^2/E \tag{7}$$

$$\sqrt{G_I}=[\pi\sqrt{a(1-\nu^2)/E}]\sigma f(a/r) \tag{8}$$

G_I will be a material constant if the material is an ideal Griffith solid. Then

$$\sqrt{G_I}[\pi\sqrt{a(1-\nu^2)/E}]^{-1}=\sigma f(a/r)=\text{constant} \tag{9}$$

When Eq. (6) is critical,

$$\sigma_c=K_{Ic}/[\sqrt{\pi a}f(a/r)] \tag{10}$$

For a specimen with no hole (control), we have

$$\sigma_o=\sigma_{c\ a/r=\infty}=K_{Ic}/[\sqrt{\pi a}(1.00)] \tag{11}$$

$$\sigma_o/\sigma_c=f(a/r),\ \sigma_c/\sigma_o=1/f(a/r) \tag{12}$$

From experimental observations, this model is found to be consistent with the observed behavior predicted for a constant value of a=0.04" [4]. However, several limitations of the Waddoups model preclude its general ultility. First the necessary development by Bowie [48] is limited to isotropic material systems. In addition, the assumption that the characteristic dimension is a material constant is invalid [49] and [50].

With the constant amplitude of stress and fixed frequency, after N cycles, fatigue crack growth can be represented by the Paris' Law [51].

$$da/dN=C(\Delta K)^m \tag{13}$$

where C and m are experimentally determined material constants.

$$\Delta K=\Delta\sigma\sqrt{\pi a}f(a/r) \tag{14}$$

where $\Delta\sigma=\sigma_{max}-\sigma_{min}$ and $\Delta K=K_{max}-K_{min}$. We use $K_{min}=0$ for $K_{min}<0$, then $\Delta K=K_{max}$ [52]. Substituting Eq. (14) into Eq. (13), we have

$$da/dN=C[\sqrt{\pi a}f(a/r)]^{m}(\Delta\sigma)^{m} \tag{15}$$

In integral form

$$\int_{a_o}^{a}Nda/[\sqrt{\pi a}f(a/r)]^{m}=C\int_{o}^{N}(\Delta\sigma)^{m}dN \tag{16}$$

The function, f(a/r), was tabulated for uniaxial and biaxial stresses [53]. Mode I & II problems are included. If we assume that $a_o\approx 0.0"$ (very small crack initiation), and the crack extends perpendicular to loading, we get

$$K_I=\sigma\sqrt{\pi L} \tag{17}$$

The effective half-crack length is (L+a), then

$$K_I=\sigma\sqrt{\pi(L+a)} \tag{18}$$

$$\sigma_o/\sigma_c=\sqrt{(L+a)/a} \tag{19}$$

When $r+a_N$ approaches L and a_N approaches a, we obtain

$$\sigma_c/\sigma_o=\sqrt{a_N/(r+a_N)} \tag{20}$$

Actually, Paris' Law is not sufficient to express the defect initiation and growth in notched composite laminates. Delamination growth is a major concern to designers of composite structures and is usually planar and self similar. Using principles of fracture mechanics as the delamination grows along the interface, the growth rate (da/dN) is related to the strain energy release rate (G) by the power law [54-55].

$$da/dN=A(G)^n \tag{21}$$

In general practice, G is the total strain energy release rate with components due to mode I, mode II, and mode III deformation. The growth rates of interfacial cracks and delaminations are particularly sensitive to the mode of cyclic loading. In the case of plane stress

$$G_I=K_I^2/E \tag{22}$$

Then,

$$da/dN=A(K_I^2/E) \tag{23}$$

Plugging Eq. (6) into Eq. (23), we get

$$da/dN=A[(\sigma\sqrt{\pi a}Y)^2/E]^n \tag{24}$$

where A and n are material properties, Y is f(a/r) and E is modulus changing with cycles. After rearrangement, we express it in the integral form

$$\int_{a_o}^{a} Nda/a^n=\int_{o}^{N}[A(\pi Y^2)^n\sigma^{2n}/E^n]dN \tag{25}$$

where σ is a function of cyclic loading (sine or step function) and E is a function of (a,N). Now we can obtain a_N'. Replacing a_N by a_N' in Eq. (20), we obtain

$$\sigma_c/\sigma_o = \sqrt{a_N'/(r+a_N')} \qquad (26)$$

However, it is hard to find a numerical solution, because some micro-damage properties around the hole due to cyclic loading are not well understood. So we express the relation between the critical and the unnotched strength in simple compact form. The further study on this work is suggested.

Chapter IV

NUMERICAL METHODS

In the case of two-dimensional plane stress quasi-isotropic, orthotropic and anisotropic composite laminates we apply finite element method to the laminate coupon with a center hole to get the approximate solutions of stress and strain fields. Two computer programs given in Ref. [56] and [57] are slightly modified for the composite materials. Here we use the program described in [57] for time and space savings. The documentation and a modified FEM computer program are listed in Appendix IV. The documentation is omitted here, refer to the implementation of the finite element method in the Appendix of Ref. [57]. The objective is to discuss finite element analysis procedures for linear problems in solid and structural mechanics. It is the displacement-based FEM that can be regarded as an extension of the displacement method of analysis. The finite element discretization procedure and derivation of the equilibrium equations are presented in general, i.e., a general three-dimensional body (generalized coordinates) was considered. The general equations derived must be specialized in specific analyses to the specific stress and strain conditions considered. In this research a two-dimensional plane stress problem is solved by using the general formulation with the appropriate displacement, stress and strain variables, i.e., the stresses in the z-plane are zero. In most practical analyses the use of isoparametric finite elements is more effec-

tive. The principal idea of the isoparametric finite element formulation is to achieve the relationship between the element displacements at any point and the element nodal point displacements directly through the use of interpolation functions (also called shape functions). This means that the transformation matrix is not evaluated; instead, the matrices corresponding to the required degrees of freedom are obtained directly. Also the continuum and structural isoparametric element formulations satisfy the convergence criteria (compatible and complete). For practical consideration in isoparametric element calculations, each element of the composite coupon has 8 nodes (8 nodes for plate, 9 nodes for shell) and 9 Gaussian points. The integration order is 3x3 and the degree of precision is 5. Each element has 8 nodes to eliminate the geometric error and has 9 Gaussian points to yield the closest results (the SCF is determined at element 1 Gaussian point 9). In addition, for notched problem there exists a new-developing method, boundary element method, to achieve numerical solution, see Ref. [58].

From experimental data of notched composite specimens, we consider 1.5"x8" specimens with a central hole with a diameterof 3/8", see Fig. 4. The ratio of hole diameter to width is 1:4, which is smaller than 0.33 [59]. In order to see the influences of length and width on the SCF, we reduce the length to half length and double the width to 3" with the length up to 10". One important point is that the aspect ratio should not be large enough to cause buckling of the specimen in compression. For symmetry, we only consider the first quarter of the

coupons of Fig. 4. For $[0/45_2/90]_s$ and $[0/45_4/90]_s$ layups, we consider the upper half of the coupons. To make meshes and nodes, the elements around the hole have to be as small as possible to meet the localized stress concentration.

Due to fatigue loadings, the circular hole will be deformed into the elliptical hole with the assumption that the diameter of the semi-axis perpendicular to the loading is unchanged. The diameter parallel to loading is enlarged with the increase of the cycles, see Fig. 5. Although it is not yet possible to predict the relation of the enlarged diameter to cycles, we can obtain such data experimentally. The stress distributions for graphite/epoxy T300/5208 specimens with various orientations and elliptic holes are tabulated. The stiffness data in Table 1 are from Ref. [60]. From Table 2 and 3 we see that the length does not influence the SCF. The changes of strains and stresses only occur at the remote points. From Table 2 and 4 we see that the width slightly influences the SCF. Comparing the data, we see that as the elliptical hole becomes slender, the SCF becomes smaller. That is a stress concentration reduction which can contribute to the increase of residual strength, see Fig. 6-18 for the variety of layups. The plotting scheme for the numerical results is to use the cubic spline function, see the subroutines from the computer library (IMSL), to achieve a smooth curve for each data set.

From plate theory, laminate theory and the finite element analysis, we can obtain the stresses and strains at all the elements of every lay-

er at the applied stress range from min to max at the first cycles. Similarly, we can obtain from X-ray radiographs of damage zones the different elliptical dimensions. The strength analysis is based on the tensor polynomial failure criterion can be applied to each ply. Then the initial laminate strength can be estimated by the first-ply failure theory on the conservative side [60]. But the ultimate laminate failure strength is based on the last-ply failure stress, that is used as base line information for comparison with the residual strength after N cyclic loads have been applied.

In this way we can determine the residual strength after N cycles by means of the simplied model. The results obtained from this procedure are within acceptable error in comparison with the experimental data.

The diameter of the semi-axis parallel to loading direction enlarges with the increase of the number of applied cycles, see Fig. 19. Actually, the longitudinal semi-axis, b, is not a hole shape change. It is a superposition of effective notch determined by the damaged region around a hole. We consider the total region of hole and effective notch as an elliptical hole for simplicity, see Fig. 20 for T300/5208 fatigued specimen with $[0/\pm45/90]_s$ layup. However, the mathematical relationship of the enlarged diameter to the number of applied cycles is difficult to predict. The determination of such a relationship requires extensive experimental data showing the deformed geometry by X-ray or C-scan at specific cycles of loading. The complexity of this problem is

increased by the fact that the response depends on ply orientations, stacking sequence, and geometrical factors.

We begin by applying the finite element method to obtain the approximate solution of stress and strain fields for a two-dimensional plane stress specimen with a central hole. Also via the FEM we can obtain the stress in each ply and, from last-ply failure theory, we can estimate the failure strength of that notched specimen.

From Table 2 and 5-10 we see the SCF decreases as the semiaxis, b, becomes larger for 0, +45, -45, 90 deg single ply laminae and twelve cases of layups. The geometry change does influence the SCF and the reduction of SCF can contribute to the increase of residual strength. Also we find that the more 90 deg plies present in the laminate, the higher is the SCF. Additionally, we also plot the stresses (axial, transverse, and shear) around the notch of the first quarter for various layups in different scales as shown in Fig. 21-29, although shear stress is not used in the present model. The above mentioned results are associated with the effect of notch geometry only.

Actually, the elastic moduli are also reduced during cyclic loading, in addition to the geometry effect changes. In order to better represent the real phenomena, we use discount theory to predict the last-ply failure of the laminate [61] [62]. In many cases, laminates have considerable strength remaining after first-ply failure and there arises the difficult and important problem of analytically determining subsequent failures. Initial failure of a layer may occur in the fiber or in the ma-

trix mode. In the first case, the stiffness in the fiber direction E_1 is reduced, and in the second case the elastic properties E_2 and G_{12} are reduced. These elastic properties are not reduced to zero, because the uncracked regions remain bonded to adjacent layers. A precise estimate of these stiffness reductions is difficult to make. The simple (but extreme) assumption is that E_1 reduces to zero in the fiber failure mode and that E_2 and G_{12} reduce to zero in the matrix mode. Since a laminate in most cases will not survive a fiber mode failure, the progressive failure cases of interest are initial and subsequent failures in the matrix mode. If it is assumed that, for failure of a lamina in the matrix mode, E_2 and G_{12} can be set equal to zero, eventually the assumptions of netting analysis result. For netting analysis, the ultimate load is defined by the state when E_2 and G_{12} vanish in all laminae.

We know that the internal stress redistribution is a driving force for subsequent subcritical element damage and critical element degradation. The basic nature of that stress redistribution can be established by considering the quasi-static strength of such a laminate since such cracks also form before fracture under quasi-static loading. When edge effects do not dominate the failure process, the ply discount method is a good engineering approach to estimate laminate strength. To apply the scheme one must calculate ply stresses, use a failure criterion to predict first ply failure (matrix cracking), reduce the moduli in the broken plies (E_2, G_{12}=0), recalculate ply stresses, test for second

ply failure, etc. until last ply failure is predicted. First consider a quasi-isotropic laminate with a $[0/\pm45/90]_s$ layup. The experimental data is shown in Table 11 [63]. The residual strength (S_n) and the measured 0 deg crack length (C) increase with increasing cycles. The radius of the circular hole, a, remains unchanged as the short semi-axis of elliptic hole with increasing cycles. The long semi-axis of elliptic hole, b, as stated in Fig. 20, enlarges with increasing cycles, but b is not a hole shape change. It is the region of effective notch which includes the hole and the damaged area. We measure the values of b before observing the residual strengths. In addition to changing the hole geometry to ellipse, we also adopt discount theory to reduce moduli after the 90, -45, +45, and 0 deg plies crack. The moduli reduction data is shown in Table 12. The stress and strain fields are obtained for all cases of geometry and moduli changes via the FEM. The data for the SCF and maximum displacement are shown in Table 13. We see that the SCF deceases when more moduli are reduced, i.e., more cracked plies are introduced for the case of constant geometry. Also, when both the hole becomes slender and the moduli are reduced, the SCF becomes less and less. Finally, the SCF will approach the asymptotic value under both conditions. The asymptotic value is 1 for ideal isotropic materials, but it is slightly higher than 1 for orthotropic or anisotropic materials. These results are shown in Fig. 30.

The literature indicates that there are several fracture models which have been used to determine the notched strength of composite

laminates. After reviewing these methods, we first choose to consider the Waddoups, Eisenmann, and Kaminski (WEK) fracture model [4]. The unnotched strength of a given quasi-isotropic laminate $[0/\pm45/90]_s$ is 550 MPa. Following the steps stated in [4], we can calculate the notched residual strength as shown in Table 14. We find that the predicted results in in Table 14 are quite different from the experimental data in Table 11. The example of calculation for T300/5208 graphite/epoxy quasi-isotropic notched strength is as follows:

Plug the first two values of column 3 in Table 14 into Eq. (12),

$f(a/r)=\sigma_o/\sigma_c=79.57/37=2.15$

From Table 7 in Ref. [53],

$a/r=0.3$

$a=0.1875"x0.3=0.05625"$

Plug into Eq. (10),

$K_{Ic}=\sigma_c\sqrt{\pi a}f(a/r)=37\sqrt{3.1416x0.05625}x2.15=33.44$ Ksi$\sqrt{in}$

Now a=0.1875" b=0.5" w=0.75"

$r=(a+b)/2=0.34375"$ (average)

$a/r=0.05625/0.34375=0.164$

From Table 7 in Ref. [53],

$f(a/r)=2.53$

$\sigma_c=K_{Ic}/[\sqrt{\pi a}f(a/r)]=33.44/[\sqrt{3.1416x0.05625}x2.53]$ =31.44 Ksi

The calculated notched strength=31.44 Ksi, is shown in Table 14 column 3.

The finite width correction factor, Y, is

$Y=[2+(1-2r/w)^3]/[3(1-2r/w)]=1.33$

The modified notched strength is

1.33x31.44 Ksi=41.77 Ksi

The modified strength=41.77 Ksi, is shown in Table 14 column 4.

The disadvantages of the WEK fracture model are 1) the SCF is not involved, 2) the change of hole geometry from circular to elliptic is not incorporated, 3) the finite width correction factor is not involved. Due to the shortcomings of the Waddoups, Eisenmann, and Kaminski fracture model we concluded that the WEK fracture model was not adequate to find the residual strength, since it only shows the decrease of static strength with the increase of hole diameter. Then we choose the Whitney and Nuismer (WN) fracture model to determine the notched strength. The SCF calculated from Eq. (4) shown in Table 15 for an infinite orthotropic laminate with a central circular hole can be used as a comparison to the SCF in Table 2 for finite width obtained via FEM. We see that there is only a small difference in the values. So the SCF, K_t^{∞}, in Table 2 can be used for the WN fracture model.

Chapter V

RESULTS AND DISCUSSIONS

Now we attempt to use the Whitney and Nuismer (WN) fracture model to determine the notched strength (the residual tensile strength) for a specific number of cycles of fatigue loading after comparing with several fracture models. At the beginning we use the point stress criterion instead of average stress criterion for simplicity, although the later generally has better accuracy than the former. From the experimental data for T300/5208 quasi-isotropic laminate in reference [63], we have the residual tensile strength (Sn) at specific cycles of T-T fatigue loading and the corresponding geometry changes. The unnotched tensile strength for those specimens is 71 ksi. The point stress criterion is shown in Eq. (5). For different cracked situations in each b value, we assume that K_{tg} is equal to K_t^{∞} when all 90, -45 and +45 deg plies have cracked, i.e. at b=0.1875" K_{tg}=1.98, at b=0.5" K_{tg}=1.73, at b=0.8" K_{tg}=1.67, and at b=1.2" K_{tg}=1.63, see column 2 in Table 16 and curve 3 in Fig. 30 for K_{tg} at each b value. With the K_{tg} value known, we obtain d_o by intersecting the base normalized stress distribution curve which is the stress state for the circular hole (a=b=R) with no ply cracking. We use the base curve to represent the WN normalized point stress criterion, since it is suitable for the circular hole. The scheme to determine the characteristic length (d_o) at the unnotched laminate strength (failure) from the WN

fracture model is shown in Fig. 31a, and d_o determined at K_{tg} in normalized stress distribution is shown in Fig. 31b. K_t^∞ is the SCF at the hole edge and K_{tg} is the SCF (normalized by the unnotched strength) corresponding to the characteristic length. It is reasonable to have larger d_o when K_t^∞ is decreasing. That can be explained by the normalized stress distribution ($\sigma_y/\sigma_{applied}$) along the x-axis used to find d_o from K_{tg} for moduli changes shown in Fig. 32. It is very important to determine d_o accurately from K_{tg} in Fig. 32, but that is not easy to do due to the small changes in the normalized stress curves in that region and the very small changes of d_o which occur. The enlarged scale of a portion of that Fig. is shown in Fig. 33. Then, we obtain d_o=0.05, 0.08, 0.09 and 0.10 respectively, see column 3. That shows d_o has a slight change in the same layup. We conclude that d_o is not necessarily a material constant for the same layup. With d_o and K_t^∞ for each case, we can predict the notched tensile strength via Eq. (5), see column 4 in Table 16.

Then, if we assume no ply cracking, we have the notched strength and the errors in comparison with experimental data listed in Table 17, where d_o is the same as Table 16 and K_t^∞ is the SCF at the hole edge without ply cracking (no moduli reduction). We also find that K_{tg}^* is close to K_{tg}, where K_{tg}^* is defined as the unnotched strength divided by the observed strength (S_n). Similarly, d_o^* determined by K_{tg}^* in the base curve is close to d_o. That sug-

gests that the empirical proof what we assumed is reasonable. To simplify the problem we set d_o=0.08 (average) as a constant for this lay-up; the result is shown in Table 18. We see the error between the experimental data and the predicted values is also small and acceptable. Due to the fact that the maximum displacement when all of the (90, -45, +45 and 0) plies have cracked reaches the order of 10E5 inch (rupture), the laminate failed before all 0 deg plies cracked. That is shown in Table 16, K_{tg} at d_o is assumed to equal K_t^∞ for the situation of all 90, -45 and +45 degree plies cracked. So K_t^∞ at that stage is the lower limit. Obviously, K_t^∞ and d_o obtained without ply cracking define the upper limit. The detailed calculation of notched strength and the determination of d_o from K_{tg} are shown in Appendix III as an example. Physically, we use K_{tg} to determine d_o in the base normalized stress distribution based on the ideas that: 1) K_{tg} corresponds to failure in Fig. 31, 2) K_{tg} equals to K_t^∞ when 90, -45 and +45 plies are cracked, and is the lower limit of values used to calculate the notched strength, i.e., on conservative side, 3) we can directly obtain the base normalized curve to find d_o from K_{tg} according to the point stress criterion, because the base curve ($\sigma_y/\sigma_{applied}$) is the same no matter what the $\sigma_{applied}$ is. But we can not directly obtain K_{tg} by normalizing the unnotched strength, because $\sigma_o/\sigma_{applied}$ is arbitrary due to $\sigma_{applied}$ between σ_{max} and σ_{min}, 4) It is not easy to observe experimentally that at the specific cycles which plies reach the saturated patterns of cracking exact-

ly, so we consider the worst case when all 90, -45 and +45 deg plies have cracked.

We assume that all 90, -45 and +45 deg plies have cracked for the cases of longitudinal semi-axis, b, =0.1875", 0.5", 0.8" and 1.2" at the corresponding cycles of 10E0, 10E1, 10E3 and 10E4 for the quasi-isotropic notched laminate. Actually, 90, -45 and +45 deg plies start to crack simultaneously as cycles of load are applied. It is certain that the 90 deg plies reach saturated crack patterns first, followed by the -45 deg plies and +45 deg plies. That can be shown by the stress concentration factor at the hole edge for a single ply, because the SCF for 90 deg plies is the largest, then the -45 deg plies followed by the +45 deg plies which the SCF is the smallest. The strength of the plies relative to the stress state will control failure. We can also observe this damage development phenomenum in Ref. [64] for three types of quasi-isotropic laminates, $[(0/\pm45/90)_s]_{3s}$, $[(0/90/\pm45)_s]_{3s}$ and $[(0/+45/90/-45)_s]_{3s}$, under T-T fatigue tests. 90 deg plies started cracking at cycles 10E1-10E3, -45 deg plies at 10E3-10E4 and +45 deg plies at 10E3-10E5. At 10E4-10E5 cycles the 90 deg ply cracking reached saturation, at 10E5-10E6 cycles -45 and +45 deg ply cracking reached saturation.

There are two sets of fatigue data from [65] which show the compliances, residual strengths and geometry changes of graphite/epoxy T300/934 laminates with a central circular hole for both $[0/\pm45/0]_{2s}$ and $[0/\pm45/90]_{2s}$ layups. Following the same procedure, the K_{tg}

equals to K_t^{∞} when all the -45 and +45 deg plies have cracked for each b value with the $[0/\pm45/0]_{2s}$ layup, and when all of the 90, -45 and +45 deg plies have cracked for the $[0/\pm45/90]_{2s}$ layup. The d_o was also determined from K_{tg} in the base curve (a=b=0.06 , no ply cracking). When we have determined K_t^{∞} and d_o we can compute the notched strength. The predicted notched strengths and errors in comparison with empirical data are shown in Table 19 and 20. We see that the WN fracture model can be used to predict the notched strength. The point stress criterion is a simple way to find the notched strength with increasing d_o while K_t^{∞} is decreasing. In Table 19 and 20 we see that compliance increases with increasing cycles, i.e., the modulus decreases with increasing cycles. That will result in a stress concentration loss and the characteristic length, d_o, will become larger with increasing cycles. Additionally, if we plot the major effective notch axis, b vs log cycles for these layups, we do not find a clearly linear relation (see Fig. 34 and 35, where the solid line represents linear and the dotted line expresses nonlinear relation). Also, the determination of d_o from K_{tg} in the normalized stress base curve for the T300/934 $[0/\pm45/0]_{2s}$ and $[0/\pm45/90]_{2s}$ layups are shown in Fig. 36 and 37 respectively, we find that for small holes the stress concentration is localized near the hole, i.e., small holes cause less strength reduction than do large holes. The longitudinal semi-axis, b, measured from X-ray radiographs are shown in Fig. 38 and 39 for these two layups. The scheme of measuring b is the same as that shown in Fig. 20.

In our analysis, we assume that when all plies which crack reach a saturated pattern, then the stress concentration factor is the lower bound, i.e., the most damaged case. As for the observed data in Table 16, we do not know exactly the number of cycles for which the 90, -45 and 45 deg plies become saturated. However, when all plies are not cracked and the laminate is subjected to fatigue loading that case is the upper bound on the stress concentration factor. As a matter of fact, it is generally not possible to have plies not cracked under T-T fatigue tests. So the predicted residual strength should be within the upper and lower bounds.

Similarly, the single ply (0, 45, -45 and 90) notched strengths are computed. The reduced moduli for a cracked ply are listed in Table 21. The SCF and maximum displacement for each ply are listed in Table 22-25. We see that the SCF for each cracked ply is almost unchanged no matter what the b value is. Then K_{tg} is equal to the average value of the SCF for each ply. Following the same procedure, we can find d_o from K_{tg} in the base normalized curve. d_o is a fixed material constant for each ply. With the knowns of the SCF, d_o and the unnotched strength, via Eq. (5) we can compute the single ply notched strength, see Table 26-29.

Chapter VI

SUMMARY AND CONCLUSTIONS

This research concerns the use of a stress redistribution material modeling method to predict the notched strength of damaged laminates, including theoretical, numerical and experimental analyses. We considered the case of a circular hole deformed into an effective elliptical shape. This model is developed in detail and shows satisfactory agreement with experimental data. This approach can be summarized as follows:

.Geometry changes; It is assumed that damage around the hole relaxes the geometrical constraint associated with the stress concentration in a manner which can be simulated analytically by assuming that a central circular hole deforms into an elliptic-shaped hole when subjected to T-T fatigue loading, which results in a progressive stress concentration loss as the elliptic hole becomes slender.

.Moduli reduction; As damage developes, the stiffness of the damaged plies is reduced using the ply discount method to solve for the redistributed stress field, by assuming that the 90, -45, +45 and 0 deg plies crack successive in stages. It was found that the ply cracking also reduced the stress concentration near the hole.

.The WN fracture model was adopted to the damage accumulation problem determine the notched laminate strength, i.e., the residual tensile strength at a given number of cycles. K_t^{∞} and d_o are

the two parameters that control notched strength. The former becomes less with increasing cycles and the later becomes larger due to loss of SCF.

.Last ply failure determines the ultimate strength of the laminate.

.The ply level strength is also predicted.

The procedure used to apply the model is described in steps as follows:

.From experimental data we determine the notched composite specimen layup, length, width, thickness and notch geometry, etc.

.Obtain estimates of the damage zone around the hole as a function of cycles from experimental data.

.Use FEM to obtain stress and strain fields with the input of loading, node, mesh and stiffnesses for each effective elliptic hole shape as a function of the number of cycles of loading. Then we have laminate and ply stress and strain fields. At the time we consider progressive moduli changes for each elliptic hole shape to determine the differences caused in the stresses and strains.

.With the output of stress and strain fields we obtain K_t^{∞} and the normalized stress curves, which are important to calculate the notched strength using a chosen fracture model, such as the WN fracture model. In the WN fracture model we predict notched strength with the knowns of unnotched strength, semi-major and -minor axes of the hole, K_t^{∞} and the characteristic length. In this research we find that the characteristic length d_o (a parameter in the WN model) is not necessarily a fixed material constant for the same layup.

.The determination of d_o for the WN fracture model is achieved as follows: 1) obtain K_t^∞ and the normalized stress distribution curve due to geometry and moduli changes, 2) take K_{tg} equal to K_t^∞ for the most damaged state (90, -45 and +45 plies cracked, moduli reduced) for each b value, i.e., for a $[0/90]_s$ layup, 90 deg plies cracked, for a $[0/\pm45/90]_s$ layup, 90, -45 and +45 deg plies cracked, for a $[0/\pm45/0]_{2s}$ layup, -45 and +45 deg plies cracked; for each cracked ply we set $E_2=G_{12}=0$, 3) use the normalized stress curve for the circular hole (no ply cracking) as the base curve, 4) intersect the base curve at K_{tg} to find d_o, 5) plug K_t^∞ and d_o into Eq. (5) to calculate the notched strength.

If there exists observed data, we can obtain K_{tg}^* and d_o^* to compare with K_{tg} and d_o. The steps to find K_{tg}^* and d_o^* are: 1) calculate K_{tg}^* which is the SCF of the unnotched strength (σ_o) divided by the observed strength (S_n), i.e., $K_{tg}^*=\sigma_o/S_n$, 2) refer to the normalized stress curve (σ_y) along x-axis corresponding to the circular hole and no ply cracking (the base curve), 3) determine the characteristic length (d_o^*) corresponding to the intersection of the stress curve at K_{tg}^*, 4) compare K_{tg}^* and d_o^* with K_{tg} and d_o.

Using this method we have found that the predicted notched strength for a laminate and single plies is within acceptable error in comparison with experimental data.

Due to the scarsity of observed data and the lack of statistics for available data, the present model has been verified for only three data sets. Furthermore, more experimental work is need to generate more residual strength data.

However, the present work suggests that even a very approximate account of stress redistribution associated with damage accumulation caused by fatigue loading of center-notched composite laminate coupons can be used to obtain engineering estimates of residual strength.

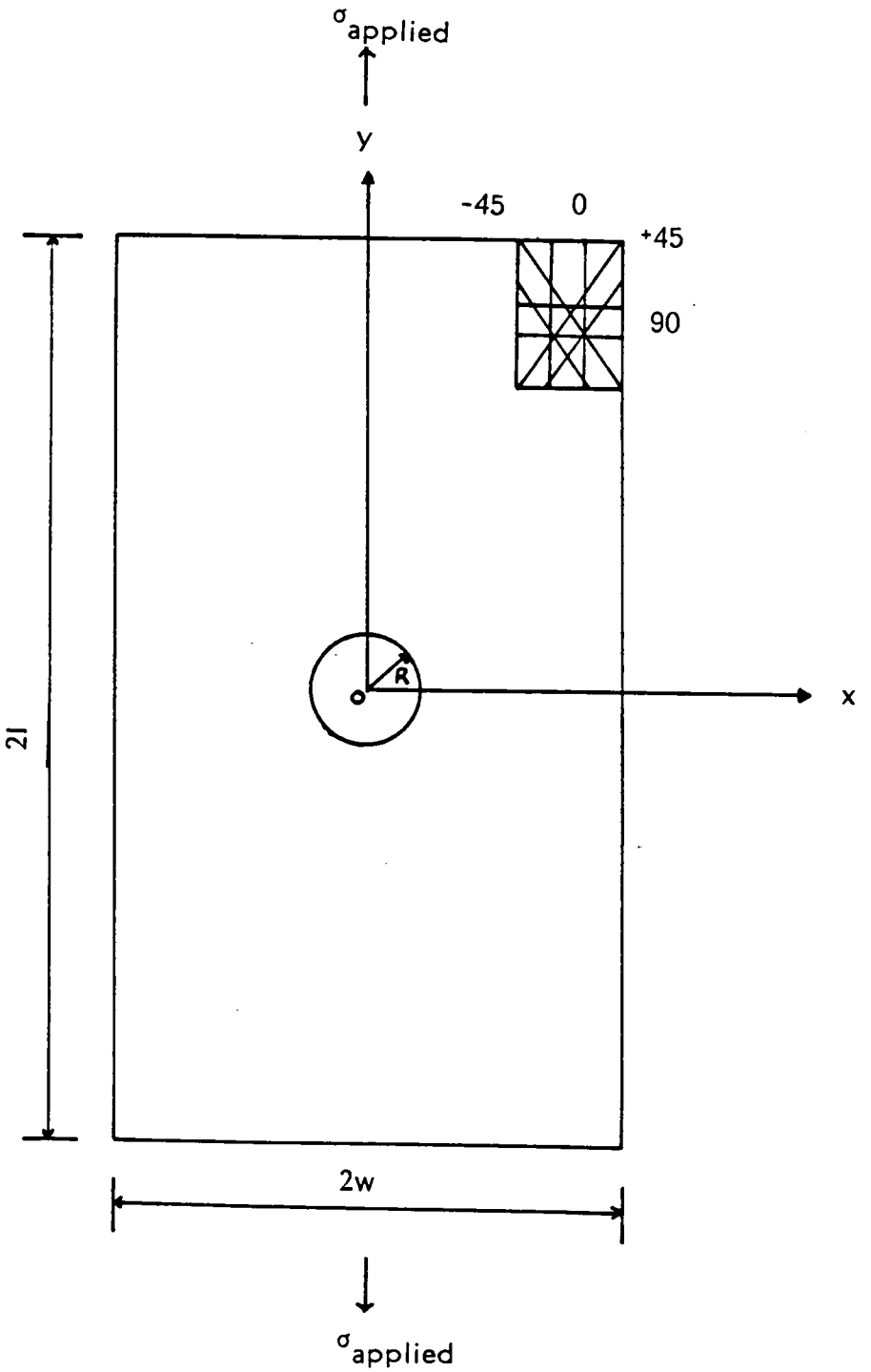

Fig. 1 Laminate with a Central Circular Hole in x-y Coordinates

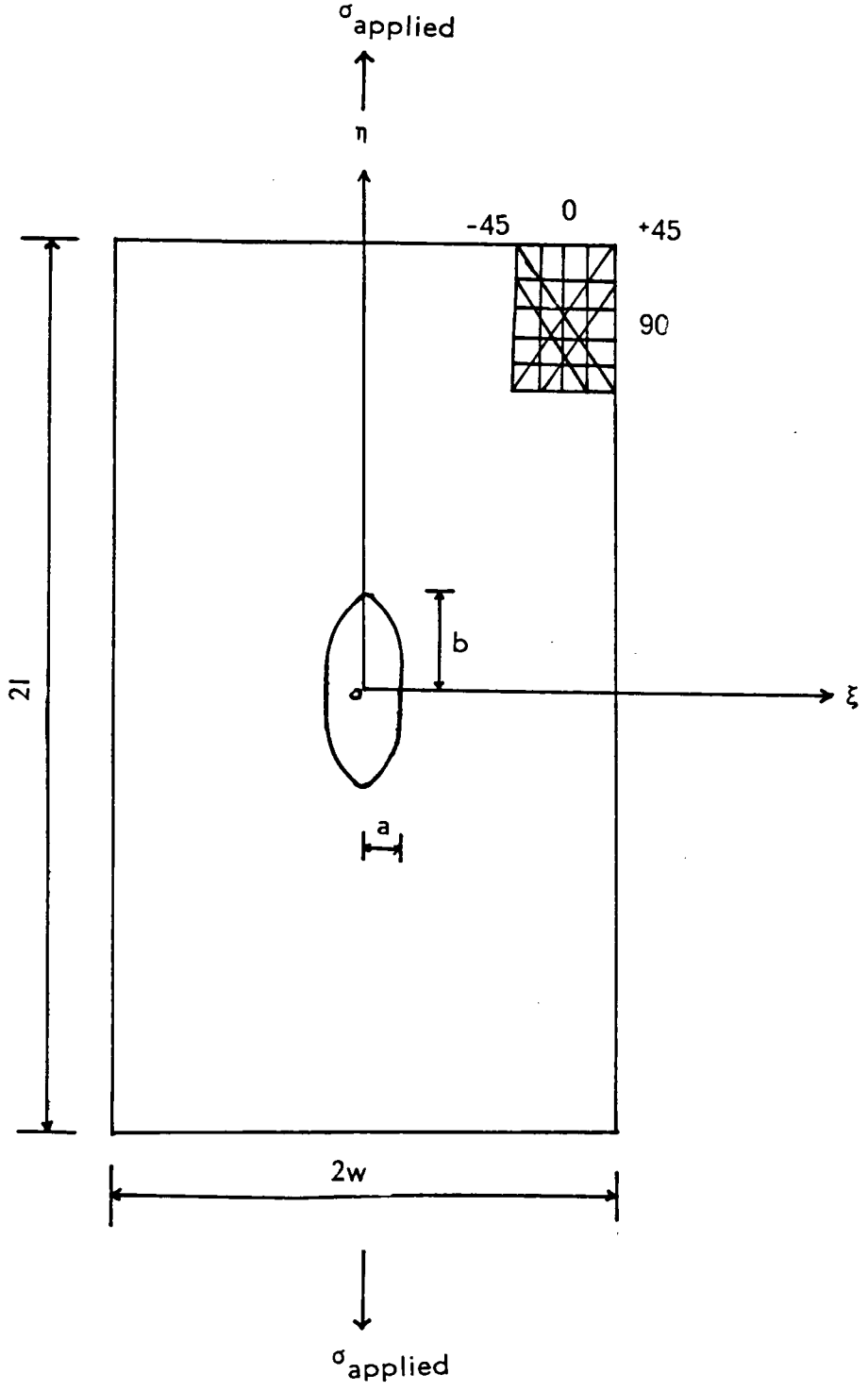

Fig. 2 Laminate with a Central Elliptical Hole in Elliptical Coordinates

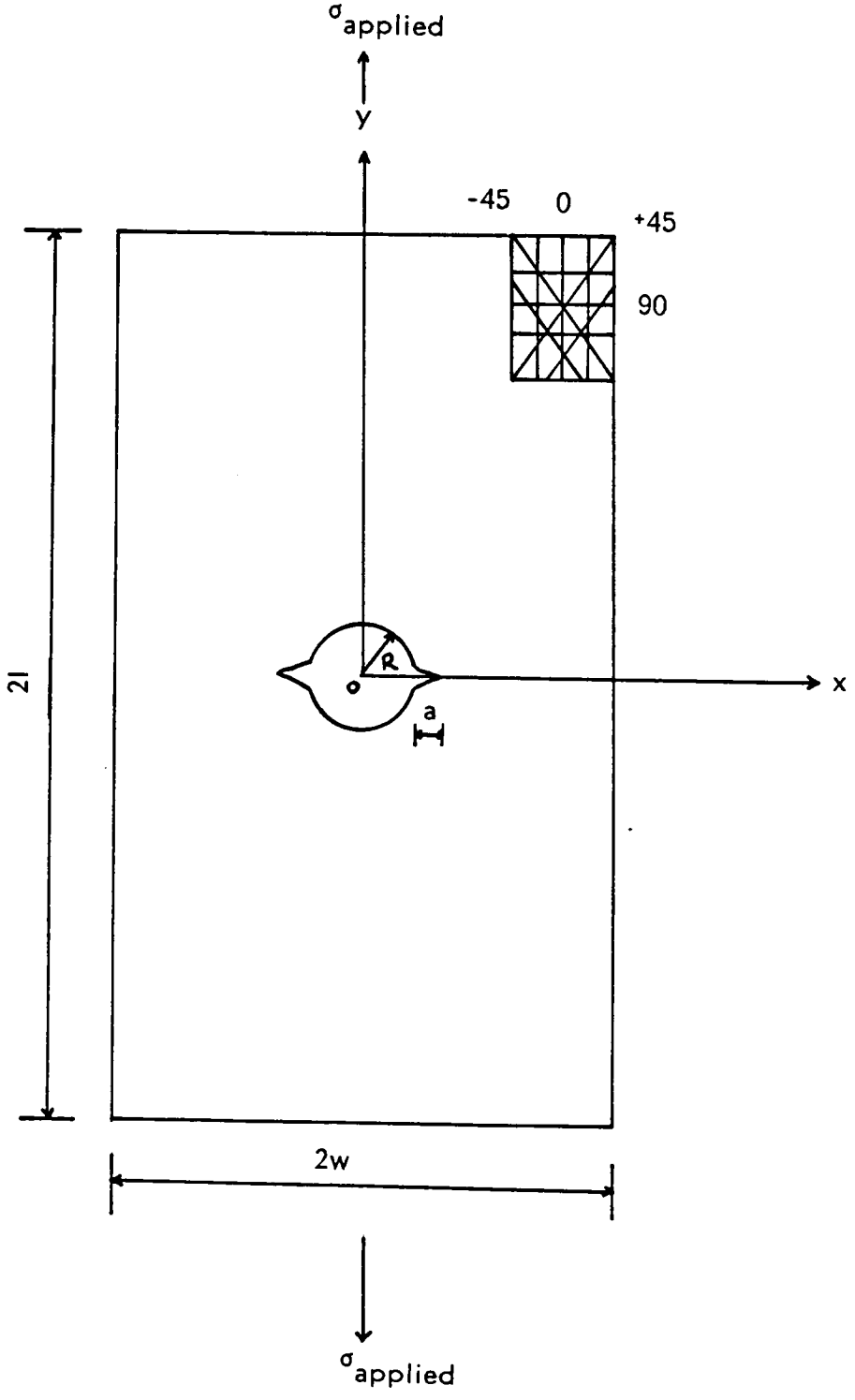

Fig. 3 Fracture Model (Mode I) for Transverse Crack Growth

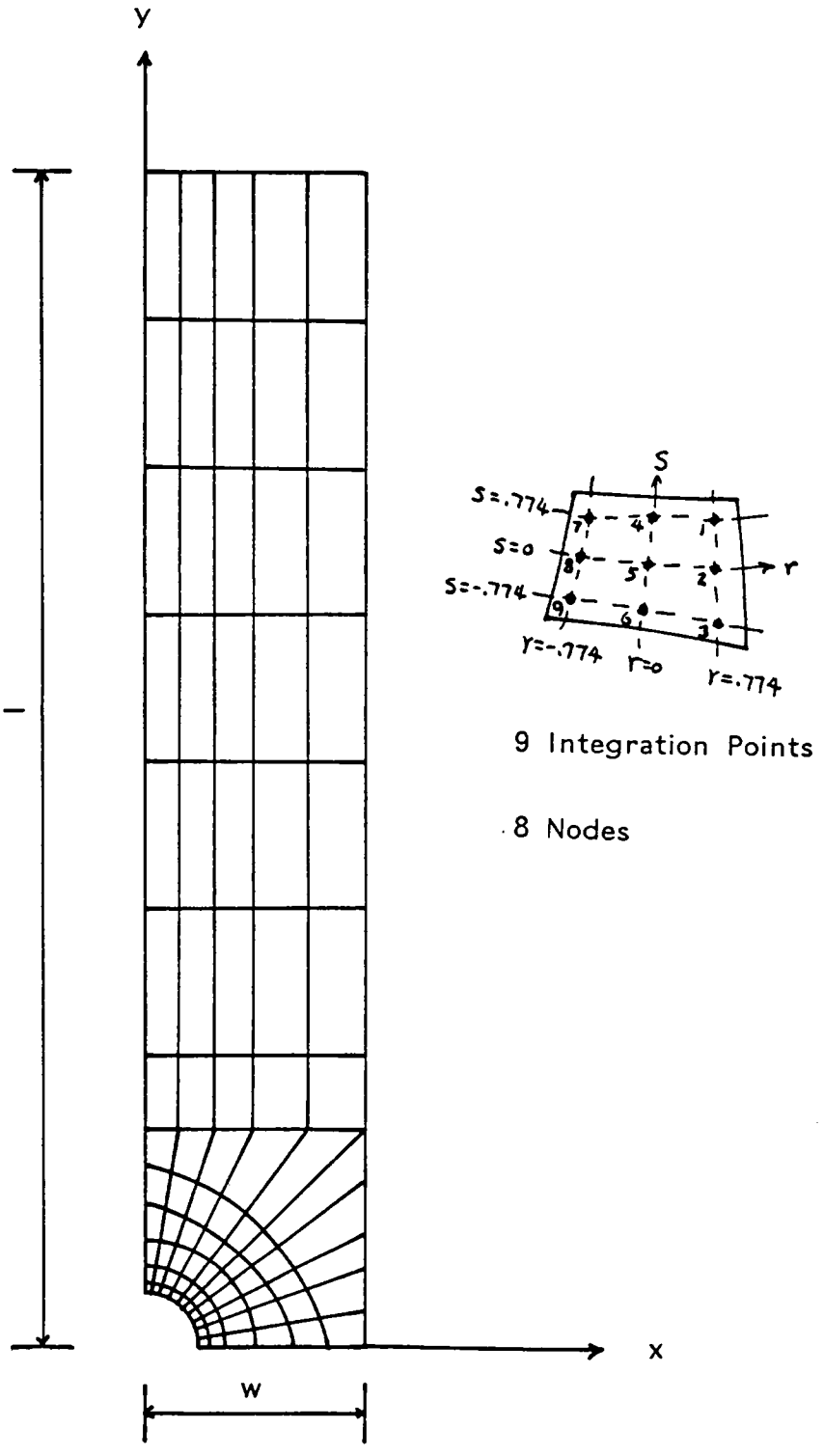

Fig. 4 FEM Meshes for Laminate with a Central Circular Hole

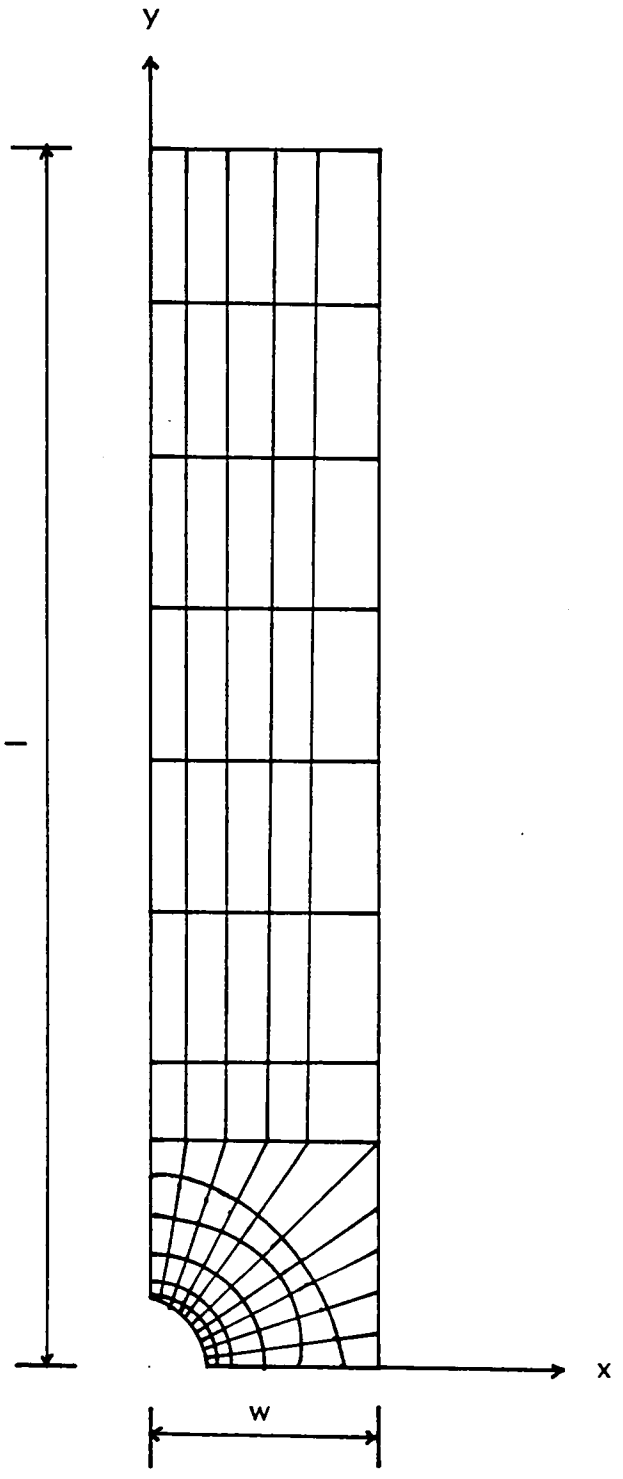

Fig. 5 FEM Meshes for Laminate with a Central Elliptical Hole

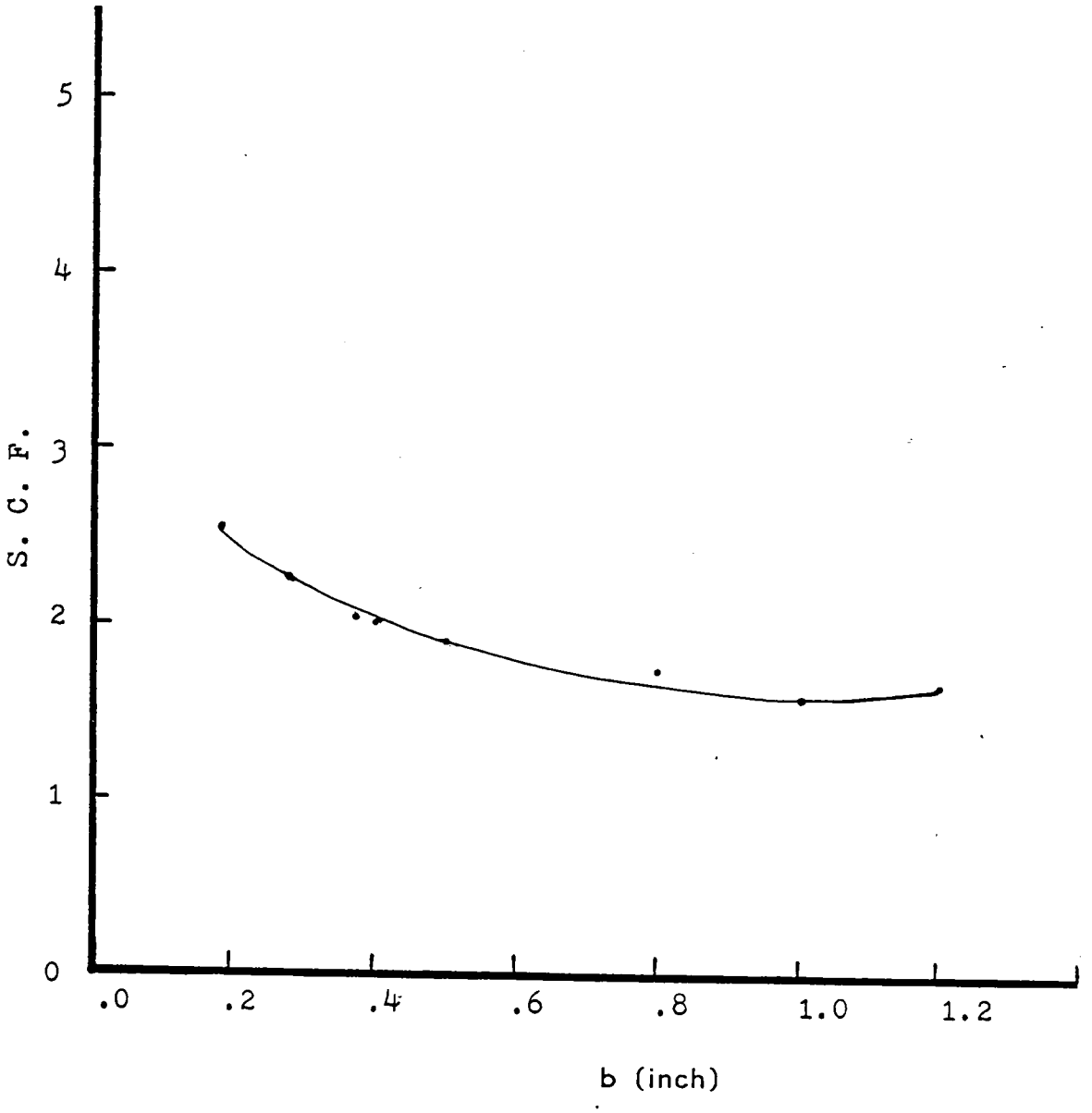

Fig. 6 SCF vs. Longitudinal Semi-axis of Elliptical Hole, b, for Graphite/Epoxy T300/5208 1.5"x8" with Layup $[0_8]_t$

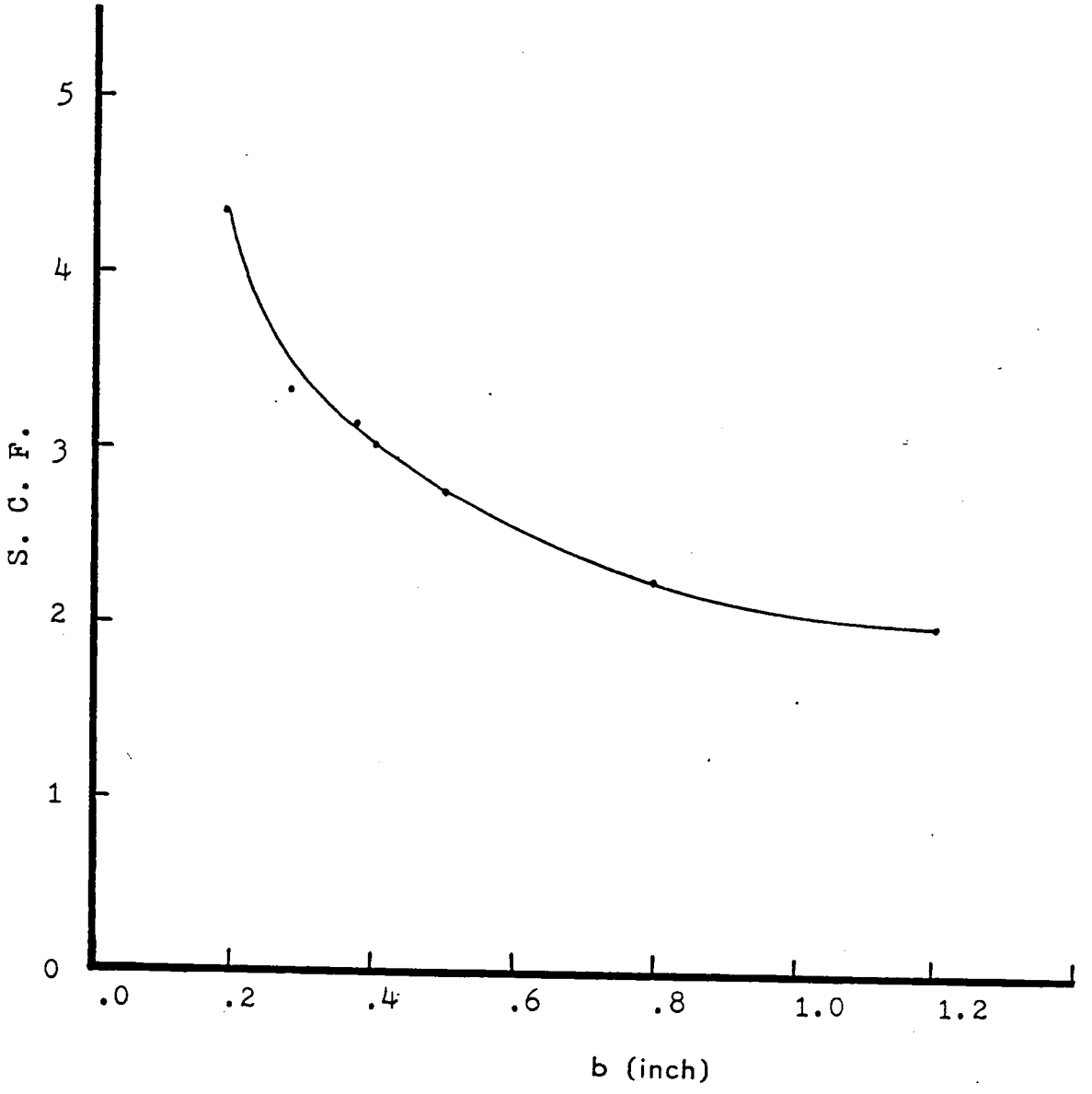

Fig. 7 SCF vs. Longitudinal Semi-axis of Elliptical Hole, b, for T300/5208 1.5"x8" with Layup $[0/90]_{2s}$

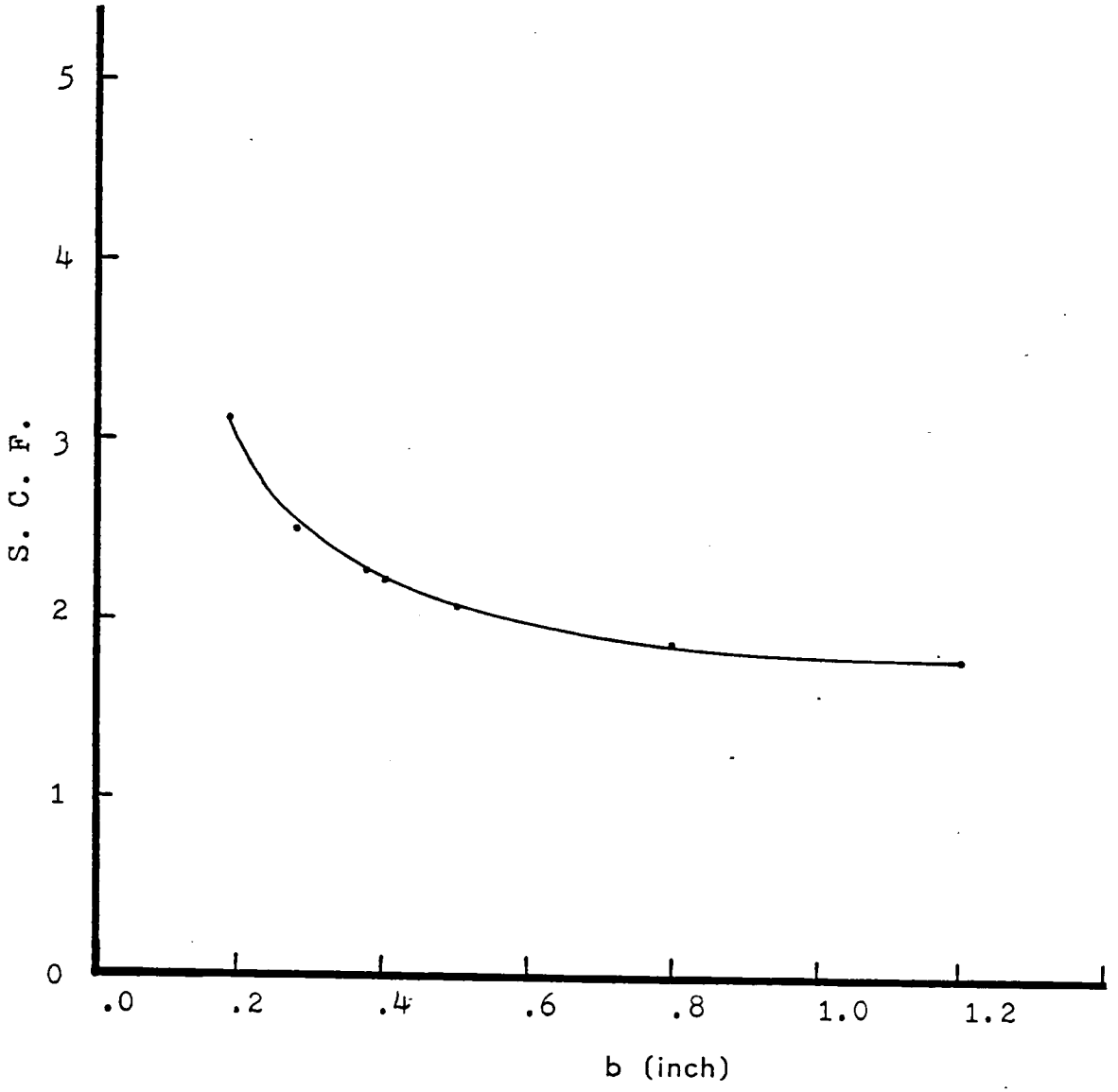

Fig. 8 SCF vs. Longitudinal Semi-axis of Elliptical Hole, b, for T300/5208 1.5"x8" with Layup $[0/\pm 45/90]_s$

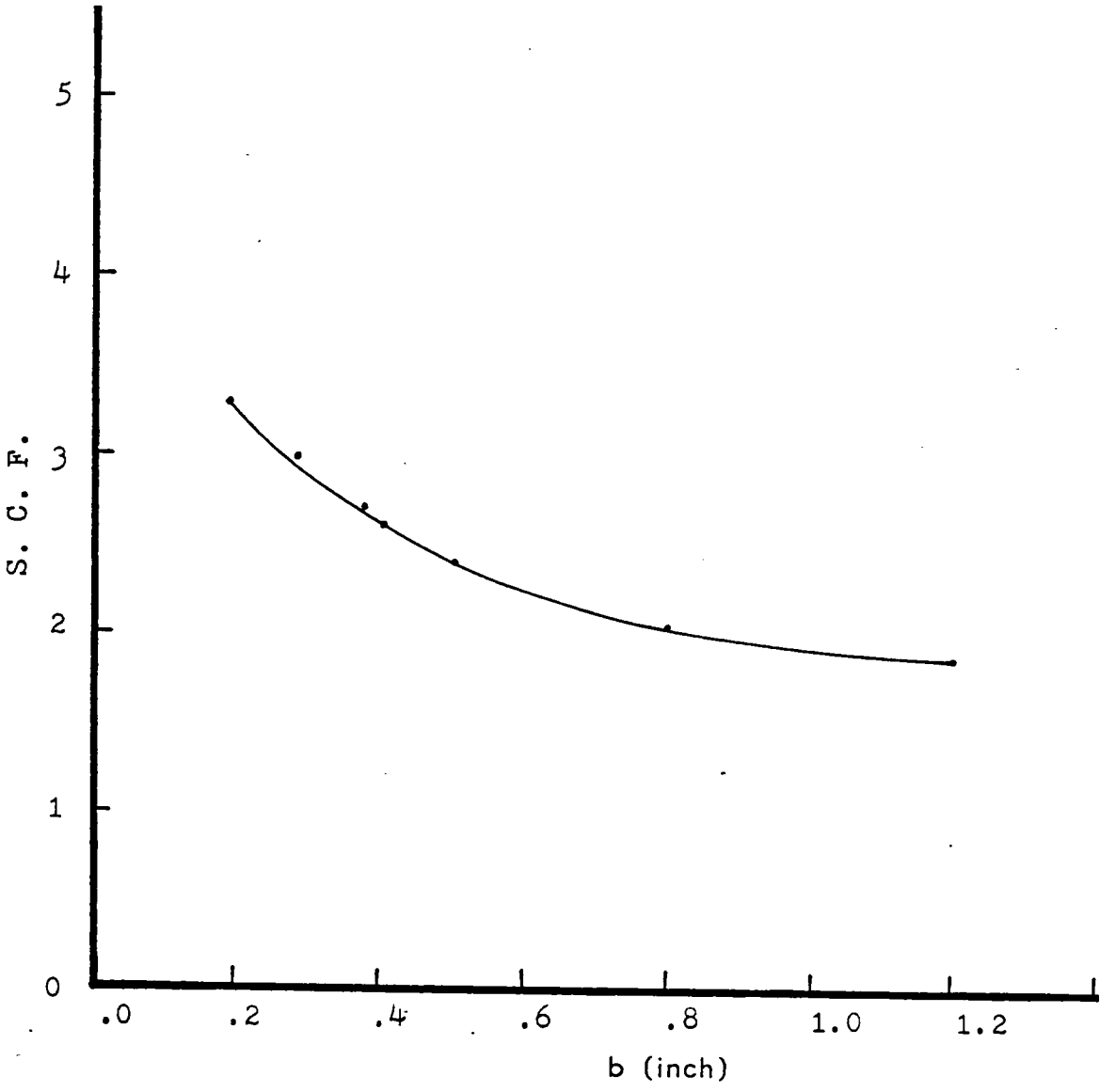

Fig. 9 SCF vs. Longitudinal Semi-axis of Elliptical Hole, b, for T300/5208 1.5"x8" with Layup $[0/\pm45/90_4]_s$

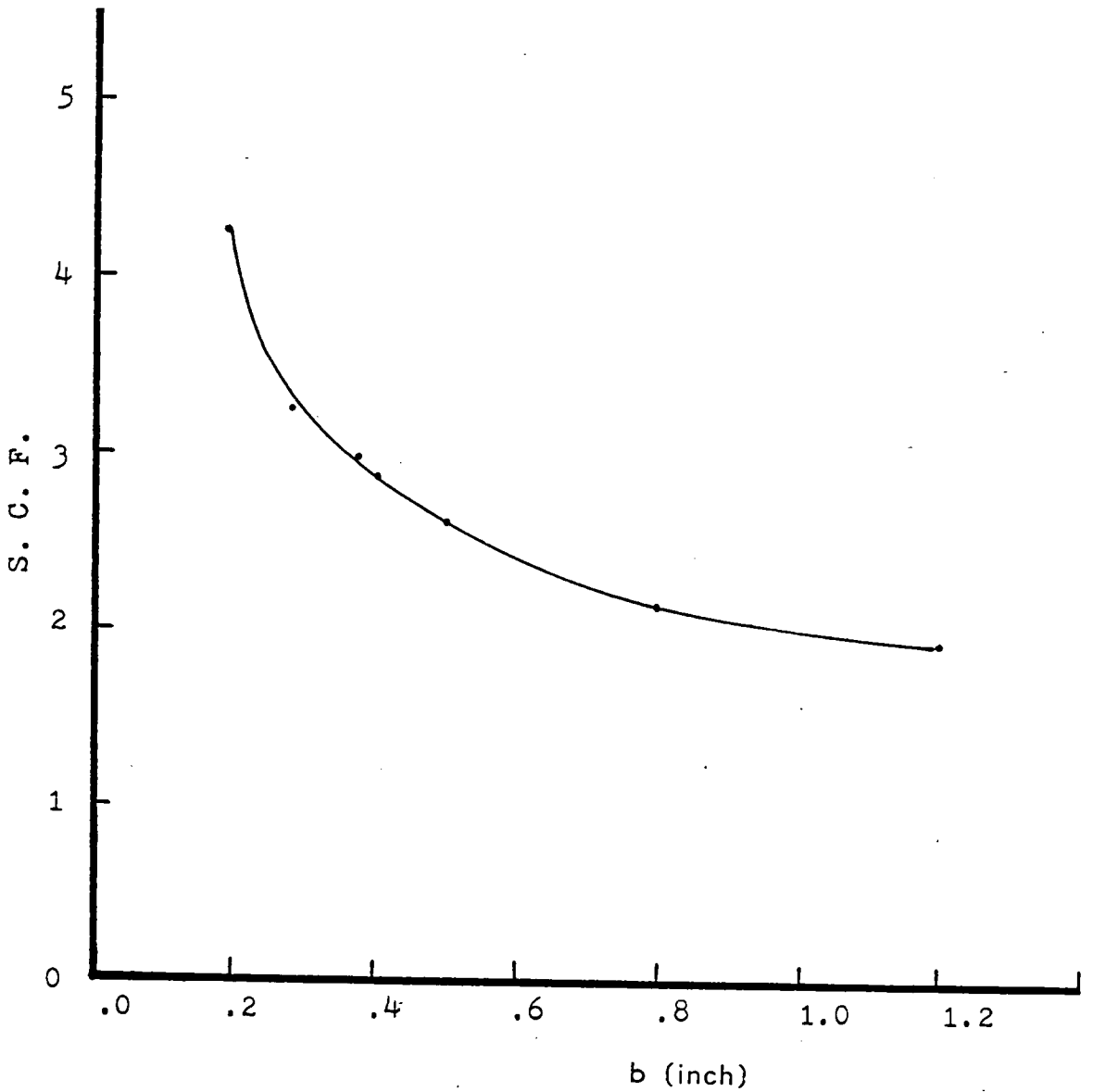

Fig. 10 SCF vs. Longitudinal Semi-axis of Elliptical Hole, b, for T300/5208 1.5"x8" with Layup $[0/\pm45/90_8]_s$

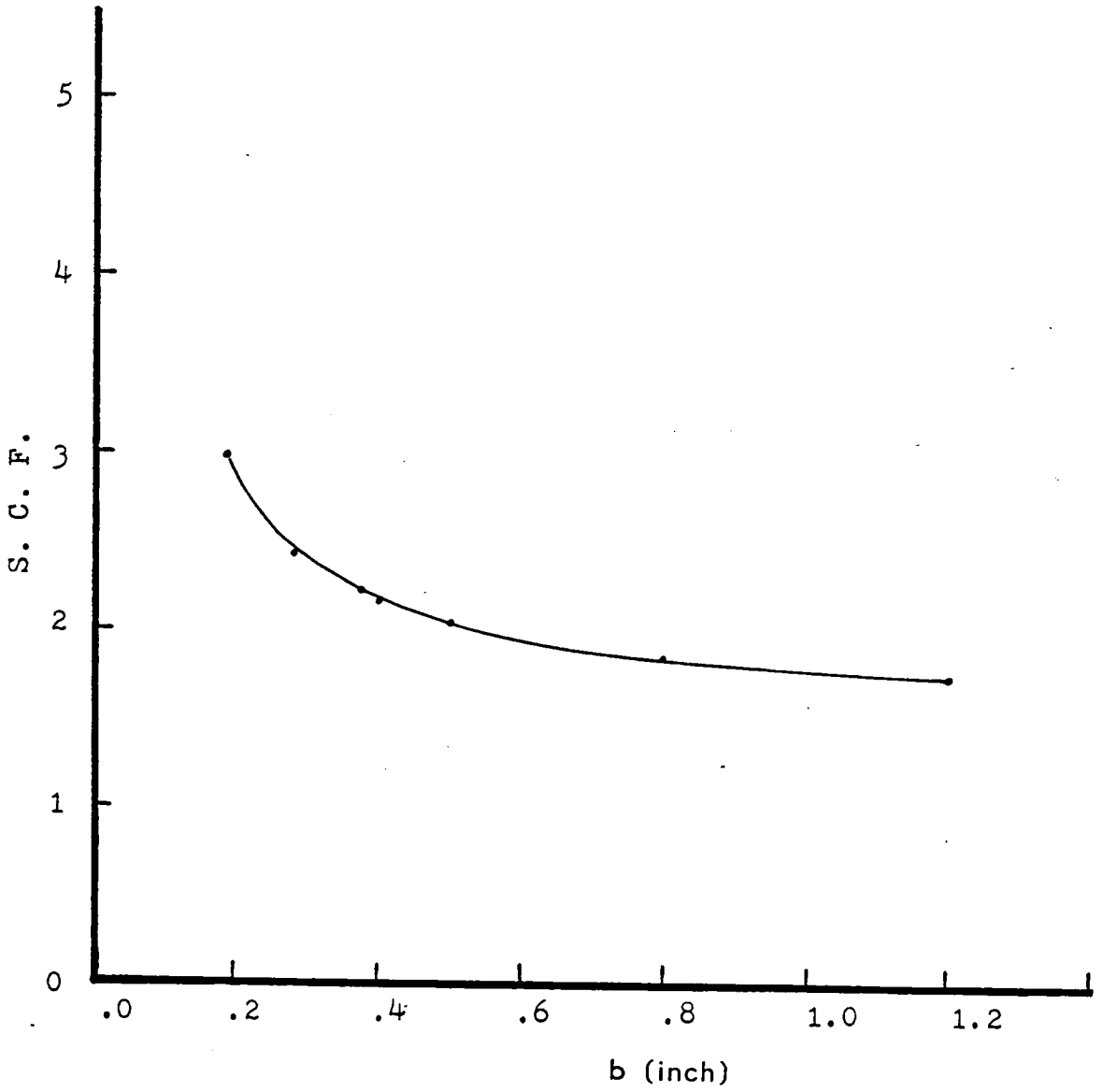

Fig. 11 SCF vs. Longitudinal Semi-axis of Elliptical Hole, b, for T300/5208 1.5"x8" with Layup $[0_4/\pm 45/90]_s$

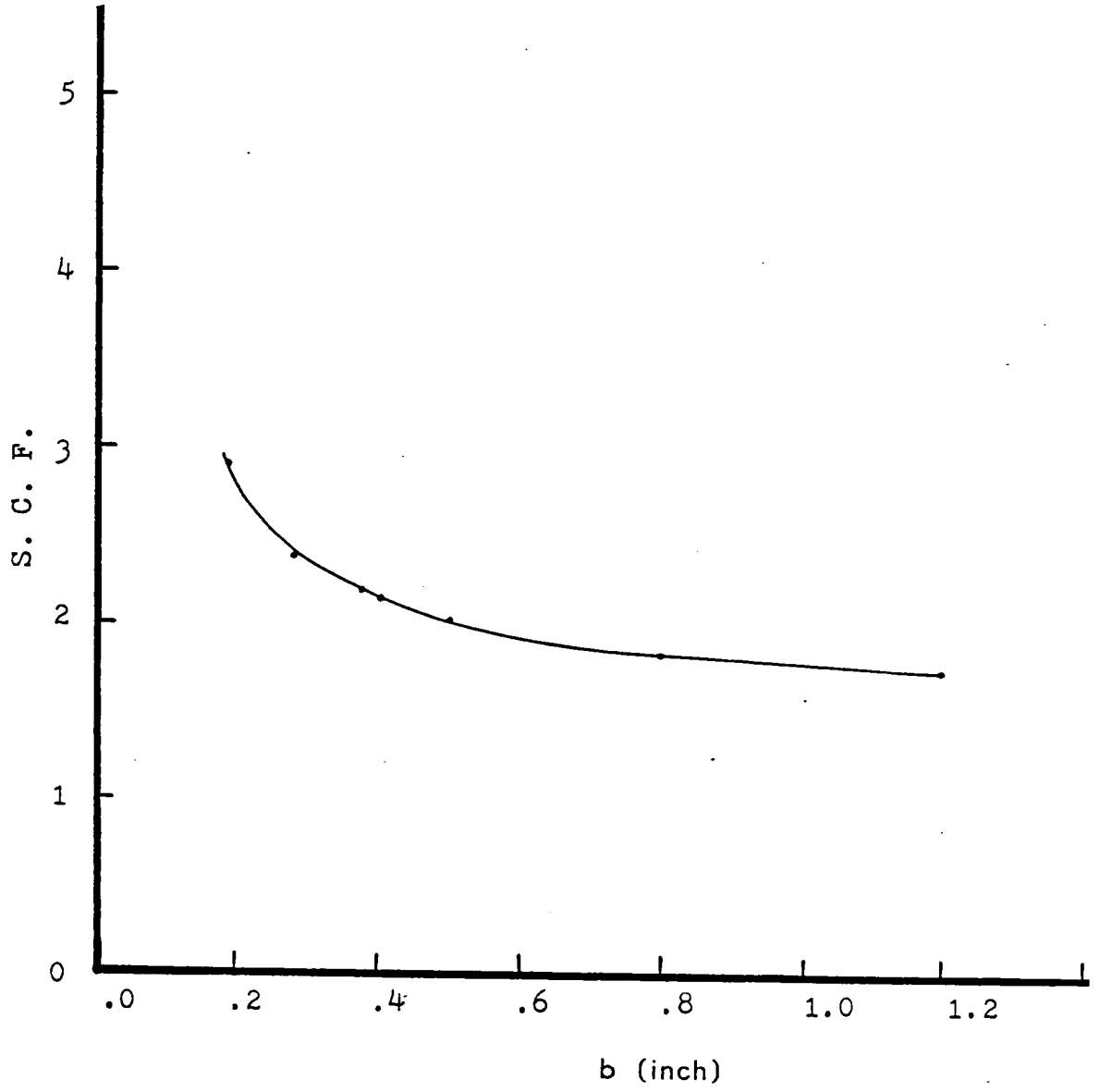

Fig. 12 SCF vs. Longitudinal Semi-axis of Elliptical Hole, b, for T300/5208 1.5"x8" with Layup $[0_8/\pm 45/90]_s$

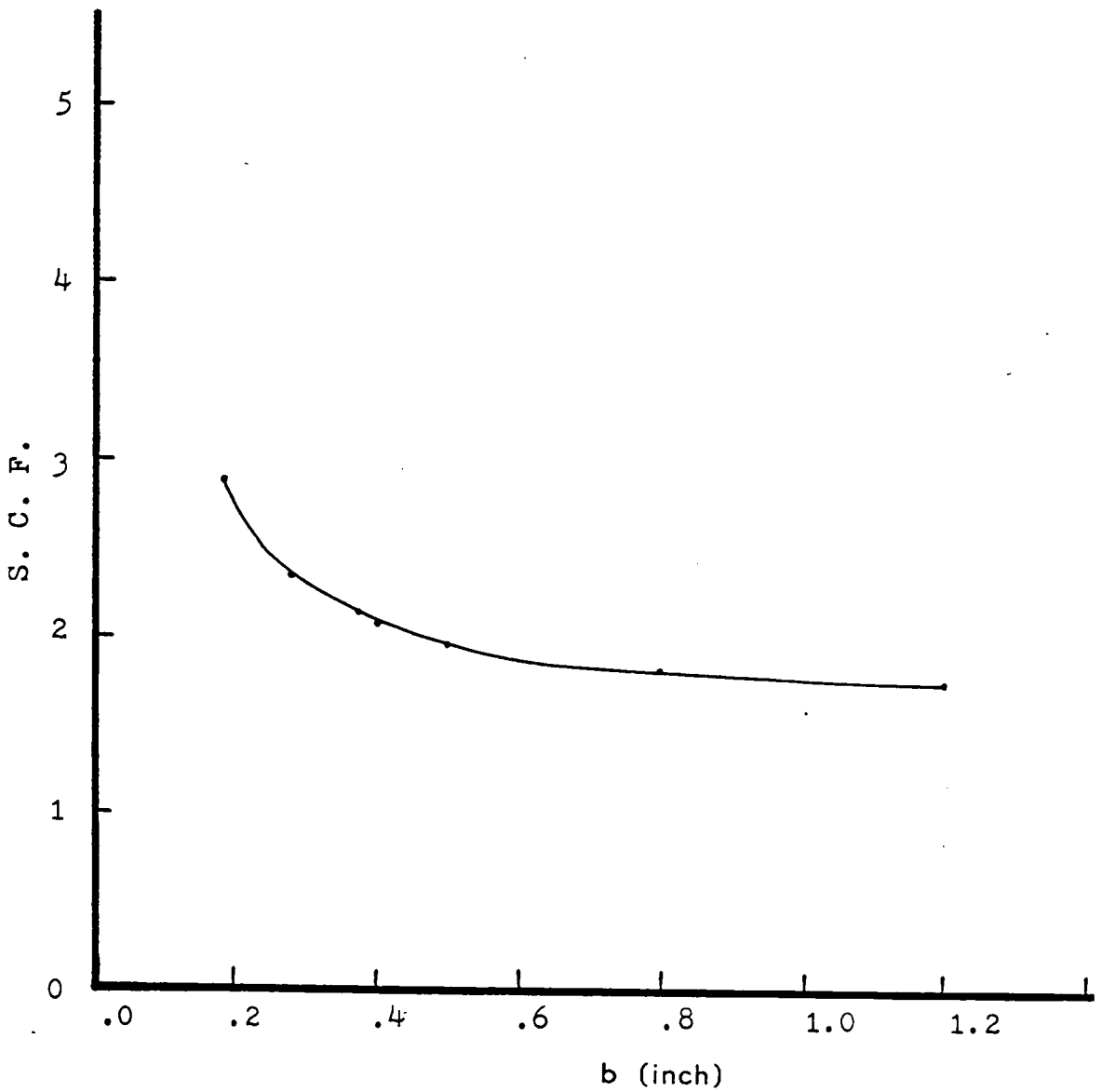

Fig. 13 SCF vs. Longitudinal Semi-axis of Elliptical Hole, b, for T300/5208 1.5"x8" with Layup $[0/\pm 45_2/90]_s$

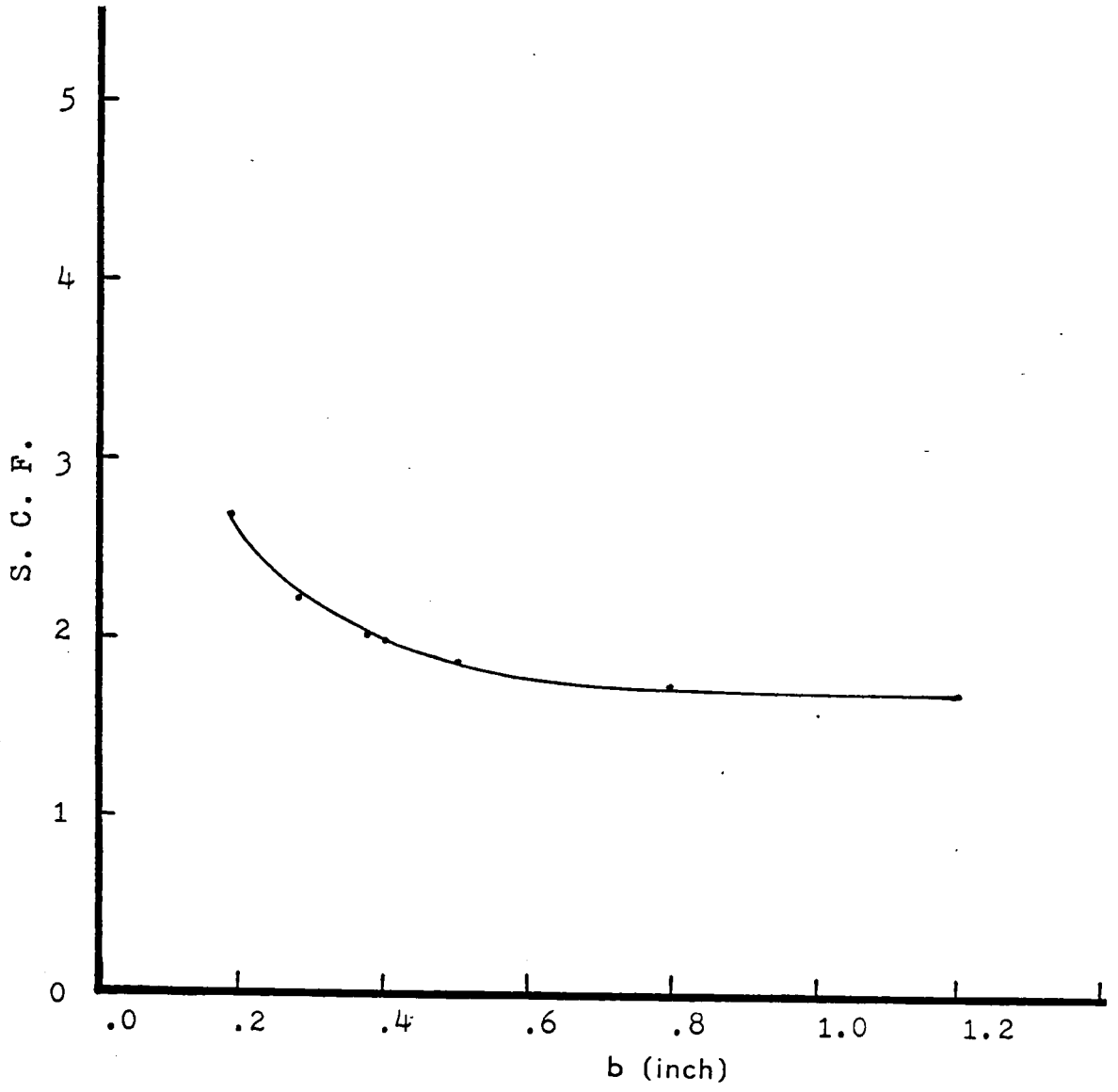

Fig. 14 SCF vs. Longitudinal Semi-axis of Elliptical Hole, b, for T300/5208 1.5"x8" with Layup $[0/\pm 45_4/90]_s$

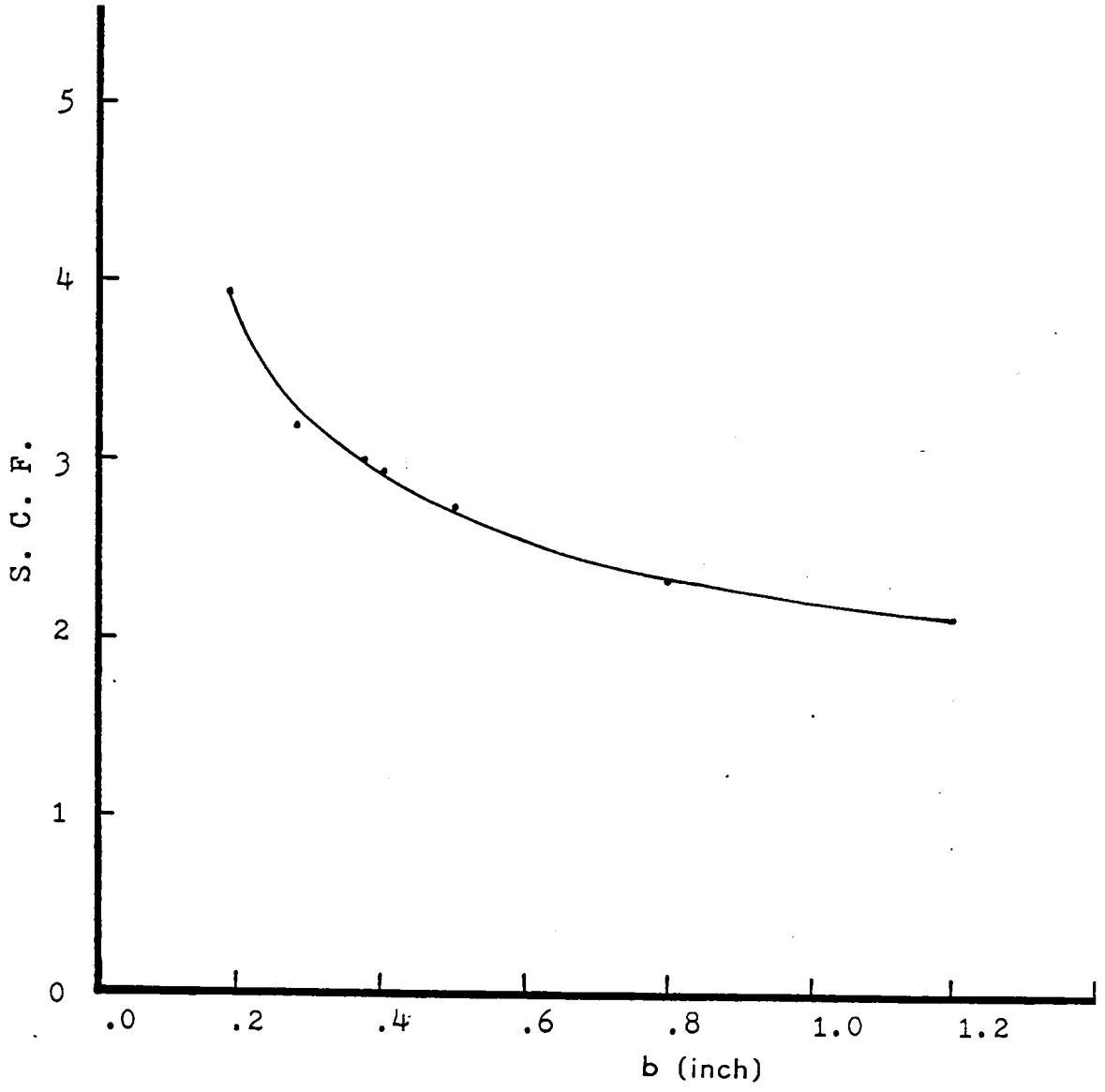

Fig. 15 SCF vs. Longitudinal Semi-axis of Elliptical Hole, b, for T300/5208 1.5"x8" with Layup $[0/45_2/90]_s$

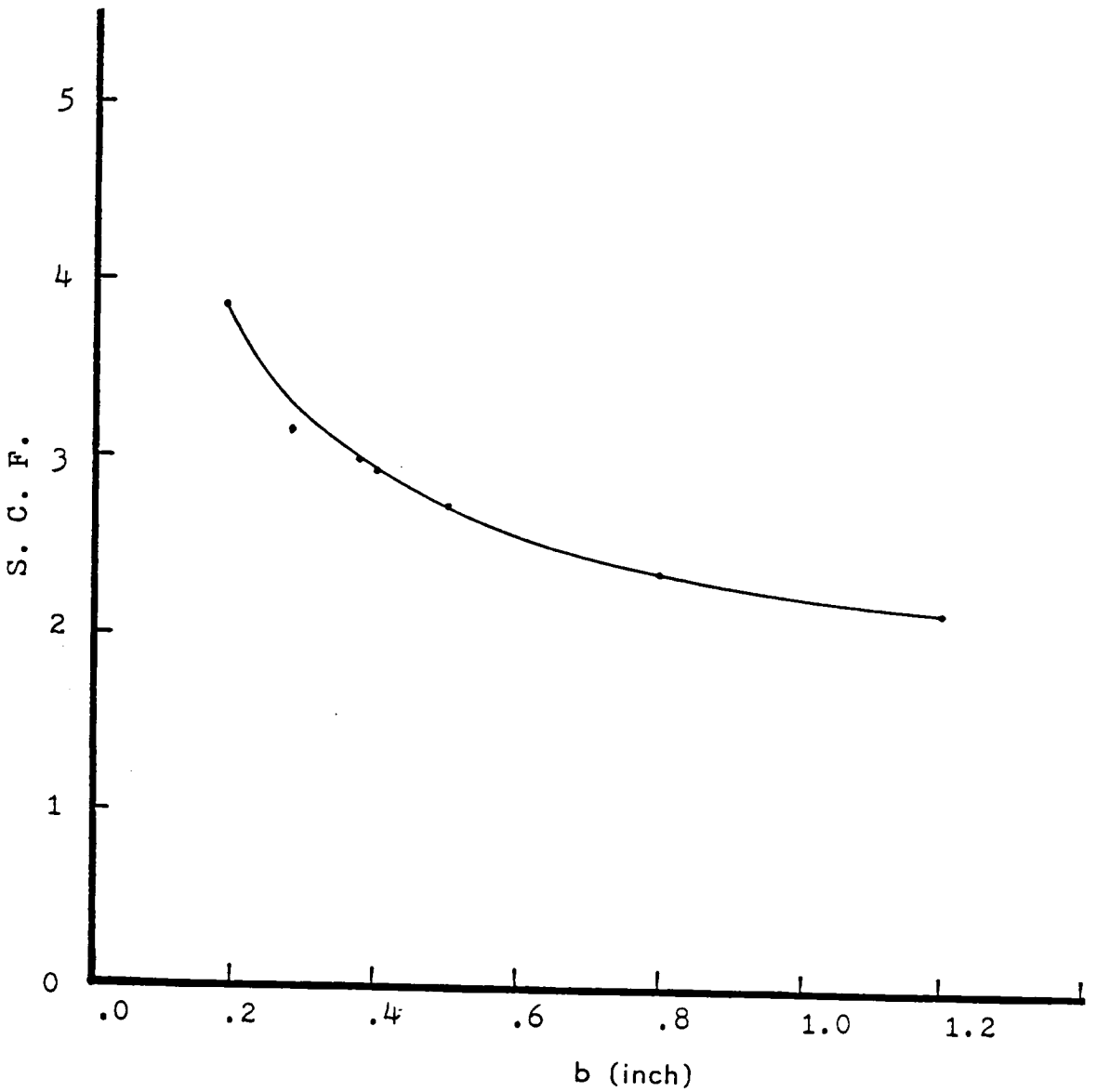

Fig. 16 SCF vs. Longitudinal Semi-axis of Elliptical Hole, b, for T300/5208 1.5"x8" with Layup $[0/45_4/90]_s$

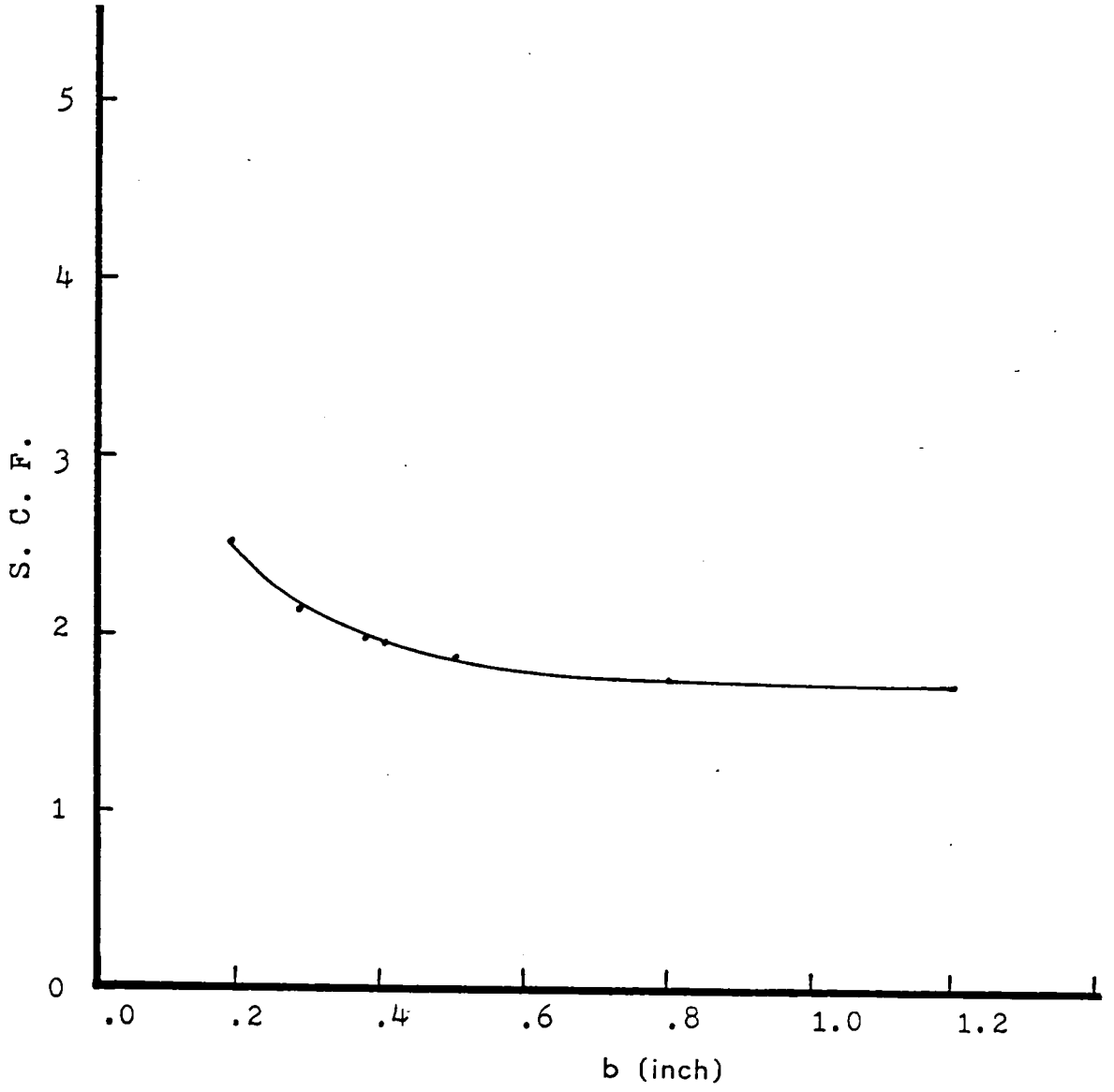

Fig. 17 SCF vs. Longitudinal Semi-axis of Elliptical Hole, b, for T300/5208 1.5"x8" with Layup $[0_2/\pm 45]_s$

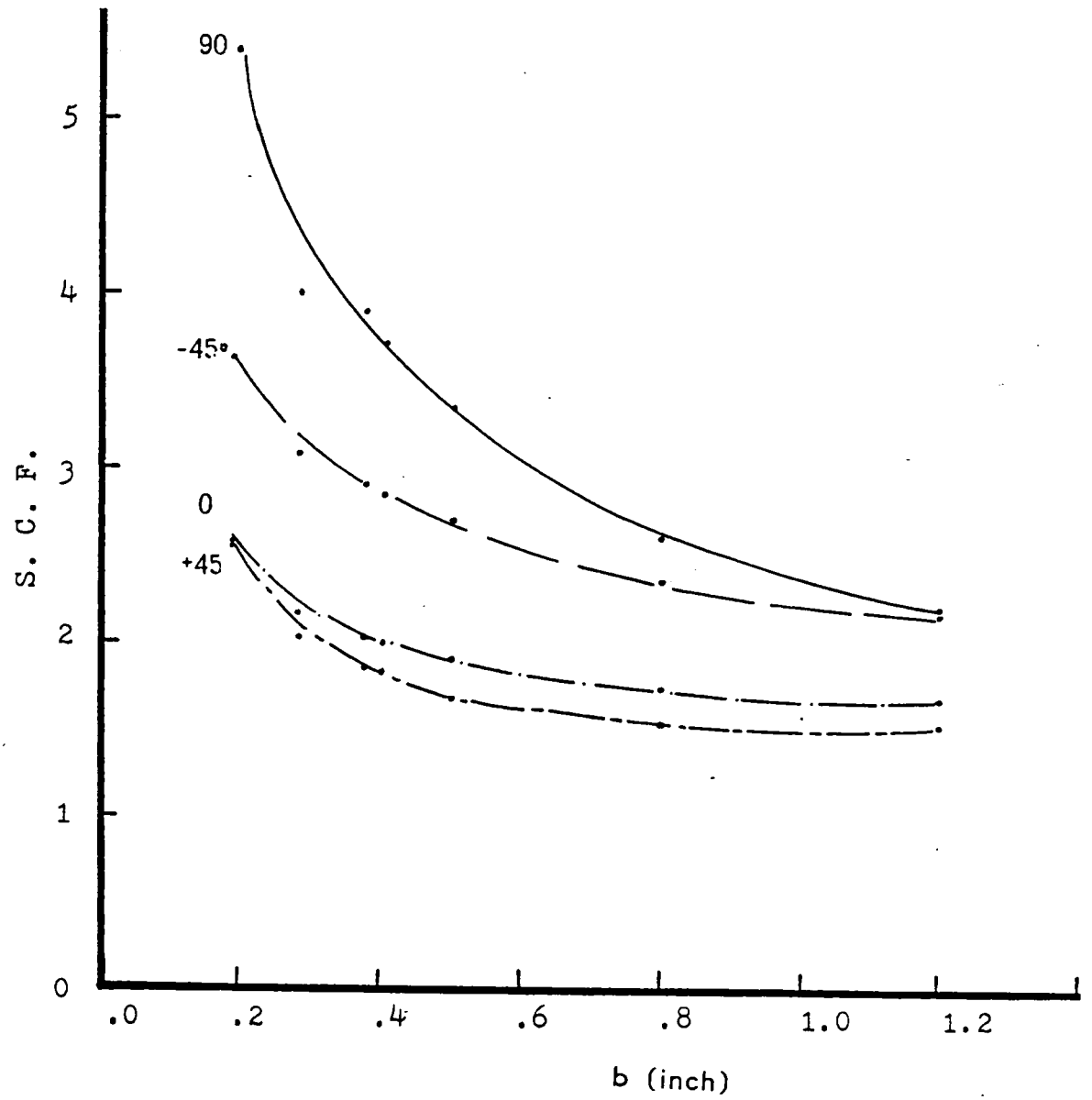

Fig. 18 SCF vs. Longitudinal Semi-axis of Elliptical Hole, b, for T300/5208 1.5"x8" one ply 0, 45, -45, 90 degree

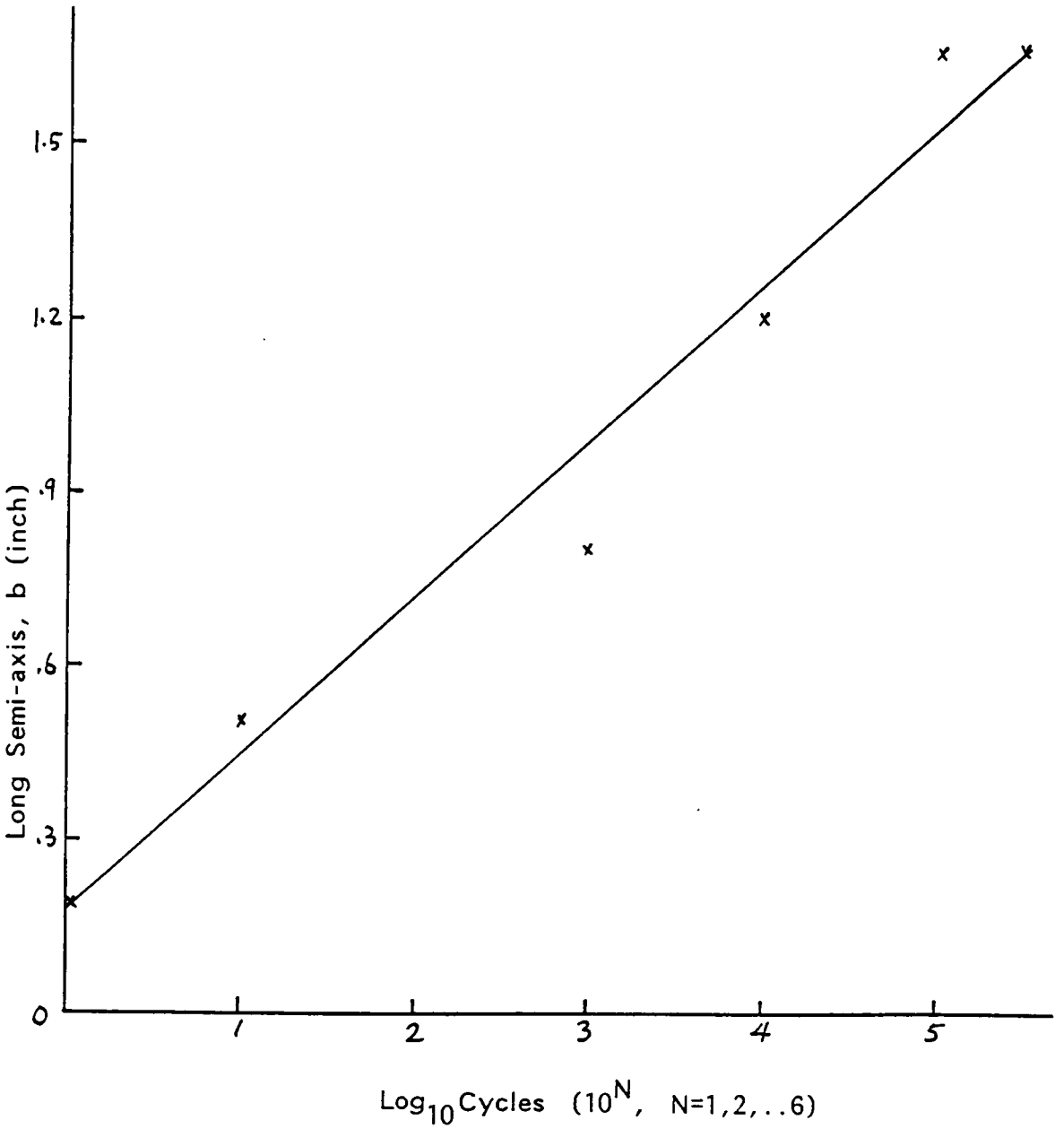

Fig. 19 Longitiudinal Semi-axis of Elliptical Hole, b vs. Cycles for T300/5208 Laminate with Layup $[0/\pm 45/90]_s$

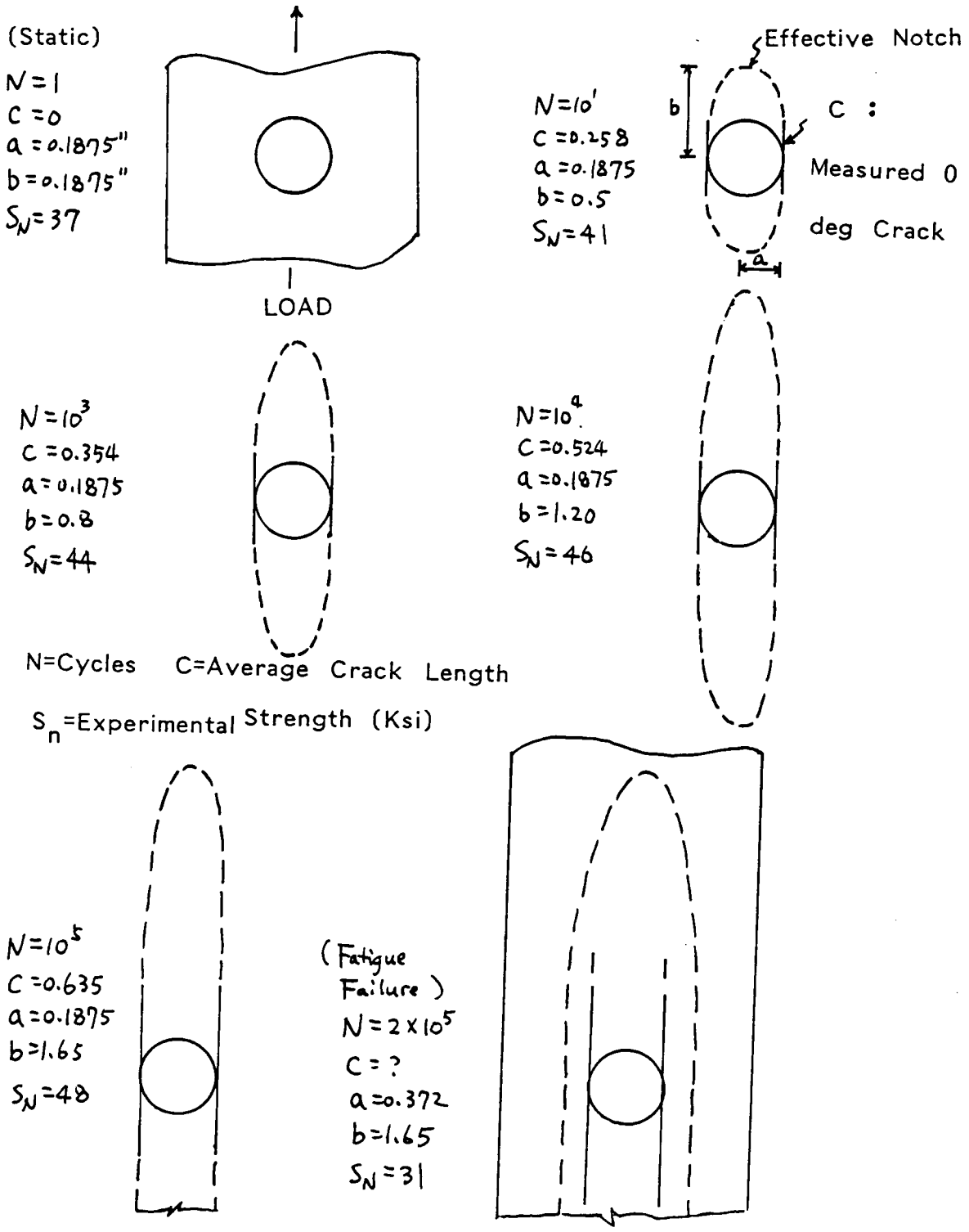

Fig. 20 Superposition of Effective Notch on Fatigued Specimen with $[0/\pm45/90]_s$ Layup

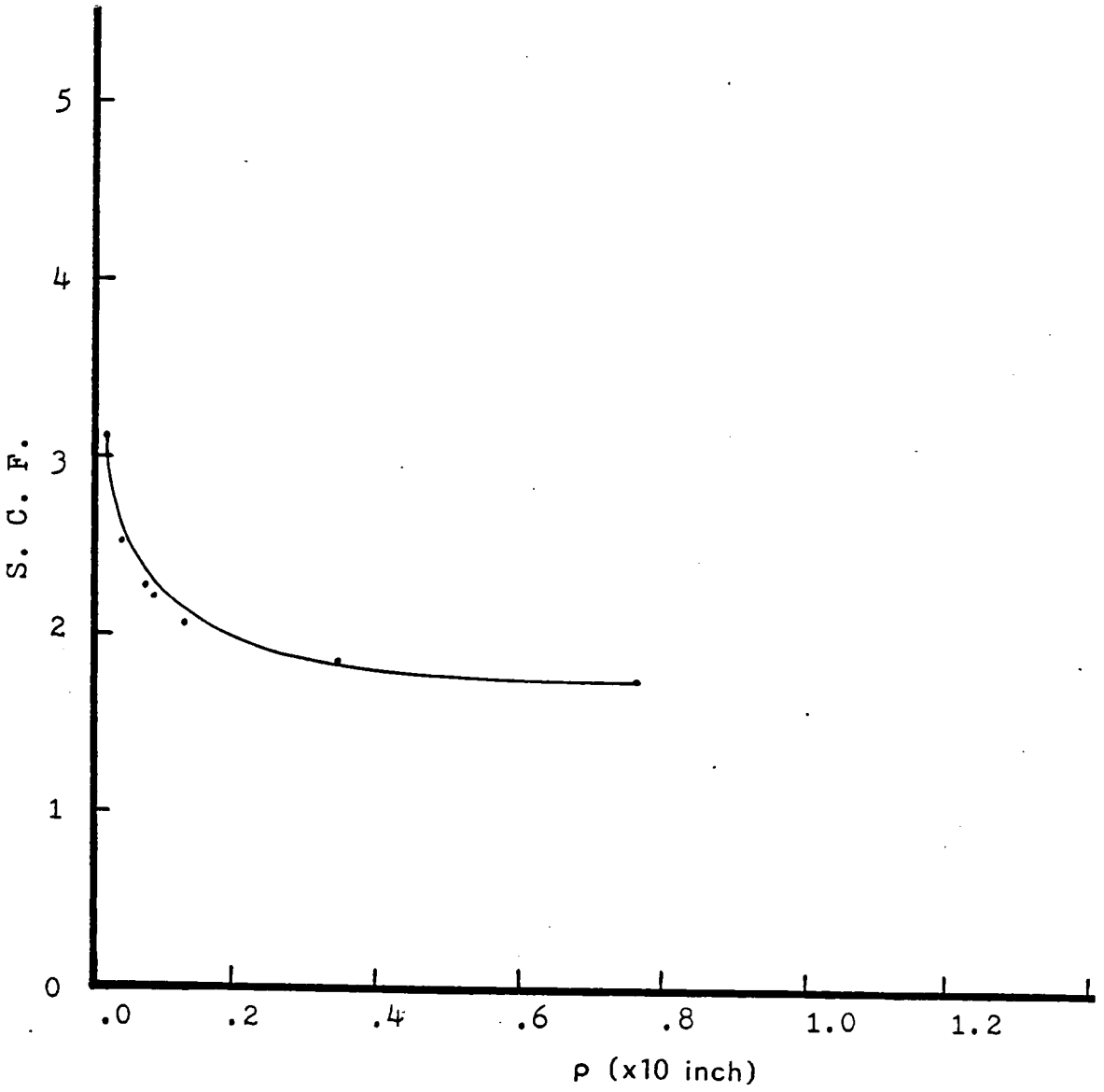

Fig. 21 SCF vs. Radius of Curvature, ρ for T300/5208 Laminate with Layup $[0/\pm45/90]_s$

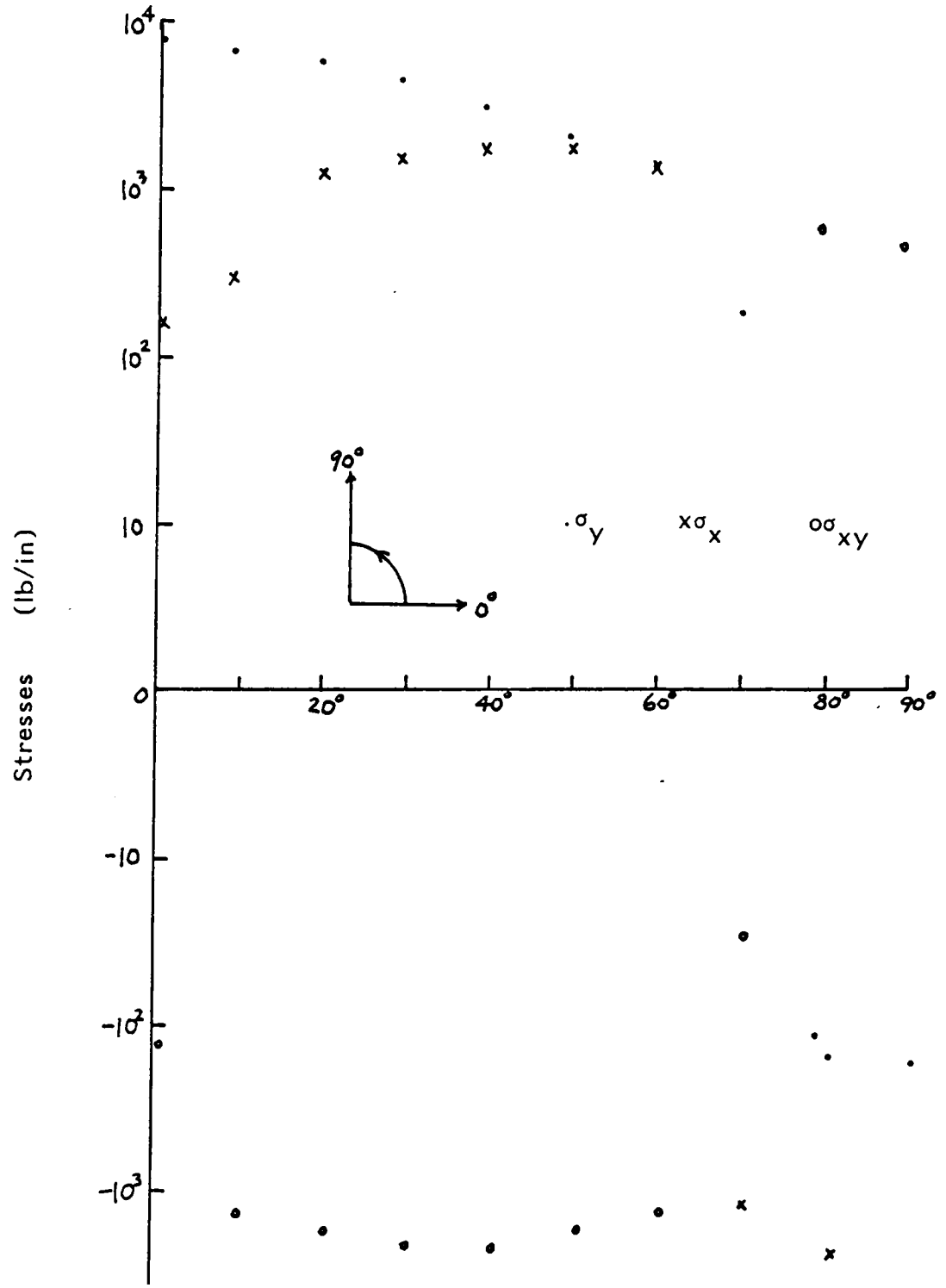

Fig. 22 Log Stresses Around the Notch of First Quarter for T300/5208 1.5"x8" with a Central Hole dia=3/8" Layup $[0_2/\pm 45]_s$

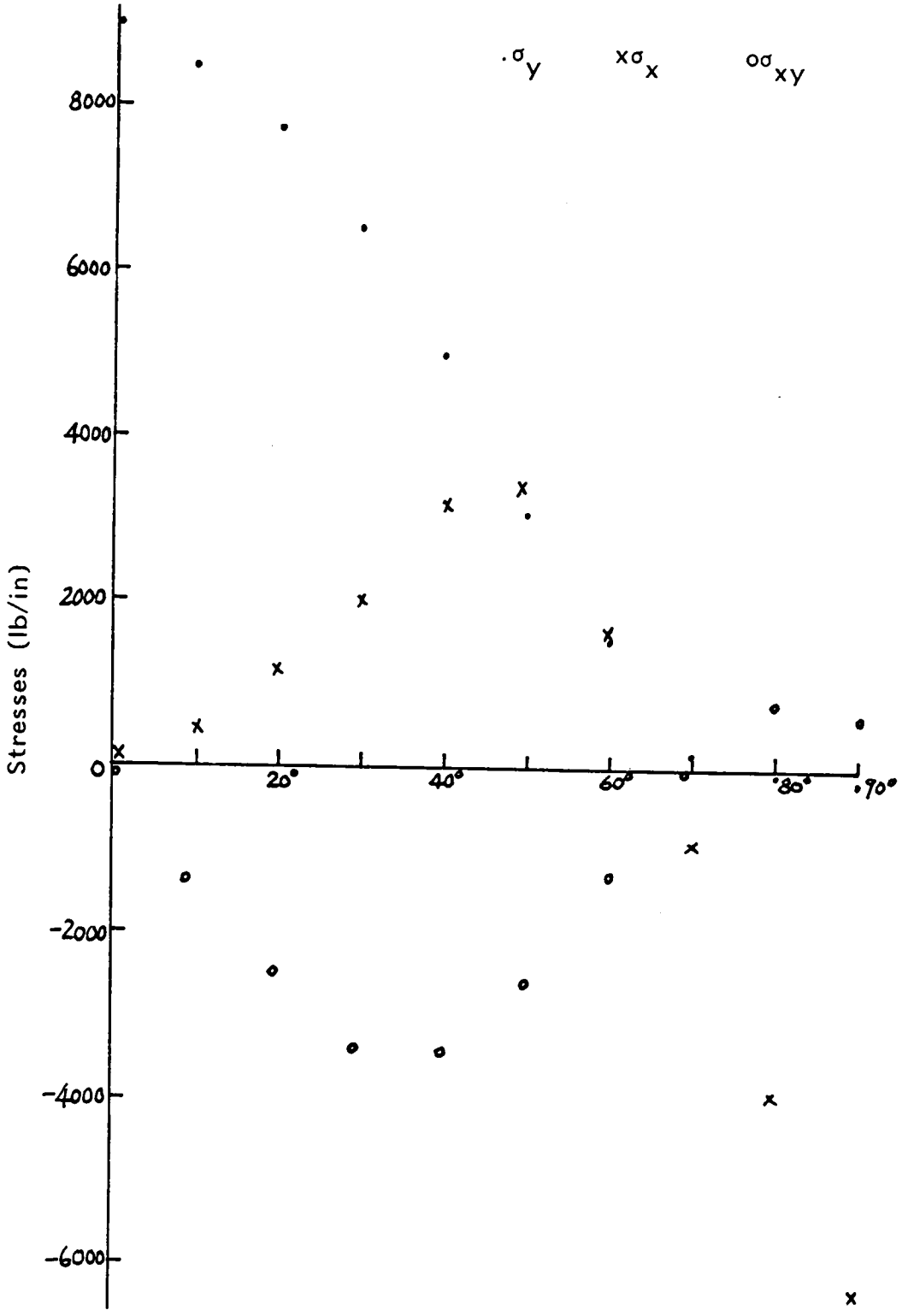

Fig. 23 Stresses Around the Notch of First Quarter for T300/5208 1.5"x8" with a Central Hole dia=3/8" Layup $[0_2/\pm 45]_s$

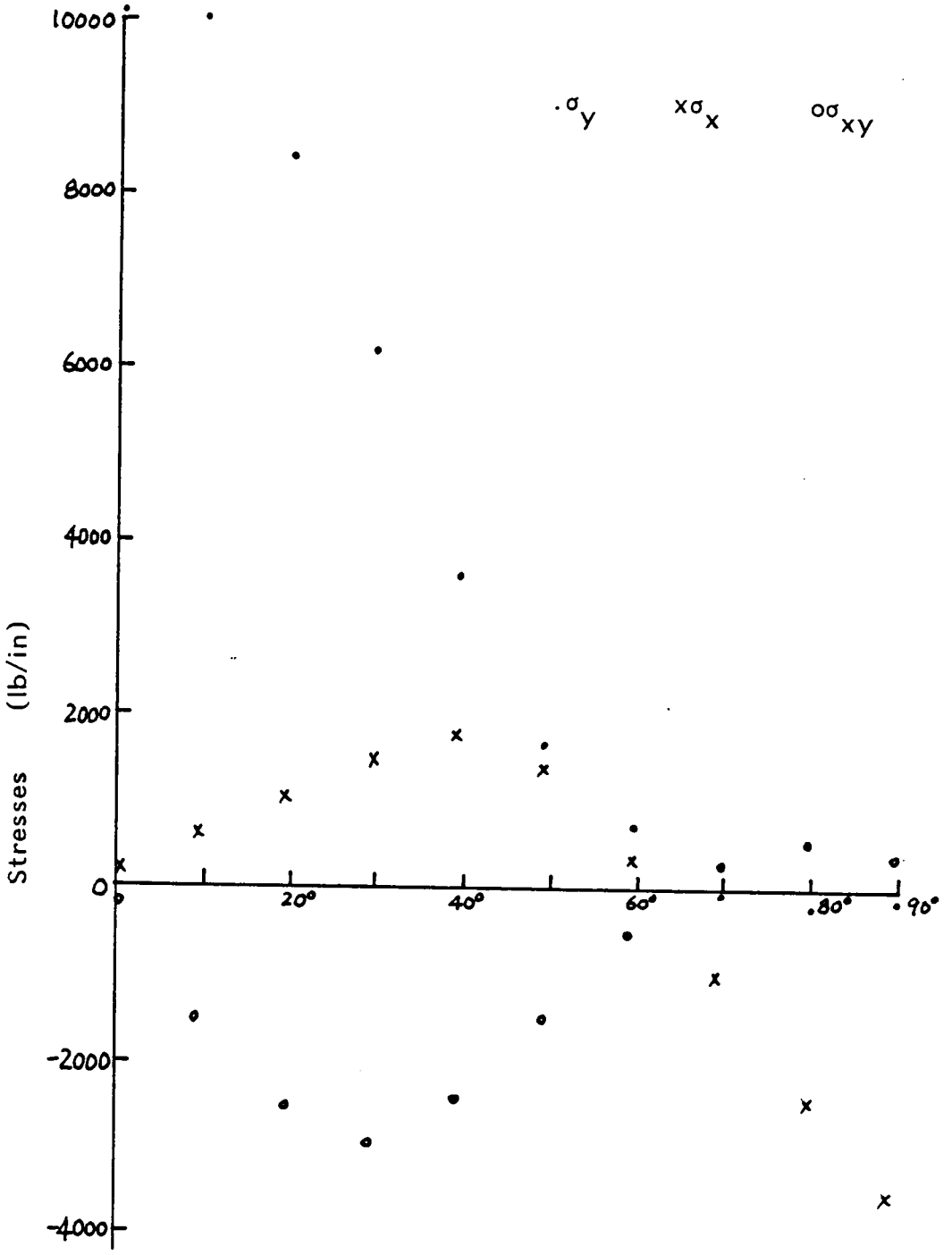

Fig. 24 Stresses Around the Notch of First Quarter for T300/5208 1.5"x8" with a Central Hole dia=3/8" Layup $[0/\pm45/90]_s$

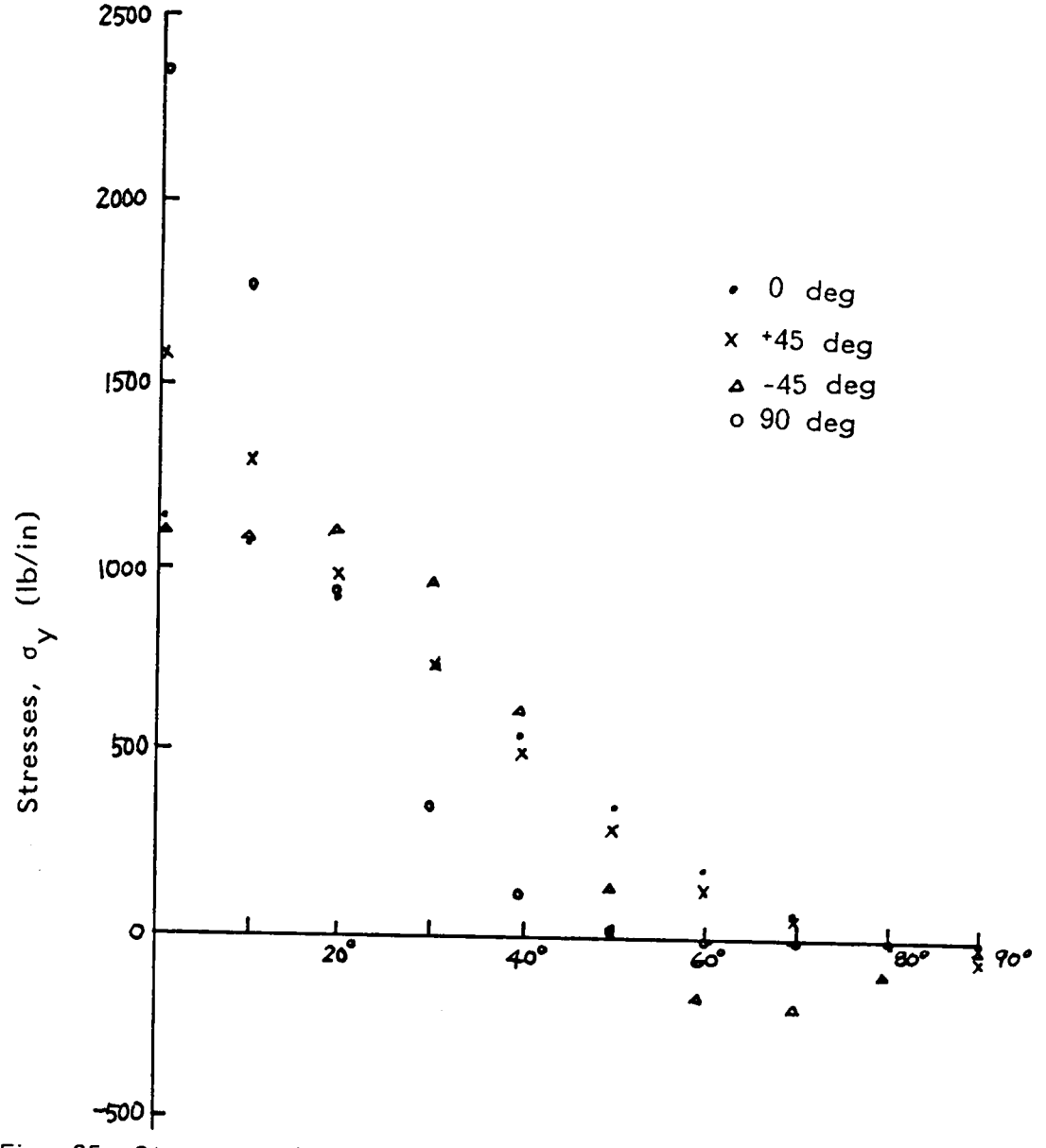

Fig. 25 Stress σ_y Around the Notch of First Quarter for T300/5208 1.5"x8" with a Central Hole dia=3/8" one ply 0, 45, -45, 90

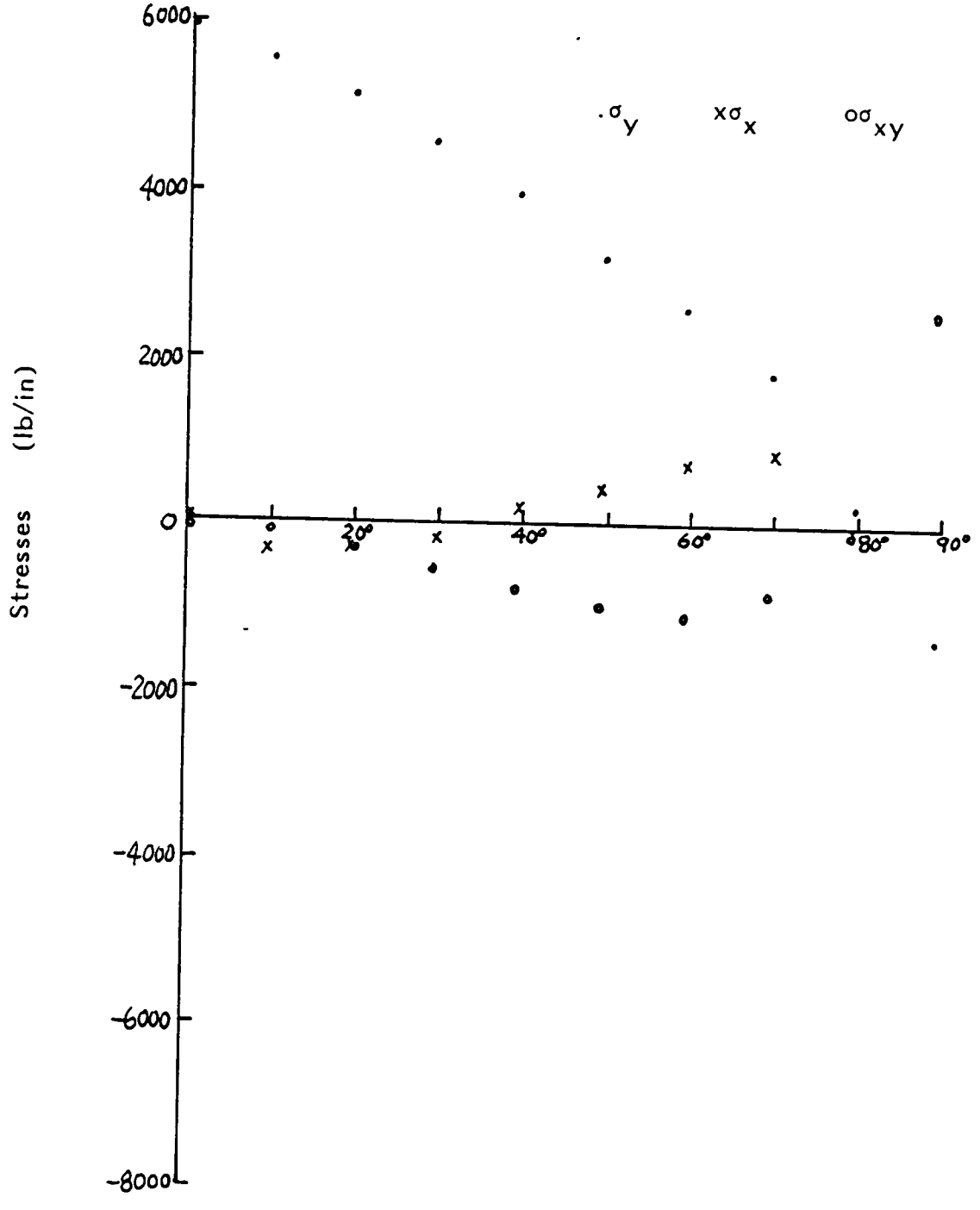

Fig. 26 Stresses Around the Notch of First Quarter for T300/5208 with an Elliptical Hole a=3/16", b=1.2" Layup $[0_2/\pm 45]_s$

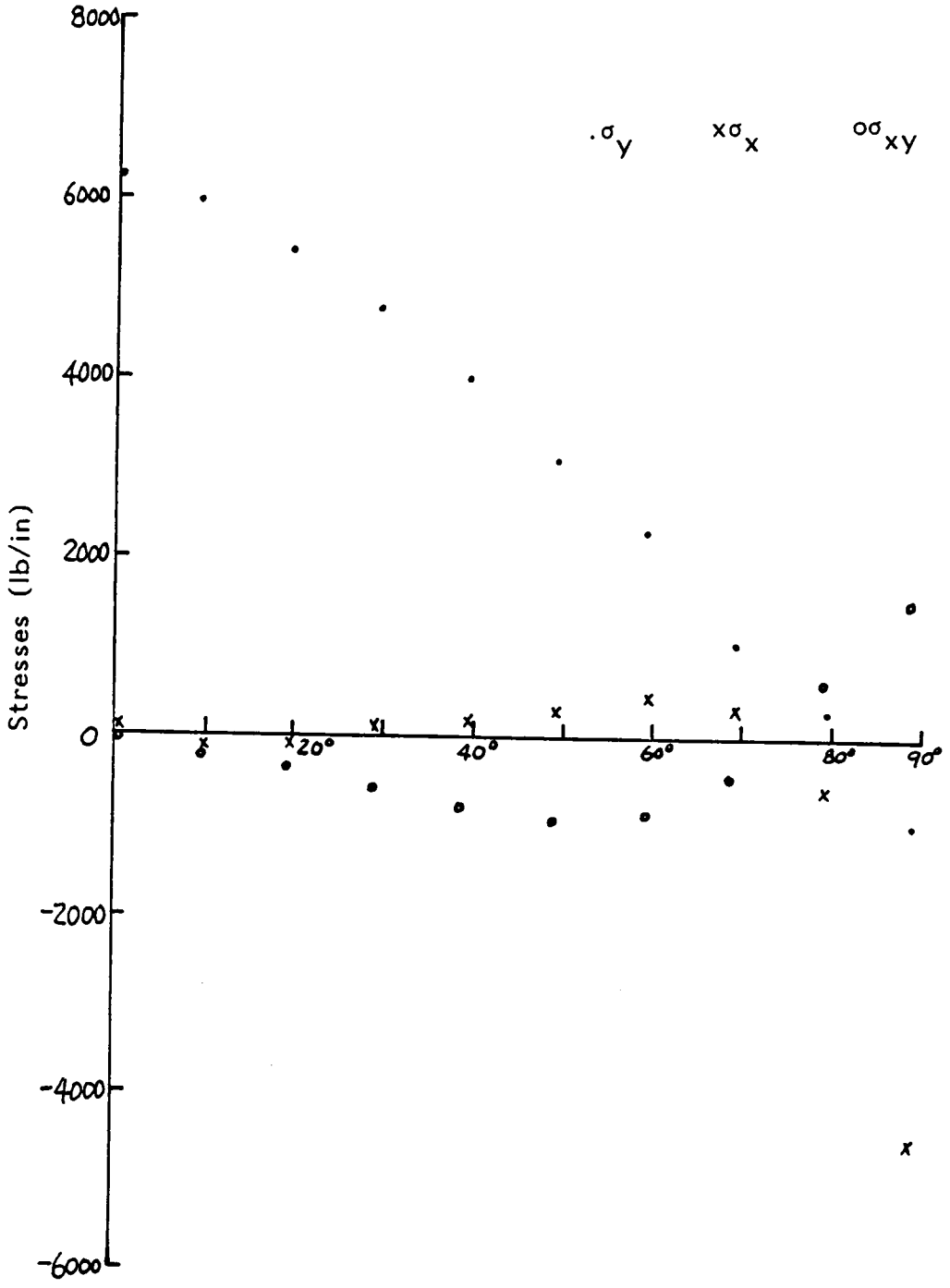

Fig. 27 Stresses Around the Notch of First Quarter for T300/5208 with an Elliptical Hole a=3/16", b=1.2" Layup $[0/\pm 45/90]_s$

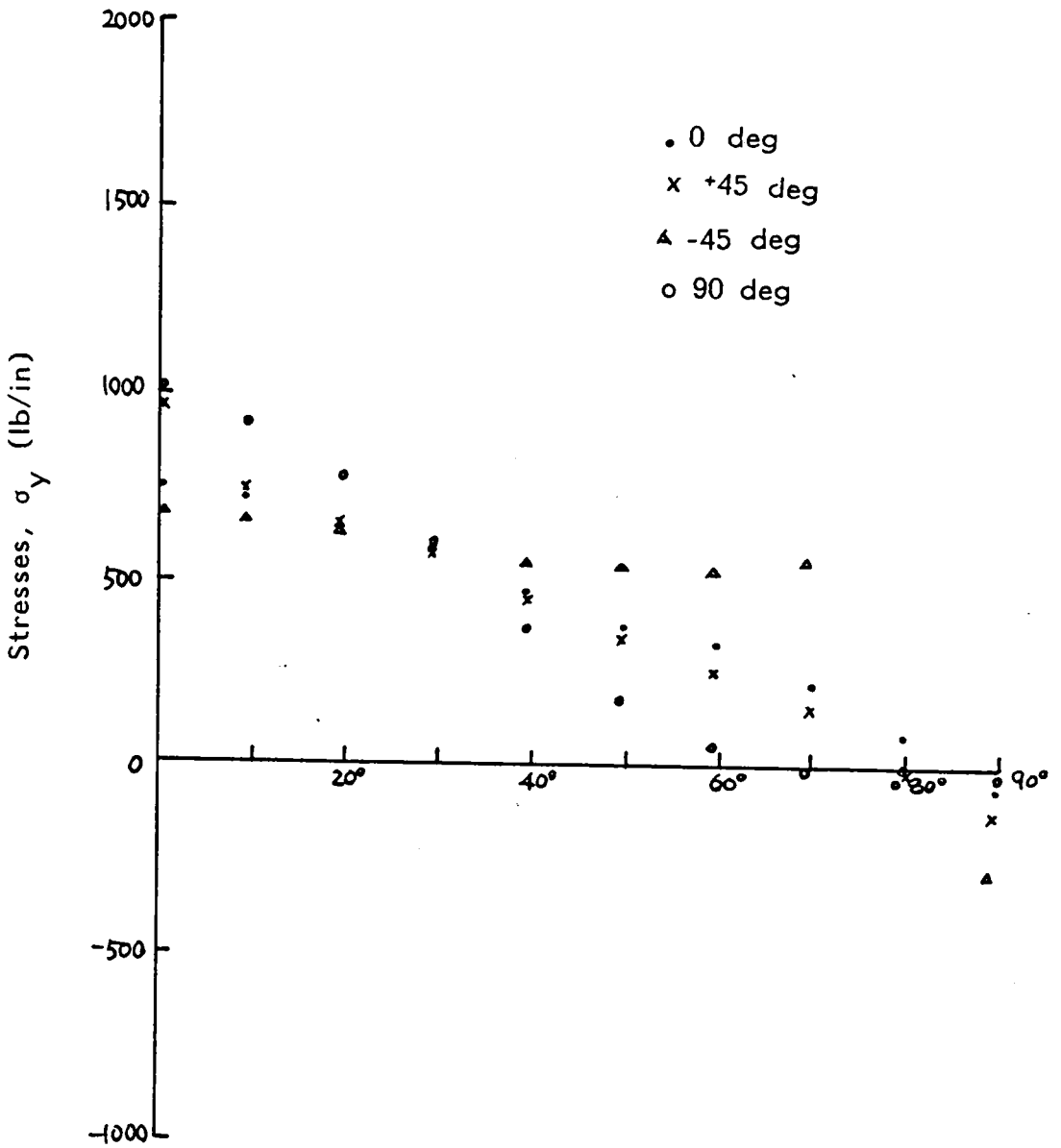

Fig. 28 Stresses Around the Notch of First Quarter for T300/5208 with an Elliptical Hole a=3/16", b=1.2" one ply 0, 45, -45, 90

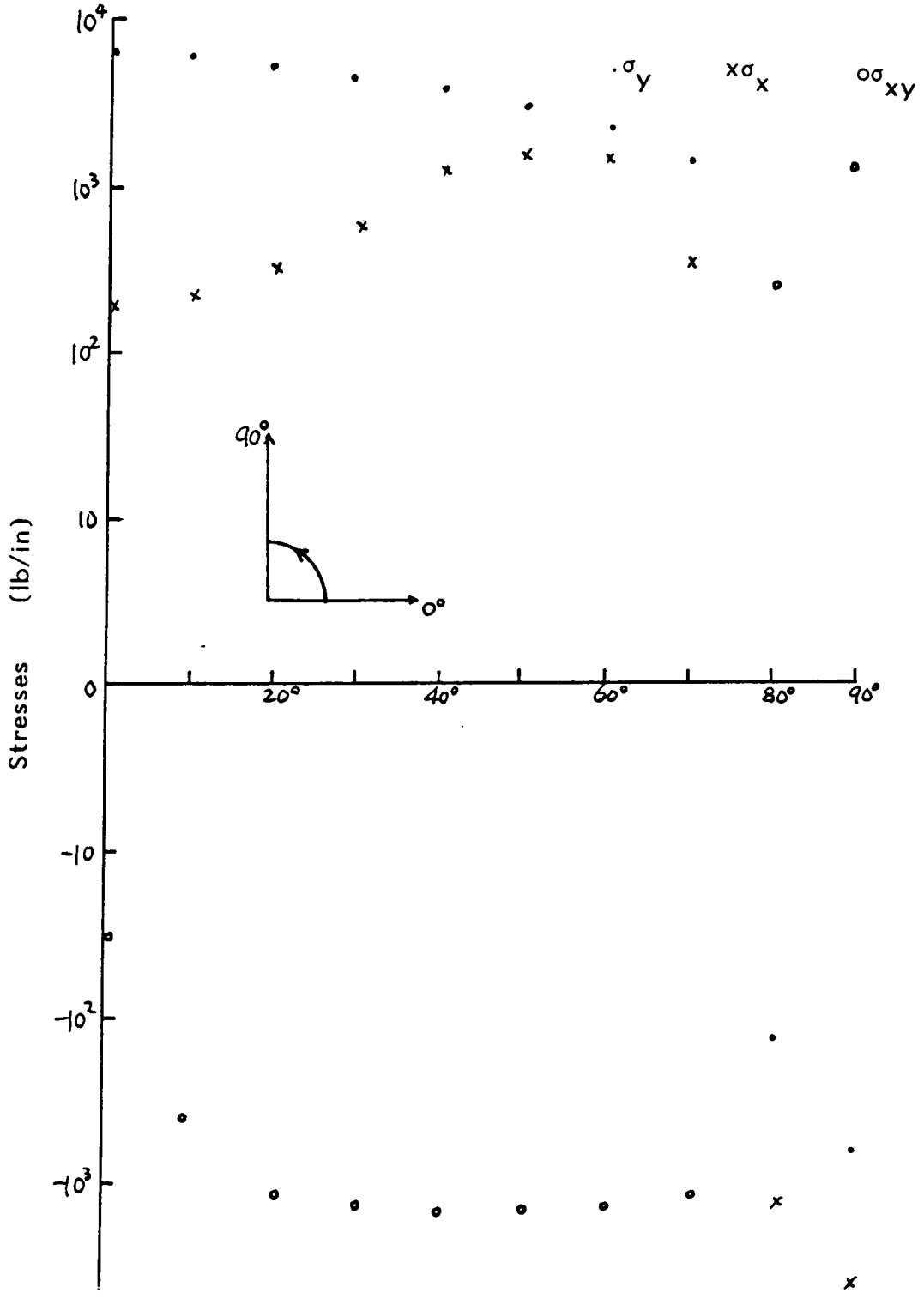

Fig. 29 Log Stresses Around the Notch of First Quarter for T300/5208 with an Elliptical Hole a=3/16", b=0.28" Layup $[0_2/\pm 45]_s$

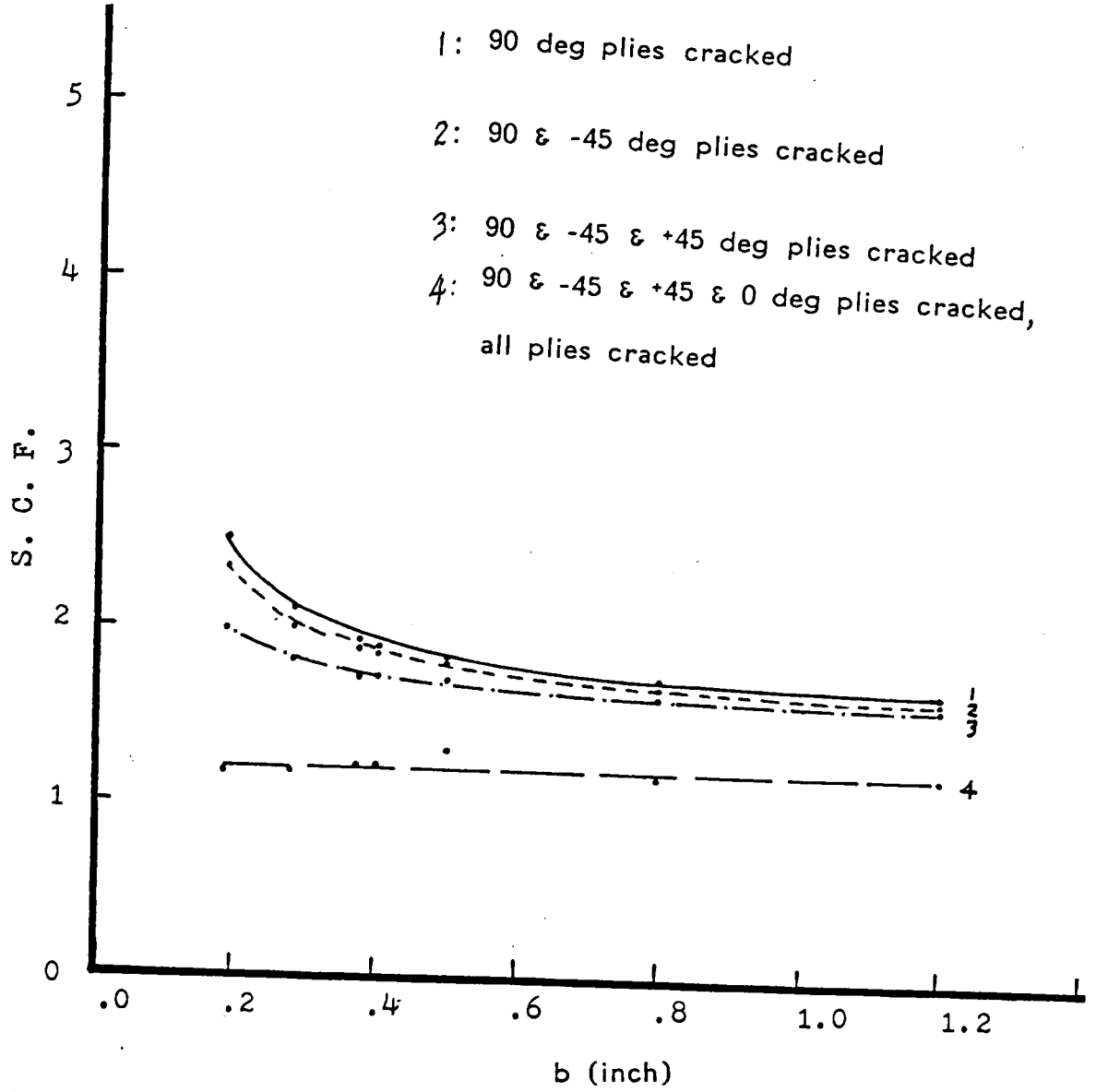

Fig. 30 SCF vs. Longitudinal Semi-axis of Elliptic Hole, b, and with Moduli Reduction for T300/5208 Laminate with Layup $[0/\pm45/90]_s$

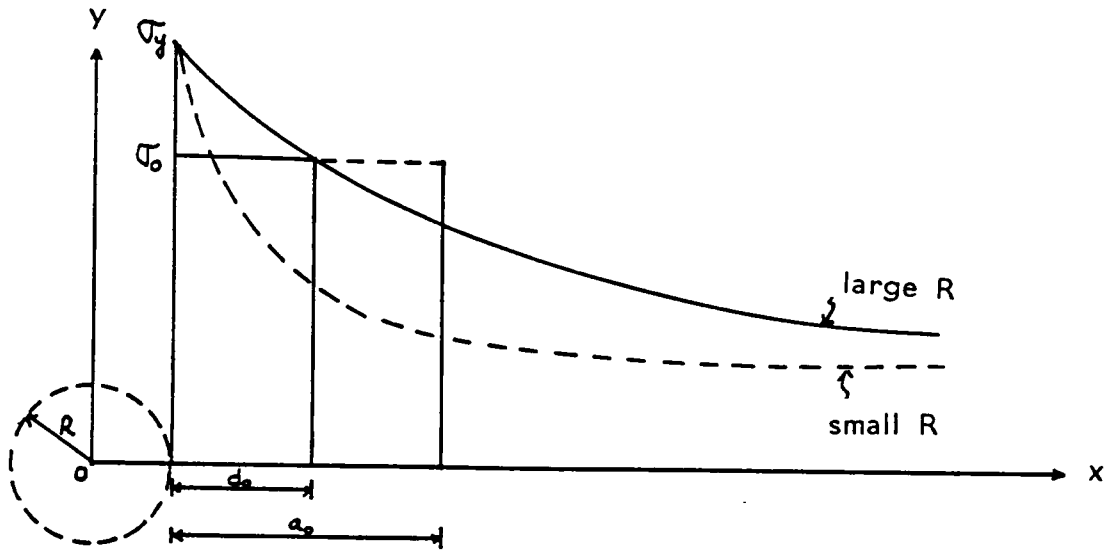

a. Stress Distribution at Failure to Determine d_o and a_o

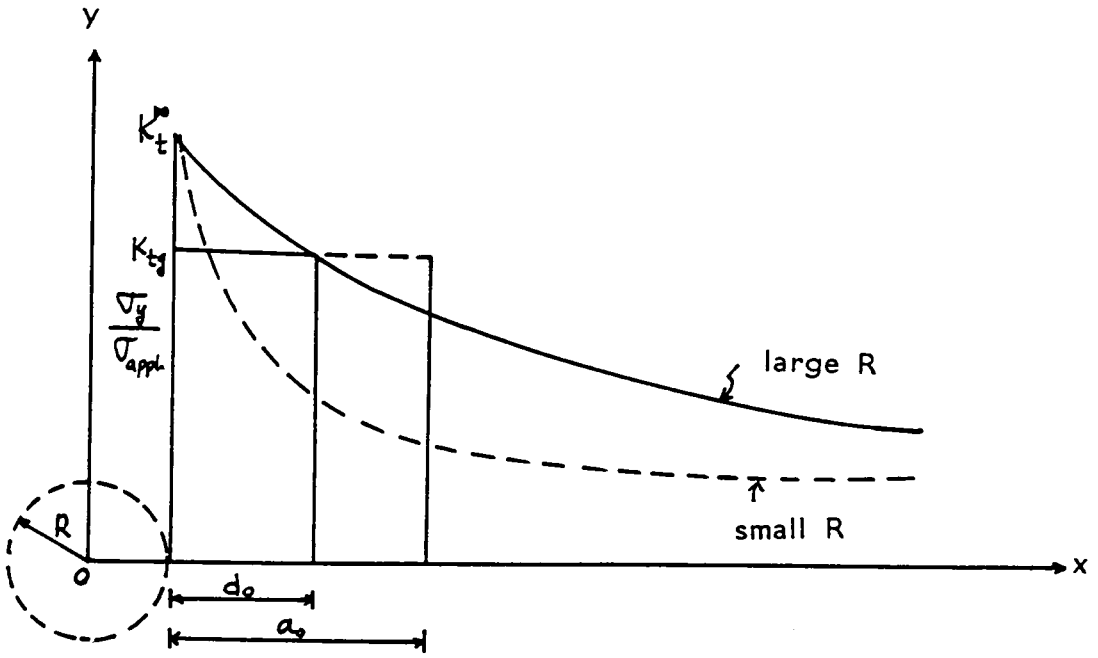

b. Normalized Stress Distribution at Failure to Determine d_o and a_o

Fig. 31 The Point Stress and Average Stress Criteria in WN Fracture Model

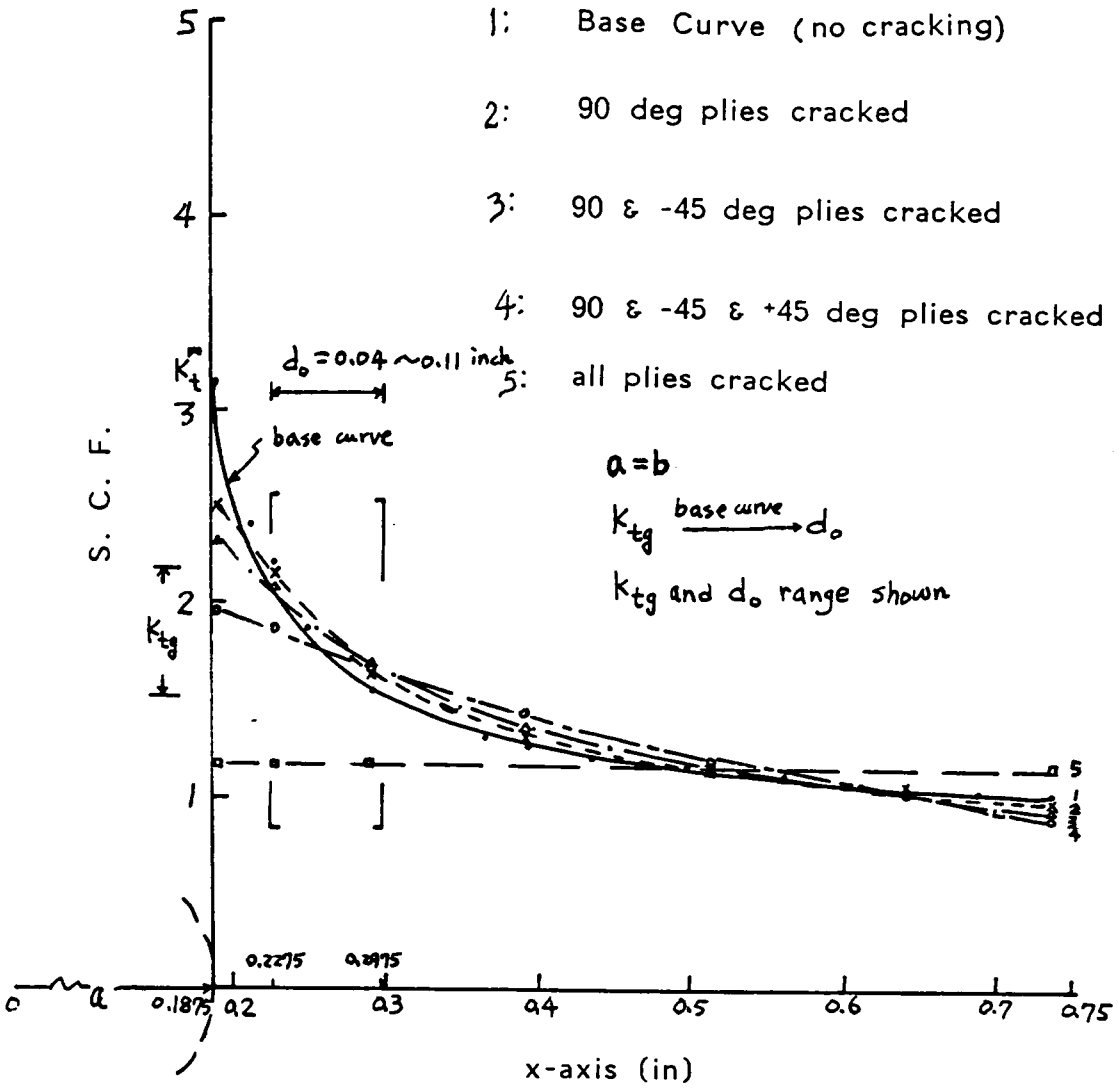

Fig. 32 Normalized Stress (σ_y) along x-axis and the Determination of d_o from K_{tg} for T300/5208 $[0/\pm45/90]_s$ Layup

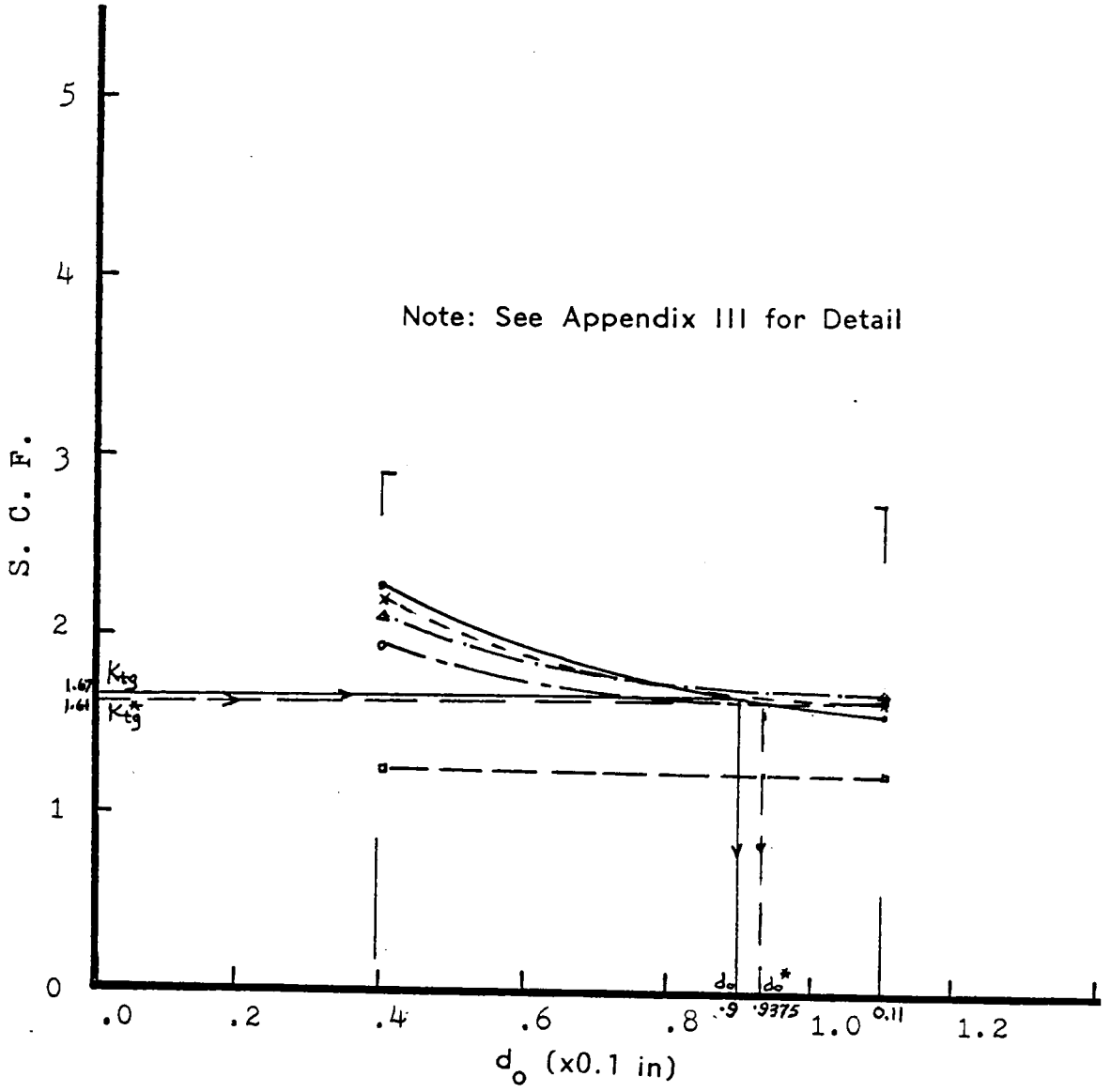

Fig. 33 Enlarged Scale of Important Portion in Fig. 31 to Determine d_o from K_{tg}

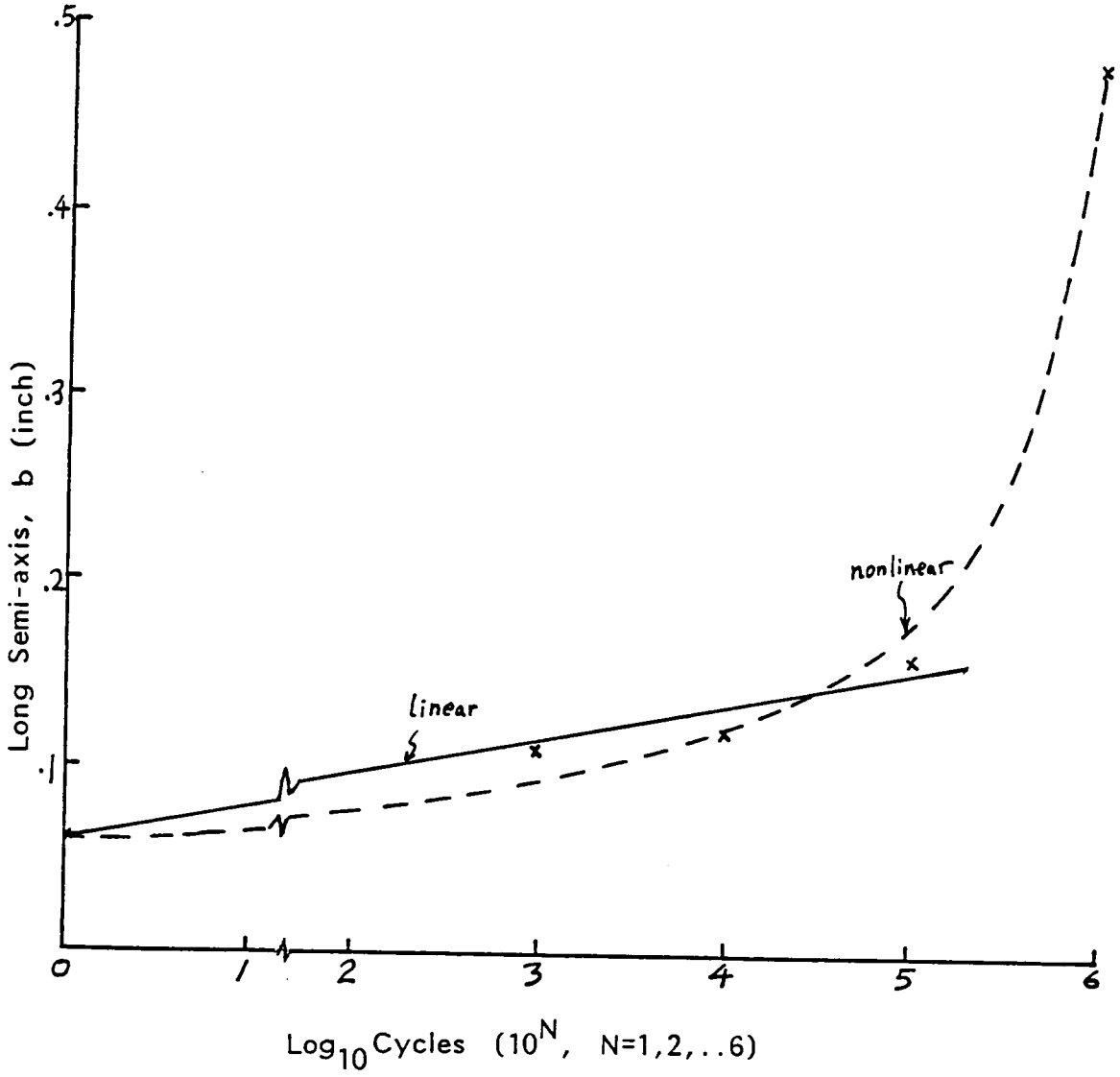

Fig. 34 Longitudinal Semi-axis of Elliptic Hole, b vs Log Cycles for T300/934 $[0/\pm 45/0]_{2s}$ Layup

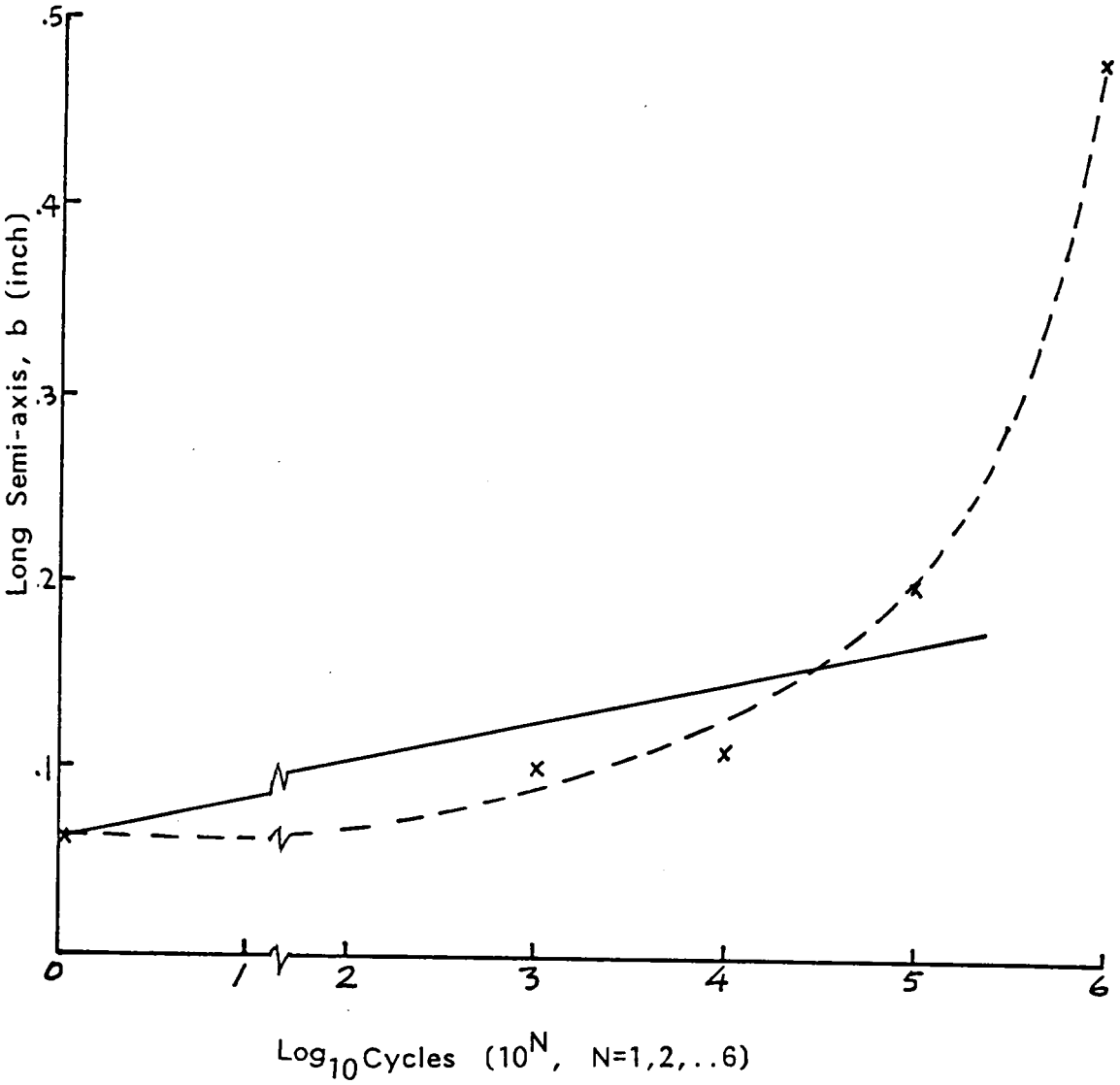

Fig. 35 Longitudinal Semi-axis of Elliptic Hole, b vs Log Cycles for T300/934 $[0/\pm45/90]_{2s}$ Layup

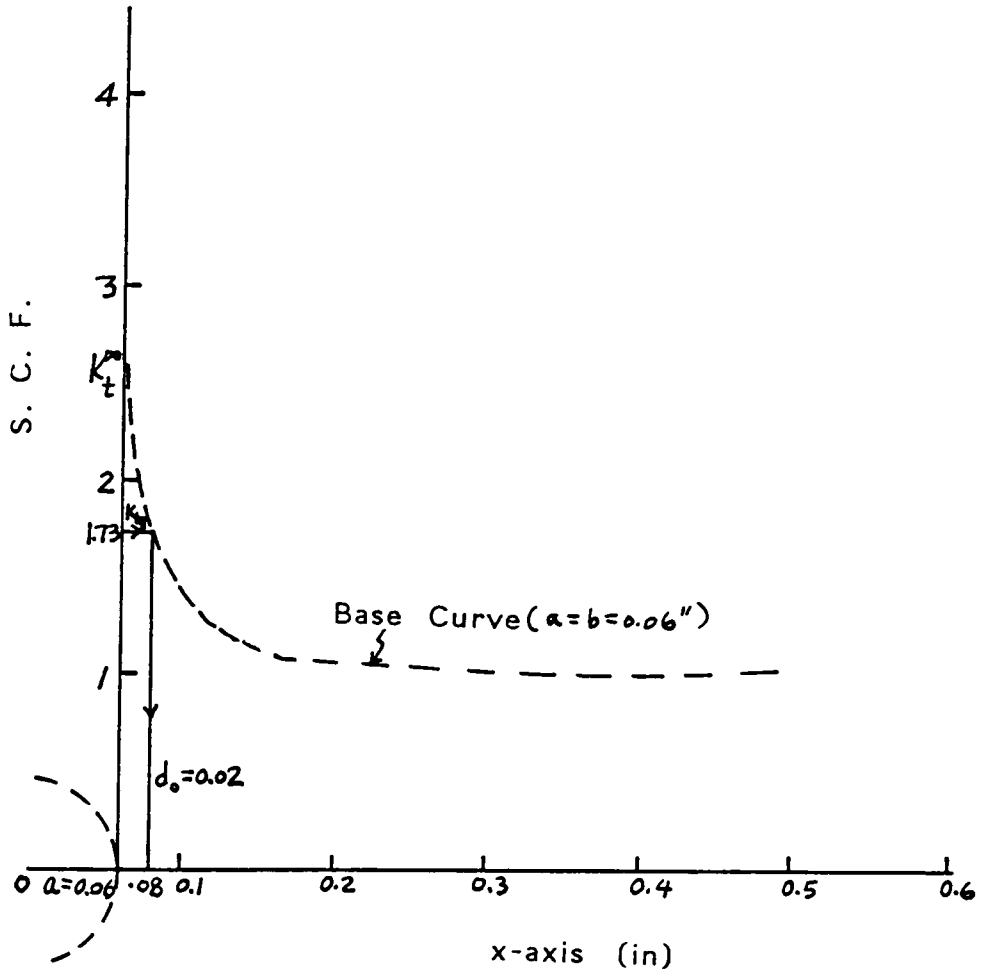

Fig. 36 Normalized Stress (σ_y) along x-axis and the Determination of d_o from K_{tg} for T300/934 $[0/\pm45/0]_{2s}$ Layup

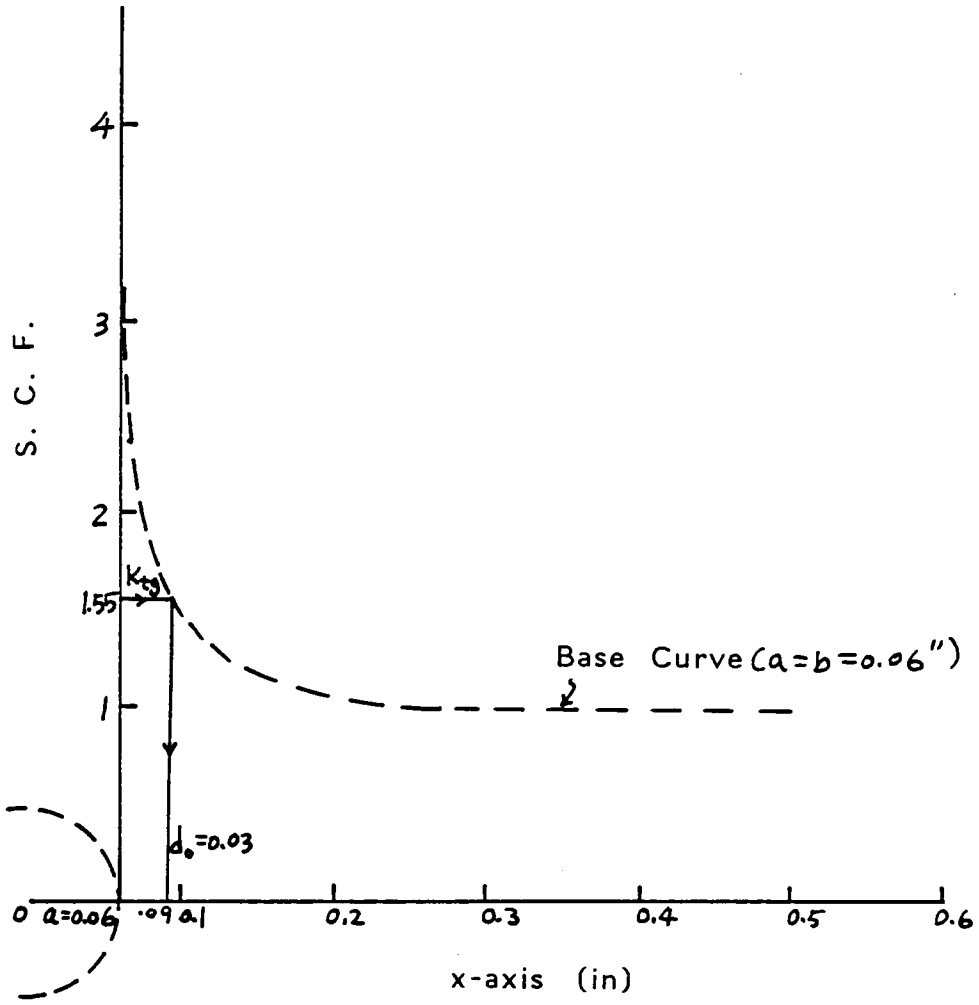

Fig. 37 Normaized Stress (σ_y) along x-axis and the Determination of d_o from K_{tg} for T300/934 $[0/\pm45/90]_{2s}$ Layup

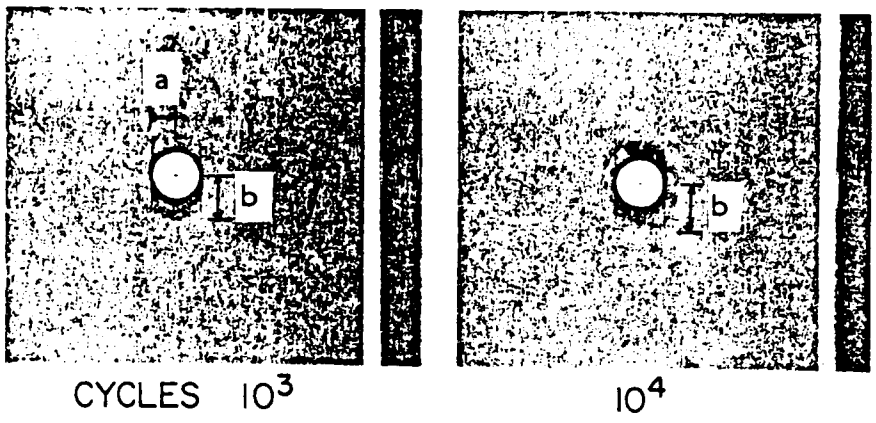

CYCLES 10^3 10^4

$a = 0.06''$ $a = 0.06''$

$b = 0.11''$ $b = 0.12''$

Fig. 38 The Measurement of Major Semi-axis, b, for T300/934 [0/±45/0] at the Specific Cycles of Loading

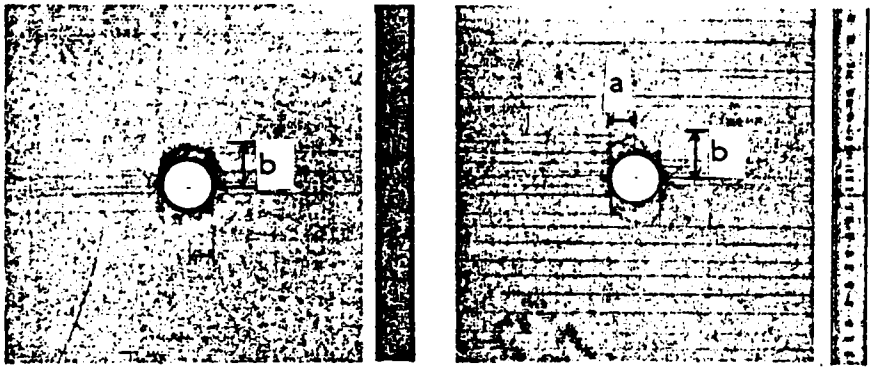

CYCLES 10^3 10^4

$a = 0.06''$ $a = 0.06''$

$b = 0.10''$ $b = 0.11''$

Fig. 39 The Measurement of Major Semi-axis, b, for T300/934 [0/±45/90] at the Specific Cycles of Loading

Table 1. Stiffnesses for Graphite/Epoxy T300/5208 Lamminates

No.	Layups	Plies	A_{11}	A_{12}	A_{16}	A_{22}	A_{26}	A_{66}
1	$[0_8]_t$	8	1054440	16820	0	59740	0	41586
2	$[0/90]_{2s}$	8	557090	16820	0	557090	0	41586
3	$[0/\pm45/90]_s$	8	442685	131138	0	442685	0	155904
4	$[0/\pm45/90_4]_s$	14	487490	143753	0	1233515	0	187094
5	$[0/\pm45/90_8]_s$	22	547230	160573	0	2287955	0	228680
6	$[0_4/\pm45/90]_s$	14	1233515	143753	0	487490	0	187094
7	$[0_8/\pm45/90]_s$	22	2287955	160573	0	547230	0	228680
8	$[0/\pm45_2/90]_s$	12	606825	253866	0	606825	0	291015
9	$[0/\pm45_4/90]_s$	20	935105	499322	0	935105	0	561237
10	$[0/45_2/90]_s$	8	442685	131138	124323	442685	124323	155904
11	$[0/45_4/90]_s$	12	606825	253866	248646	606825	248646	291015
12	$[0_2/\pm45]_s$	8	691360	131138	0	194010	0	155904
13	[0]	1	131805	2103	0	7468	0	5198
14	[-45]	1	41035	30682	-31081	41035	-31081	33778
15	[+45]	1	41035	30682	31081	41035	31081	33778
16	[90]	1	7468	2103	0	131805	0	5198

Notes: 1. Each ply is 0.005 inch thick

2. The unit of stiffness A_{ij} is lb/in

Table 2. Graphite/Epoxy T300/5208 Coupons 1.5"x8" with a Centered Circular Hole Dia=3/8", Total Nodes=332, Elements=95

No.	Layups	Total Plies	Max Displacement Δl (inch)	Max Stress σ_y (lb/in)	SCF
1	$[0_8]_t$	8	0.239668	0.896601 E4	2.58
2	$[0/90]_{2s}$	8	0.026249	0.151108 E5	4.34
3	$[0/\pm45/90]_s$	8	0.0354944	0.108267 E5	3.11
4	$[0/\pm45/90_4]_s$	14	0.0182147	0.200396 E5	3.29
5	$[0/\pm45/90_8]_s$	22	0.0178664	0.407125 E5	4.25
6	$[0_4/\pm45/90]_s$	14	0.0532301	0.182233 E5	2.99
7	$[0_8/\pm45/90]_s$	22	0.0734037	0.278502 E5	2.91
8	$[0/\pm45_2/90]_s$	12	0.0428343	0.150359 E5	2.88
9	$[0/\pm45_4/90]_s$	20	0.053348	0.233788 E5	2.69
10	$[0/45_2/90]_s$	8	0.0454244	0.137247 E5	3.94
11	$[0/45_4/90]_s$	12	0.0596081	0.201470 E5	3.86
12	$[0_2/\pm45]_s$	8	0.0842416	0.883823 E4	2.53
13	[0]	1	0.239684	0.112075 E4	2.58
14	[-45]	1	0.159766	0.157455 E4	3.62
15	[45]	1	0.1549	0.111432 E4	2.56
16	[90]	1	0.142629	0.23373 E4	5.37

Notes: 1. Applied uniform stress 600 MPa (87000psi)

2. Max displacement at remote loading points

3. Max stress σ_y at (0.00353",0.00331") away from the

hole edge, (0.1875",0")

4. $[-45_8]$ max stress=0.125962 E5; $[45_8]$ max stress=0.89146 E4; $[90_8]_t$ max stress=0.186982 E5
5. SCF stands for stress concentration factor

Table 3. Graphite/Epoxy T300/5208 Coupons 1.5"x4" with a Centered Circular Hole Dia=3/8", Total Nodes=264, Elements=75

No.	Layups	Total Plies	Max Displacement Δl (inch)	Max Stress σ_y (lb/in)	SCF
1	$[0_8]_t$	8	0.122659	0.896602 E4	2.58
2	$[0/90]_{2s}$	8	0.014252	0.152466 E5	4.38
3	$[0/\pm45/90]_s$	8	0.0182659	0.108269 E5	3.11
4	$[0/45_2/90]_s$	8	0.0250203	0.137256 E5	3.94
5	$[0/45_4/90]_s$	12	0.0328529	0.201471 E5	3.86

Notes: 1. Applied uniform stress 600 MPa (87000psi)

2. Max displacement at remote loading points
3. Max stress σ_y at (0.00353",0.00331") away from the hole edge, (0.1875",0.0")
4. This is half length of the previous case, other conditions are the same
5. SCF has no change, i.e., length does not influence SCF
6. The stress and displacement fields have large change at the remote loading points
7. St. Vernant's Principle can explain this phenomena

Table 4. Graphite/Epoxy T300/5208 Coupons 3"x8" with a Centered Circular Hole Dia=3/8", Total Nodes=332, Elements=95

No.	Layups	Total Plies	Max Displacement Δl (inch)	Max Stress σ_y (lb/in)	SCF
1	$[0_8]_t$	8	--------	0.823384 E4	2.37
2	$[0/90]_{2s}$	8	--------	0.145243 E5	4.17
3	$[0/\pm45/90]_s$	8	--------	0.102002 E5	2.93
4	$[0/\pm45_2/90]_s$	12	--------	0.140653 E5	2.69
5	$[0/45_2/90]_s$	8	--------	0.141387 E5	4.06
6	$[0/45_4/90]_s$	12	--------	0.208388 E5	3.99

Notes: 1. Applied uniform stress 600 MPa (87000psi)

2. Max displacement at remote loading points

3. Max stress σ_y at (0.00353",0.00331") away from the hole edge, (0.1875",0.0")

4. This is double width of the first case with hole dia. and other conditions unchanged

5. Width change influences SCF slightly

6. $[-45_8]$ max stress=0.128189 E5; $[45_8]$ max stress=0.76822 E4; $[90_8]$ max stress=0.18278E5

Table 5. Graphite/Epoxy T300/5208 Coupons 1.5"x8" with a Centered Elliptical Hole a=0.1875" b=0.28", Nodes=332, Elements=95

No.	Layups	Total Plies	Max Displacement Δl (inch)	Max Stress σ_y (lb/in)	SCF
1	$[0_8]_t$	8	0.240983	0.759887 E4	2.18
2	$[0/90]_{2s}$	8	0.0263677	0.115844 E5	3.33
3	$[0/\pm45/90]_s$	8	0.0356767	0.873614 E4	2.51
4	$[0/\pm45/90_4]_s$	14	0.0213508	0.181758 E5	2.98
5	$[0/\pm45/90_8]_s$	22	0.0179462	0.311862 E5	3.26
6	$[0_4/\pm45/90]_s$	14	0.0535091	0.148421 E5	2.44
7	$[0_8/\pm45/90]_s$	22	0.0737927	0.228481 E5	2.39
8	$[0/\pm45_2/90]_s$	12	0.0430598	0.123391 E5	2.36
9	$[0/\pm45_4/90]_s$	20	0.0536377	0.195112 E5	2.24
10	$[0/45_2/90]_s$	8	0.0457003	0.110720 E5	3.18
11	$[0/45_4/90]_s$	12	0.0599876	0.165024 E5	3.16
12	$[0_2/\pm45]_s$	8	0.0847028	0.748689 E4	2.15
13	[0]	1	0.240999	0.949856 E3	2.18
14	[-45]	1	0.160848	0.134289 E4	3.09
15	[45]	1	0.155673	0.884514 E3	2.03
16	[90]	1	0.0143144	0.173817 E4	4.00

Notes: 1. Applied uniform stress 600 MPa (87000psi)

2. Max displacement at remote loading points

3. Max stress σ_y at (0.0141",0.00331") away from the edge

Table 6. Graphite/Epoxy T300/5208 Coupons 1.5"x8" with a Centered Elliptical Hole a=0.1875" b=0.375",Nodes=332, Elements=95

No.	Layups	Total Plies	Max Displacement Δl (inch)	Max Stress σ_y (lb/in)	SCF
1	$[0_8]_t$	8	0.24241	0.710511 E4	2.04
2	$[0/90]_{2s}$	8	0.0265293	0.109211 E5	3.14
3	$[0/\pm45/90]_s$	8	0.0358846	0.790634 E4	2.27
4	$[0/\pm45/90_4]_s$	14	0.0214735	0.164847 E5	2.71
5	$[0/\pm45/90_8]_s$	22	0.0180518	0.286429 E5	2.99
6	$[0_4/\pm45/90]_s$	14	0.0538219	0.136127 E5	2.24
7	$[0_8/\pm45/90]_s$	22	0.0742253	0.210667 E5	2.20
8	$[0/\pm45_2/90]_s$	12	0.0433122	0.111589 E5	2.14
9	$[0/\pm45_4/90]_s$	20	0.0539555	0.176927 E5	2.03
10	$[0/45_2/90]_s$	8	0.0460032	0.104582 E5	3.01
11	$[0/45_4/90]_s$	12	0.0603962	0.156229 E5	2.99
12	$[0_2/\pm45]_s$	8	0.0852091	0.694139 E4	1.99
13	[0]	1	0.242426	0.888137 E3	2.04
14	[-45]	1	0.161993	0.126783 E4	2.91
15	[45]	1	0.156485	0.808762 E3	1.86
16	[90]	1	0.0144191	0.169794 E4	3.90

Notes: 1. Applied uniform stress 600 MPa (87000psi)

2. Max displacement at remote loading points

3. Max stress σ_y at (0.001875",0.008749") away from the edge

Table 7. Graphite/Epoxy T300/5208 Coupons 1.5"x8" with a Centered Elliptical Hole a=0.1875" b=0.4",Nodes=332, Elements=95

No.	Layups	Total Plies	Max Displacement Δl (inch)	Max Stress σ_y (lb/in)	SCF
1	$[0_8]_t$	8	0.242782	0.698501 E4	2.01
2	$[0/90]_{2s}$	8	0.0265665	0.105041 E5	3.02
3	$[0/\pm45/90]_s$	8	0.0359383	0.771487 E4	2.22
4	$[0/\pm45/90_4]_s$	14	0.0215039	0.159383 E5	2.62
5	$[0/\pm45/90_8]_s$	22	0.0180768	0.275687 E5	2.88
6	$[0_4/\pm45/90]_s$	14	0.0539032	0.133064 E5	2.18
7	$[0_8/\pm45/90]_s$	22	0.0743378	0.206154 E5	2.15
8	$[0/\pm45_2/90]_s$	12	0.0433783	0.109234 E5	2.09
9	$[0/\pm45_4/90]_s$	20	0.054039	0.173681 E5	2.00
10	$[0/45_2/90]_s$	8	0.0460786	0.101633 E5	2.92
11	$[0/45_4/90]_s$	12	0.0604981	0.152188 E5	2.92
12	$[0_2/\pm45]_s$	8	0.085342	0.683386 E4	1.96
13	[0]	1	0.242798	0.873125 E3	2.01
14	[-45]	1	0.162277	0.124133 E4	2.85
15	[45]	1	0.156692	0.79156 E3	1.82
16	[90]	1	0.014439	0.162024 E4	3.72

Notes: 1. Applied uniform stress 600 MPa (87000psi)

2. Max displacement at remote loading points

3. Max stress σ_y at (0.001875",0.009385") away from the edge

Table 8. Graphite/Epoxy T300/5208 Coupons 1.5"x8" with a Centered Elliptical Hole a=0.1875" b=0.5", Nodes=332, Elements=95

No.	Layups	Total Plies	Max Displacement Δl (inch)	Max Stress σ_y (lb/in)	SCF
1	$[0_8]_t$	8	0.244293	0.665502 E4	1.91
2	$[0/90]_{2s}$	8	0.0267448	0.955703 E4	2.75
3	$[0/\pm45/90]_s$	8	0.0361602	0.719931 E4	2.07
4	$[0/\pm45/90_4]_s$	14	0.0216363	0.145928 E5	2.40
5	$[0/\pm45/90_8]_s$	22	0.0181925	0.250721 E5	2.62
6	$[0_4/\pm45/90]_s$	14	0.0542360	0.124833 E5	2.05
7	$[0_8/\pm45/90]_s$	22	0.0747972	0.193958 E5	2.03
8	$[0/\pm45_2/90]_s$	12	0.0436491	0.102739 E5	1.97
9	$[0/\pm45_4/90]_s$	20	0.0543805	0.164554 E5	1.89
10	$[0/45_2/90]_s$	8	0.0463868	0.949852 E4	2.73
11	$[0/45_4/90]_s$	12	0.0609096	0.143012 E5	2.74
12	$[0_2/\pm45]_s$	8	0.0858802	0.654046 E4	1.88
13	[0]	1	0.244309	0.831876 E3	1.91
14	[-45]	1	0.163403	0.117821 E4	2.71
15	[45]	1	0.157545	0.731406 E3	1.68
16	[90]	1	0.0145642	0.145752 E4	3.35

Notes: 1. Applied uniform stress 600 MPa (87000psi)

2. Max displacement at remote loading points

3. Max stress σ_y at (0.001875",0.01173") away from the edge

Table 9. Graphite/Epoxy T300/5208 Coupons 1.5"x8" with a Centered Elliptical Hole a=0.1875" b=0.8",Nodes=298, Elements=85

No.	Layups	Total Plies	Max Displacement Δl (inch)	Max Stress σ_y (lb/in)	SCF
1	$[0_8]_t$	8	0.2535	0.617671 E4	1.77
2	$[0/90]_{2s}$	8	0.0284035	0.782478 E4	2.25
3	$[0/\pm45/90]_s$	8	0.038077	0.649940 E4	1.87
4	$[0/\pm45/90_4]_s$	14	0.0230463	0.124659 E5	2.05
5	$[0/\pm45/90_8]_s$	22	0.0194691	0.207913 E5	2.17
6	$[0_4/\pm45/90]_s$	14	0.0568521	0.113074 E5	1.86
7	$[0_8/\pm45/90]_s$	22	0.0782063	0.176311 E5	1.84
8	$[0/\pm45_2/90]_s$	12	0.0458466	0.946611 E4	1.81
9	$[0/\pm45_4/90]_s$	20	0.0570038	0.154192 E5	1.77
10	$[0/45_2/90]_s$	8	0.0458248	0.817368 E4	2.35
11	$[0/45_4/90]_s$	12	0.0602274	0.123973 E5	2.37
12	$[0_2/\pm45]_s$	8	0.087448	0.614592 E4	1.77
13	[0]	1	0.248762	0.772096 E3	1.77
14	[-45]	1	0.166526	0.103913 E4	2.39
15	[45]	1	0.160159	0.675495 E3	1.55
16	[90]	1	0.0148801	0.113916 E4	2.62

Notes: 1. Applied uniform stress 600 MPa (87000psi)

2. Max displacement at remote loading points

3. Max stress σ_y at (0.001875",0.02635") away from the edge

Table 10. Graphite/Epoxy T300/5208 Coupons 1.5"x8" with a Centered Elliptical Hole a=0.1875" b=1.2", Nodes=298, Elements=85

No.	Layups	Total Plies	Max Displacement Δl (inch)	Max Stress σ_y (lb/in)	SCF
1	$[0_8]_t$	8	0.2596	0.593054 E4	1.70
2	$[0/90]_{2s}$	8	0.02894	0.692228 E4	1.99
3	$[0/\pm45/90]_s$	8	0.03898	0.616314 E4	1.77
4	$[0/\pm45/90_4]_s$	14	0.0235567	0.114198 E5	1.88
5	$[0/\pm45/90_8]_s$	22	0.0198593	0.186394 E5	1.95
6	$[0_4/\pm45/90]_s$	14	0.0582026	0.107202 E5	1.76
7	$[0_8/\pm45/90]_s$	22	0.08007	0.167478 E5	1.75
8	$[0/\pm45_2/90]_s$	12	0.0469466	0.908671 E4	1.74
9	$[0/\pm45_4/90]_s$	20	0.0583733	0.149442 E5	1.72
10	$[0/45_2/90]_s$	8	0.04696	0.743726 E4	2.14
11	$[0/45_4/90]_s$	12	0.0617235	0.113106 E5	2.17
12	$[0_2/\pm45]_s$	8	0.0896431	0.593962 E4	1.71
13	[0]	1	0.254866	0.741325 E3	1.70
14	[-45]	1	0.170565	0.95884 E3	2.20
15	[45]	1	0.163846	0.679173 E3	1.56
16	[90]	1	0.0153575	0.970891 E3	2.23

Notes: 1. Applied uniform stress 600 MPa (87000psi)

2. Max displacement at remote loading points

3. Max stress σ_y at (0.001875",0.03954") away from the edge

Table 11. Experimental Fatigue Data for T300/5208 Quasi-isotropic Laminates

Cycles	% Increase of S_n	S_n (Ksi)	Crack (in) C	K_{tg}	a (in)	b (in)
10E0	0.00	37	0.000	1.92	0.1875	0.1875
10E1	11.5	41	0.258	1.73	0.1875	0.5
10E3	18.0	44	0.354	1.61	0.1875	0.8
10E4	24.4	46	0.524	1.54	0.1875	1.2
10E5	29.6	48	0.635	1.48	0.1875	1.65

Notes: 1. S_n: Residual strength calculated over gross area, i.e., observed data

2. C: Measured crack length at 0 degree
3. K_{tg}: SCF at 0.06 inch away from the hole edge
4. Short semi-axis of elliptic hole, a, remains unchanged; long semi-axis of elliptic hole, b, enlarges with increasing cycles and b is the effective notch which includes the hole and the damaged area

Table 12. Moduli Reduction for T300/5208 $[0/\pm45/90]_s$ Laminates

Plies Cracked	A_{11}	A_{12}	A_{16}	A_{22}	A_{26}	A_{66}
90	442685	126933	0	179075	0	155904
-45	442685	65569	0	97005	0	155904
+45	442685	4205	0	14935	0	155904
0	442685	1	0	1	0	155904

Notes: 1. Plies cracked means first 90 degree plies cracked with moduli reduction, then 90 and -45 degree plies cracked with more moduli reduction and so on.

2. To avoid singularity of the stiffness matrix via FEM, set value 1 instead of zero for A_{12} and A_{22} with all plies cracked.

Table 13. SCF and Displacement of Notched T300/5208 $[0/\pm45/90]_s$ Laminates with both Geometry and Moduli Changes

Hole Radius	Ply Cracked	Max Displacement Δl (in)	Max Stress σ_y	SCF
0.1875"	90	0.0998133	0.869582E4	2.50
	-45	0.162891	0.81409E4	2.34
	+45	0.951125	0.687725E4	1.98
	0	0.140641E5	0.413523E4	1.19
0.28"	90	0.100361	0.739051E4	2.12
	-45	0.163802	0.705769E4	2.03
	+45	0.956668	0.637531E4	1.83
	0	0.141371E5	0.416517E4	1.20
0.375"	90	0.100962	0.683048E4	1.96
	-45	0.164794	0.661331E4	1.90
	+45	0.962591	0.616664E4	1.77
	0	0.142178E5	0.440157E4	1.26
0.4"	90	0.10112	0.672865E4	1.93
	-45	0.165055	0.653419E4	1.88
	+45	0.964137	0.613071E4	1.76
	0	0.142388E5	0.443315E4	1.27

0.5"	90	0.101762	0.645079E4	1.85
	-45	0.166106	0.631993E4	1.82
	+45	0.970295	0.601554E4	1.73
	0	0.143261E5	0.462214E4	1.33
0.8"	90	0.103671	0.610895E4	1.76
	-45	0.169219	0.602998E4	1.73
	+45	0.988070	0.579937E4	1.67
	0	0.145477E5	0.41575E4	1.19
1.2"	90	0.106241	0.592263E4	1.70
	-45	0.173414	0.584027E4	1.68
	+45	1.01254	0.567321E4	1.63
	0	0.148935E5	0.421274E4	1.21

Notes: 1. SCF decreases with both the moduli reduction (plies cracked) and the slenderness of elliptic hole

2. Hole radius means the semi-axis of elliptic hole parallel to the loading direction

3. At last 0 degree plies cracked, we see the maximum displacement reaches the order of E5 inch, i.e., the rupture of the specimen

4. At all plies cracked A_{11} still unchanged by the assumption that in the matrix mode of failure transverse stiffnesses reduced to zero, i.e., A_{22} and A_{12}=0. It is reasonable to

have maximum displacement reaches 10E5 inch, since not in the fiber mode of failure

Table 14. The Notched Strength for Quasi-isotropic Laminate via the WEK Model

Semi-axis (in)		Calculated Notched	Multiplied by Finite
a=	b=	Strength (Ksi)	Width Correction Factor (Ksi)
0.0	0.0	79.75	
0.1875	0.1875	37	
0.1875	0.5	31.44	41.77
0.1875	0.8	29.57	58.85
0.1875	1.2	27.81	247.24

Notes: 1. Calculated notched strength decreases while b increasing

2. Modified by finite width correction factor, the calculated notched strength becomes very bad and unacceptable

Table 15. SCF for an Infinite Orthotropic Laminate with a Central Circular Hole from Eq. (4)

Layups	SCF
1. $[0_8]_t$	2.37
2. $[0/90]_{2s}$	4.91
3. $[0/\pm45/90]_s$	3.00
4. $[0/\pm45/90_4]_s$	3.99
5. $[0/\pm45/90_8]_s$	4.65
6. $[0_4/\pm45/90]_s$	2.88
7. $[0_8/\pm45/90]_s$	2.78
8. $[0/\pm45_2/90]_s$	2.70
9. $[0/\pm45_4/90]_s$	2.46
10. $[0/45_2/90]_s$	3.00
11. $[0/45_4/90]_s$	2.70
12. $[0_2/\pm45]_s$	2.33
13. [0]	2.37
14. [-45]	2.02
15. [+45]	2.02
16. [90]	6.75

Notes: 1. Switch A_{11} with A_{22} in Table 1 while using Eq. (4) to calculate SCF

2. SCF in this Table for infinite orthotropic laminate has some difference from that in Table 2 which obtained via FEM for

finite width

3. A_{16} and A_{26} are not involved in Eqn. (4), so that cases 3, 10; cases 8, 11; cases 14, 15 have same SCF
4. SCF for elliptic holes all via FEM

Table 16. Notched Strength for T300/5208 Quasi-isotropic Laminate with Plies Cracked

Plies Cracked	K_t^{∞}	d_o (in)	Prdct (ksi) Strength	K_{tg}*	d_o* (in)	S_n (Ksi)
N=10E0						37
b=0.1875"						
90	2.50	0.05	36.73	1.92	0.052	
-45	2.34	0.05	36.50	1.92	0.052	
+45	1.98	0.05	35.99	1.92	0.052	
0	1.19	0.05	34.91	1.92	0.052	
N=10E1						41
b=0.5"						
90	1.85	0.08	41.42	1.73	0.09	
-45	1.82	0.08	41.35	1.73	0.09	
+45	1.73	0.08	41.15	1.73	0.09	
0	1.33	0.08	40.29	1.73	0.09	
N=10E3						44
b=0.8"						
90	1.76	0.09	43.10	1.61	0.09375	
-45	1.73	0.09	43.03	1.61	0.09375	
+45	1.67	0.09	42.90	1.61	0.09375	

0	1.19	0.09	41.86	1.61	0.09375
N=10E4					46
b=1.2"					
90	1.70	0.10	44.78	1.54	0.11
-45	1.68	0.10	44.74	1.54	0.11
+45	1.63	0.10	44.62	1.54	0.11
0	1.21	0.10	43.73	1.54	0.11

Notes: 1. K_{tg} equal to K_t^{∞} at 90, -45 and +45 degree plies crack, i.e., K_{tg}=1.98, 1.73, 1.67 and 1.63 for b=0.1875, 0.5, 0.8 and 1.2

2. d_o is determined from K_{tg} in the base curve
3. d_o is not a fixed constant for different b in the same layup
4. Prdct strength is the predicted strength via WN fracture model
5. $K_{tg}^*=\sigma_o/S_n$ (unnotched strength/observed strength)
6. d_o^* is determined from K_{tg}^* in the base curve

Table 17. T300/5208 Notched Quasi-isotropic Laminate Residual Strength via the WN Fracture Model Point Stress Criterion with No Ply Cracking

Cycles	S_n (ksi)	K_t^∞	b (in)	d_o (in)	Prdct (ksi) Strength	Error (%)
10E0	37	3.11	0.1875	0.05	37.31	0.84
10E1	41	2.07	0.500	0.08	41.92	2.24
10E3	44	1.87	0.800	0.09	43.35	1.48
10E4	46	1.77	1.200	0.10	44.94	2.30
10E5	48					
2x10E5	31					

Notes: 1. a=0.1875 in for all cases

2. d_o is characteristic length, not constant

3. S_n is observed strength

4. Prdct strength is the predicted strength via WN fracture model

Table 18. Notched Strength for T300/5208 Quasi-isotropic Laminate with All Plies Cracked and Constant Characteristic Length d_o

Cycles	S_n (ksi)	K_t^∞	b (in)	d_o (in)	Prdct (ksi) Strength	Error (%)
10E0	37	1.19	0.1875	0.08	39.99	8.08
10E1	41	1.33	0.500	0.08	40.29	1.73
10E3	44	1.19	0.800	0.08	39.99	9.11
10E4	46	1.21	1.200	0.08	40.04	12.96

Notes:
1. K_t^∞ is SCF at hole edge with moduli reduction of all plies cracked
2. a is 0.1875 inch for all cases
3. b is the measured long semi-axis of effective notch which includes the hole and the damaged region
4. d_o is the average value of those do in Table 17
5. Prdct strength is the predicted strength via WN fracture model

Table 19. The Notched Strength for T300/934 $[0/\pm45/0]_{2s}$ Laminate with a Central Circular Hole due to T-T Fatigue Loading

Cycles	S_n (MPa)	% Incrse Cmpnce	C (in)	a (in)	b (in)	K_t^∞	d_o (in)	Prdct (MPa)	Error (%)
10E0	505	0	0	0.06	0.06	2.53	0.02	472.17	6.50
10E3	525	0	0.16	0.06	0.11	2.01	0.03	531.05	1.15
10E4	560	1.7	0.18	0.06	0.12	1.99	0.03	530.50	5.27
10E5	613	3.3	0.32	0.06	0.16	1.88	0.04	590.61	3.65
10E6	682	4	0.96	0.06	0.48	1.71	0.05	638.57	6.37
2x10E6	707	5		0.076					
5x10E6	Failure								

Notes:
1. Laminate is 6 in long, 1 in wide
2. A central circular hole diameter is 0.12 in
3. The unnotched strength is 850 MPa
4. Maximum stress is 430 MPa, stress ratio, R=0
5. 1 MPa= 0.145 ksi
6. The third item is the % of compliance increase
7. C is the measured 0 degree crack length
8. b is the measured long semi-axis of effective notch which includes the hole and damaged region
9. K_{tg}=1.73, 1.65, 1.58, 1.42 and 1.26 respectively
10. K_{tg}*=1.68, 1.62, 1.52, 1.39 and 1.25 respectively
11. d_o*=0.0225, 0.03, 0.035, 0.0435 and 0.0515 inch
12. Prdct is the predicted strength via WN fracture model

Table 20. Notched strength for T300/934 $[0/\pm45/90]_{2s}$ Laminate with a Central Circular Hole due to T-T fatigue Loading

Cycles	S_n (MPa)	% Incrs Cmplnce	C (in)	a (in)	b (in)	K_t^∞	d_o (in)	Prdct (MPa)	Error (%)
10E0	370	0	0	0.06	0.06	3.11	0.03	364.38	1.52
10E3	374	2	0.18	0.06	0.10	2.51	0.03	352.76	5.68
10E4	415	3	0.20	0.06	0.11	2.27	0.04	388.24	6.45
10E5	433	5	0.34	0.06	0.20	1.87	0.04	382.00	11.78
10E6	401	14	0.96	0.06	0.48	1.77	0.04	380.48	5.12
2x10E6	Failure								

Notes:
1. Laminate is 6 in long, 1 in wide
2. A central circular hole diameter is 0.12 in
3. The unnotched strength is 550 MPa
4. Maximum stress is 315 MPa, stress ratio, R=0
5. 1 MPa= 0.145 ksi
6. The third item is the % of compliance increase
7. C is the measured 0 degree crack length
8. b is the measured long semi-axis of effective notch which includes the hole and damaged region
9. K_{tg}=1.55, 1.52, 1.41, 1.39 and 1.39 respectively
10. K_{tg*}=1.49, 1.47, 1.33, 1.27 and 1.37 respectively
11. d_o*=0.0315, 0.032, 0.042, 0.0415 and 0.043 inch
12. Prdct is the predicted strength via WN fracture model

Table 21. Stiffnesses for a Cracked Single Ply by Reducing Moduli

Ply	A_{11}	A_{12}	A_{16}	A_{22}	A_{26}	A_{66}
[0]	131805	1	0	1	0	5198
[45]	41035	1	100	1	100	33778
[-45]	41035	1	-100	1	-100	33778
[90]	7468	1	0	1	0	5198

Notes: 1. A_{12} and A_{22} equal to 1 instead of zero to avoid singularity

2. To avoid negative definite stiffness matrix, A_{16} and A_{26} equal to 100 and -100 for 45 and -45 degree ply

Table 22. Maximum Stress and Displacement for T300/5208 [0] Ply with Moduli Reduction and Geometry Change

a= (in)	b= (in)	Max Displace. (in)	Max Stress (lb/in)	SCF
0.1875	0.1875	0.176039E4	0.595864E3	1.37
0.1875	0.28	0.177014E4	0.600485E3	1.38
0.1875	0.375	0.178024E4	0.596400E3	1.37
0.1875	0.4	0.178284E4	0.595016E3	1.37
0.1875	0.5	0.179345E4	0.591767E3	1.36
0.1875	0.8	0.182484E4	0.593238E3	1.36
0.1875	1.2	0.186628E4	0.579497E3	1.33

Notes: 1. SCF at hole edge almost unchanged for 7 cases of b

2. The average value of SCF is 1.36

3. Use SCF=1.36 as K_{tg} to find d_o in the base curve, d_o=0.17 in

Table 23. Maximum Stress and Displacement for T300/5208 [45] Ply with Moduli Reduction and Geometry Change

a= (in)	b= (in)	Max Displace. (in)	Max Stress (lb/in)	SCF
0.1875	0.1875	0.250008E4	0.565617E3	1.30
0.1875	0.28	0.25135E4	0.613992E3	1.41
0.1875	0.375	0.252830E4	0.590079E3	1.36
0.1875	0.4	0.2532E4	0.590907E3	1.36
0.1875	0.5	0.254715E4	0.590140E3	1.36
0.1875	0.8	0.258876E4	0.558815E3	1.28
0.1875	1.2	0.264847E4	0.563902E3	1.30

Notes: 1. SCF for seven cases of b changes slightly

2. The average SCF is 1.34

3. Set K_{tg}=1.34 in the base curve to find d_o, d_o=0.18 in

Table 24. Maximum Stress and Displacement for T300/5208 [-45] Ply with Moduli Reduction and Geometry Change

a= (in)	b= (in)	Max Displace. (in)	Max Stress (lb/in)	SCF
0.1875	0.1875	0.24996E4	0.575962E3	1.32
0.1875	0.28	0.251168E4	0.547542E3	1.26
0.1875	0.375	0.252631E4	0.594622E3	1.37
0.1875	0.4	0.252999E4	0.596109E3	1.37
0.1875	0.5	0.254508E4	0.602226E3	1.38
0.1875	0.8	0.258685E4	0.561328E3	1.29
0.1875	1.2	0.264631E4	0.52979E3	1.22

Notes: 1. SCF changes slightly.

2. The average of SCF is 1.32

3. Set K_{tg}=1.32 in the base curve to find d_o, d_o=0.09 in

Table 25. Maximum Stress and Displacement for T300/5208 [90] Ply with Moduli Reduction and Geometry Change

a= (in)	b= (in)	Max Displace. (in)	Max Stress (lb/in)	SCF
0.1875	0.1875	0.176178E4	0.635071E3	1.46
0.1875	0.28	0.177174E4	0.650189E3	1.49
0.1875	0.375	0.178224E4	0.640486E3	1.47
0.1875	0.4	0.178482E4	0.637742E3	1.47
0.1875	0.5	0.179529E4	0.632509E3	1.45
0.1875	0.8	0.182586E4	0.605048E3	1.39
0.1875	1.2	0.186815E4	0.589966E3	1.36

Notes: 1. SCF almost the same for the first five cases

2. The average value of SCF is 1.44

3. Set K_{tg}=1.44 in the base curve to find d_o, d_o=0.08 in

Table 26. The Predicted Residual Strength for T300/5208 [0] Ply

a (in)	b (in)	SCF	d_o (in)	Predicted Strength (MPa)
0.1875	0.1875	2.58	0.17	1186.26
0.1875	0.28	2.18	0.17	1174.38
0.1875	0.375	2.04	0.17	1170.27
0.1875	0.4	2.01	0.17	1169.39
0.1875	0.5	1.91	0.17	1166.49
0.1875	0.8	1.77	0.17	1162.44
0.1875	1.2	1.70	0.17	1160.42

Notes: 1. The unnotched strength for a 0 degree ply is 1500 MPa

2. K_{tg}=1.36
3. d_o=0.17 for all values of b
4. d_o is the same for single ply
5. 1 MPa= 0.145 Ksi

Table 27. The Predicted Residual Strength for T300/5208 [45] Ply

a (in)	b (in)	SCF	d_o (in)	Predicted Strength (MPa)
0.1875	0.1875	2.56	0.18	79.41
0.1875	0.28	2.03	0.18	78.48
0.1875	0.375	1.86	0.18	78.18
0.1875	0.4	1.82	0.18	78.11
0.1875	0.5	1.68	0.18	77.87
0.1875	0.8	1.55	0.18	77.65
0.1875	1.2	1.56	0.18	77.66

Notes: 1. The unnotched strength for a 45 degree ply is 98.8 MPa

2. K_{tg}=1.34
3. d_o=0.18 for all values of b
4. d_o is the same for single ply
5. 1 MPa= 0.145 Ksi

Table 28. The Predicted Residual Strength for T300/5208 [-45] Ply

a (in)	b (in)	SCF	d_o (in)	Predicted Strength (MPa)
0.1875	0.1875	3.62	0.09	61.03
0.1875	0.28	3.09	0.09	59.22
0.1875	0.375	2.91	0.09	58.63
0.1875	0.4	2.85	0.09	58.44
0.1875	0.5	2.71	0.09	57.99
0.1875	0.8	2.39	0.09	56.99
0.1875	1.2	2.20	0.09	56.27

Notes: 1. The unnotched strength for a -45 degree ply is 90.8 MPa

2. K_{tg}=1.32
3. d_o= 0.09 for all values of
4. d_o is the same for single ply
5. 1 MPa= 0.145 Ksi

Table 29. The Predicted Residual Strength for T300/5208 [90] Ply

a (in)	b (in)	SCF	d_o (in)	Predicted Strength (MPa)
0.1875	0.1875	5.37	0.08	39.70
0.1875	0.28	4.00	0.08	36.38
0.1875	0.375	3.90	0.08	36.16
0.1875	0.4	3.72	0.08	35.77
0.1875	0.5	3.35	0.08	34.99
0.1875	0.8	2.62	0.08	33.55
0.1875	1.2	2.23	0.08	32.83

Notes: 1. The unnotched strength for a 90 degree ply is 55.12 MPa

2. K_{tg}=1.44
3. d_o=0.08 for all values of b
4. d_o is the same for single ply
5. 1 MPa= 0.145 Ksi

REFERENCES

1. Chou, P.C., et al, "Statistical Analysis of Strength and Life of Composite Materials," AFWAL-TR-80-4049, April 1980.
2. Reifsnider, K.L.,Stinchcomb, W.W., and O'Brien, T.K., " Frequency Effects on a Stiffness-Based Fatigue Criterion in Flawed Composite Specimens," in Fatigue of Filamentary Composite Materials, STP 636, ASTM, 1977, pp. 171-184.
3. Kulkarni,S.V., McLaughlin, P.V., Jr. and Pipes, R.B., " Fatigue of Notched Fiber Composite Laminates Part II: Analytical and Experimental Evaluation," NASA, Contract NAS1-13931, NASA-CR-145039, Materials Science Corp. Blue Bell, Pa. 19422.
4. Waddoups,M.E., Eisenmann, J.R., and Kaminski, B.E., " Macroscopic Fracture Mechanics of Advanced Composite Materials," Journal of Composite Materials, Vol. 5, October 1971, pp. 446-454.
5. Chang, F.H., Gordon, D.E., and Gardner, A.H., "A Study of Fatigue Damage in Composites by Nondestructive Testing Technique," in Fatigue of Filamentary Composite Materials, ASTM STP 636, 1977, pp. 57-72.
6. Chang,F.H.,et al, "Real-Time Characterization of Damage Growth in Graphite/Epoxy Laminates," J. of Composite Materials, Vol. 10, July 1976, pp. 182-192.
7. Zweben, C., "Fracture Mechanics and Composite Materials: A Critical Analysis," in Analysis of the Test Methods for

High Modulus Fibers and Composites, ASTM STP 521, American Society for Testing and Materials, 1973, pp. 65-97.

8. Sendeckyj, G.P., "Fatigue Damage Accumulation in Graphite/Epoxy Laminates," in Failure Modes in Composites III, edited by T.T. Chiao and D.M. Schuster, The Metallurgical Society of AIME, New York, N.Y., Feburary 1976, pp. 100-114.
9. Chou, P.C., and Croman, R., "Residual Strength in Fatigue Based on the Strength-Life Equal Rank assumption," J. of Composite Materials, Vol. 12, April 1978, pp. 177-194.
10. Awerbuch,J., and Hahn, H.T., "Fatigue and Proof-Testing of Unidirectional Graphite/Epoxy Composites," in Fatigue of Filamentary Composite Materials, ASTM STP 636, 1977, pp. 248-266.
11. Askins, D.R., "Development of Engineering Data on Advanced Composite Materials," AFWAL-TR-81-4172, Feb. 1982.
12. Lauraitis, K.N., et al, "Advanced Residual Strength Degradation Rate Modeling for Advanced Composite Materials, Vol. II-Task II and III," AFWAL-TR-79-3095, Vol. II, July 1981.
13. Christensen, R.M., "Residual-Strength Determination in Polymeric Materials," in J. of Rheology, 25(5), 1981, pp. 529-536.
14. Christensen, R.M., and Wu, E.M., Engineering Fracture Mechanics, Vol. 14, 1981, p 215.
15. Owen, M.J., "Static and Fatigue Strength of Glass Chopped

Strand Mat/Polyester Resin Laminates," in Short Fiber Reinforced Composite Materials, ASTM STP 772, B.A. Sanders, Ed., 1982, pp.64-84.

16. Owen, M.J., and Bishop, P.T., "The Significance of Micro Damage in Glass-Reinforced Plastics at Macroscopic Stress Concentrators," in J. of Physics D: Applied Physics, Vol. 5, 1972.
17. Whitney, J.M., and Nuismer, R.J.," Stress Fracture Criterion for Laminated Composites Containing Stress Concentraions," J. of Composite Materials, Vol. 8, July 1974, pp. 253-265.
18. Zweben, C., J. of the Mechanics and Physics of Solids, Vol. 19, 1971, pp. 103-116.
19. Kanninen, M.F., et al, "Fundamental Analysis of the Failure of Polymer-Based Fiber Reinforced Composites," Final Report, Battelle Memorial Laboratories, Columbus, Ohio, Sept. 1975.
20. Kulkarni, S.V., Rice, J.S., and Rosen, B.W., Composites, Vol. 6, Sept. 1975, pp. 217-225.
21. Chou, P.C., and Croman, R., "Degradation and Sudden-Death Models of Fatigue of Graphite/Epoxy Composites," in Composite Materials: Testing and Design (Fifth Conference), ASTM STP 674, S.W. Tsai, Ed., 1979, pp. 431-454.
22. Inglis, C.E., Trans. Roy. Inst. Naval Architects, 60, 1913, p. 219.
23. Kolosoff, G., Doctor Dissertation, Dorpat, 1909.
24. Muskhelishvili, N.I., Some Basic Problems of Mathematical Theory

of Elasticity, Noordhoff, Groaingen, Holland, 1953.

25. Leknitskii, S.G., Theory of Elasticity of an Anisotropic Elastic Body, Holden-Day, San Francisco, 1963.
26. Leknitskii, S.G., Anisotropic Plates, Goldon and Breach, London, 1968.
27. Timoshenko, S., and Goodier, J.N., Theory of Elasticity, Third edition, McGraw-Hill, New York, 1970.
28. Savin, G.N., Stress Concentration Around Holes, Pergamon, New York, 1961.
29. Jeffery, G.B., Phil. Trans. Ser. A, Vol. 221, 1920, pp.265-293.
30. Mindlin, R.D., Proc. Soc. Exptl. Stress Anal., Vol. 5, 1948, p. 56.
31. Koiter, W.T., Quart. Appl. Math., Vol. 15, 1957, p. 303.
32. Howland, R.C.J., Trans. Roy. Soc. (London), Ser. A, Vol. 229, 1930, p.49.
33. Stevenson, A.C., Proc. Roy. Soc. (London), Ser. A, Vol. 184, 1945, p.129 and p. 218.
34. Peterson, R.E., Stress Concentration Design Factors, John Wiley, New York, 1974.
35. Roark, R.J., and Young, W.C., Formulas for Stress and Strain, Fifth edition, McGraw-Hill, 1975.
36. Goodier, J.N., and Hodge, P.G., Elasticity and Plasticity, New York, 1958.
37. Durelli, A.J., Parks, V.J., and Feng, H.C., "Stress Around an Elliptic Hole in a Finite Plate Subjected to Axial Loading,"

Trans. ASME, Ser. E, Vol. 88, No. 1, March 1966, pp. 192-195.

38. Wahl, A.M., and Beeuwkes, "Stress Concentration Produced by Holes and Notches," Trans. ASME, Vol. 1, 1934, pp. 617-623.

39. Jones, N., and Hozos, D., "A Study of the Stress Around Elliptic Holes in Flat Plates," Trans. ASME, Vol. 93, Ser. B, J. of Eng. for Industry, 1971, p.688.

40. Broek, D., Elementary Engineering Fracture Mechanics, Sijthoff & Noordhoff, 1978.

41. Soni, S.R., "Failure Analysis of Composite Laminates with a Fastener Hole," in Joining of Composite Materials, ASTM STP 749, K.T. Kedward, Ed., 1981, pp. 145-164.

42. Muskhelishvili, N.I., Math. Ann., Vol. 107, pp. 282-312, 1932.

43. Timoshenko, S.P., and Goodier, J.N., Theory of Elasticity, Third edition, Chapter 6.

44. Lekhnitskii, S.G., Theory of Elasticity of an Anisotropic Elastic Body, Holden-Day, Inc., San Francisco, 1963.

45. Lekhnitskii, S.G., Anisotropic Plates, translated from the Second Russian Edition by S.W. Tsai and T. Cheron, Gordan and Breach, Science Publishers, Inc., New York 1968.

46. Nuismer, R.J., and Whitney, J.M., "Uniaxial Failure of Composite Laminates Containing Stress Concentrations," in Fracture Mechanics of Composites, ASTM STP 593, 1975, pp. 117-142.

47. Whitney, J.M. and Nuismer, R.J., "Stress Fracture Criterion for Laminated Composites Containing Stress Concentration,"

J. of Comp. Matls., Vol. 8, July 1974, pp. 253-65.

48. Bowie, O.L., "Analysis of an Infinite Plate Containing Radial Cracks Originating from the Boundary of an Internal Circular Hole," J. Math. Physics, Vol. 35, 1956, p. 60.

49. Karlak, R.F., "Hole Effects in a Related Series of Symmetrical Laminates," Proceedings of Failure Modes in Composites IV, AIME, October 1977, p. 105.

50. Pipes, R.B., et al, "Notched Strength of Composite Materials," J. of Composite Materials, Vol. 13, April 1979, p. 148.

51. Paris, P.C., and Erdogan, F., "A Critical Analysis of Crack Propagation Laws," Trans. ASME, J. Basic Engineering, 85, 1963, pp. 528-534.

52. Parker, A.P., The Mechanics of Fracture and Fatigue: an Introduction, E.&F.N. Spon Ltd., 1981, Chapter 7.

53. Paris, P.C., and Sih, G.C., "Stress Analysis of Cracks," ASTM STP 381, 1970, p. 70.

54. Wilkins, J.D., et al, "Characterizing Delamination Growth in Graphite/Epoxy," ASTM STP no. 775, 1982.

55. O'Brien, T.K., "Characterization of Delamination Onset and Growth in a Composite Laminates," ASTM STP no. 775, 1982, pp. 140-168.

56. Reddy, J.N., An Introduction to the Finite Element Method, McGraw-Hill, 1984.

57. Bathe, K.J., Finite Element Procedures in Engineering Analysis, Prentice-Hall, 1982.

58. Crouch, S.L., and Starfield, A.M., Boundary Methods in Solid Mechanics: with applications in rock mechanics and geological engineering, George Allen & Unwin (Publishers) Ltd., London, 1983.

59. Hong, C.S., and Crews, J.H., Jr.,"Stress-Concentration Factors for Finite Orthotropic Laminates with a Circular Hole and Uniaxial Loading," NASA Technical Paper 1469, pp. 1-26, 1979.

60. Tsai, S.W., and Hahn, H.T., Introduction to Composite Materials, Technomic Publishing Co., Inc. 1980.

61. Rosen, B.W., "Failure of Fiber Composite Laminates," Mechanics of Composite Materials-Recent Advances, Proceedings of the IUTAM Symposium on Mechanics of Composite Materials, August 1982, p. 105.

62. Reifsnider, K.L., et al, "Damage Mechanics and NDE of Composite Laminates," Mechanics of Composite Materials-Recent Advances, Proceedings of the IUTAM Symposium on Mechanics of Comp. Matls., August 1982, p.399.

63. Stinchcomb, W.W., et al, "Fatigue Damage in Notched Composite Laminates Under Tension-Tension Cyclic Loads," Second Annual Progress Report NAG-1-232, NASA Langley Research Center, 1982.

64. Liechti, K.M., et al, "Cumulative Damage Model for Advanced Comp. Materials," AFWAL-TR-82-4094, July 1982, Section IV.

65. Ramani, S.V. and Williams, D.P., "Notched and Unnotched

Fatigue Behavior of Angle-Ply Graphite/Epoxy Composites," Fatigue of Filamentary Composite Materials, ASTM STP 636, 1977, pp. 27-46.

APPENDIX I: NOMENCLATURE

A	material constant
a	crack length of symmetrically double crack propagation; short semi-axis of elliptic hole
a_o	initial crack length
a_N	crack length at N cycles
b	measured effective notch as long semi-axis of elliptic hole
C	cracked region length
d	diameter of hole
d_o	characteristic length from Ktg of WN fracture model
d_o*	observed characteristic length from Ktg*
E	Young's modulus
G	total strain energy release rate
K	SIF, sub I means mode I and so on
K_t^∞	elastic SCF at the hole edge
K_{tg}	SCF at the characteristic length corresponding to normalized unnotched strength
K_{tg}*	unnotched strength divided by observed strength, σ_o/S_n
L	crack length
l	specimen half length
m	material constant
N	number of cycles
n	material constant
R	radius
r	radius of hole
S_n	observed notched strength from experimental data

s symmetry

t total

w specimen half width

x axis vertical to loading

Y crack correction factor

y axis parallel to loading

σ stress

σ_η longitudinal stress in the curvilinear coordinates

σ_ξ transverse stress in the curvilinear coordinates

$\sigma_{\eta\xi}$ shear stress in the curvilinear coordinates

σ_c critical stress

σ_o unnotched strength

σ_N^∞ notched strength

ν Poisson's ratio

APPENDIX II: EQUATION

Eq. (1) is expressed as:

$$\sigma_{\eta}=\frac{S}{2}\{e^{2\xi}_{o}\mathrm{Cos}2\beta+[\mathrm{Sinh}2\xi(1-e^{2\xi}_{o}\mathrm{Cos}2\beta)-e^{2\xi}_{o}\mathrm{Sin}2\beta\mathrm{Sin}2\eta)]/$$
$$(\mathrm{Cosh}^{2}\xi-\mathrm{Cos}2\eta)\}+$$
$$+\frac{S}{4}\{\{[(e^{2\xi}_{o}\mathrm{Cos}2\beta-1)(1-2\mathrm{Sin}^{2}\eta)\mathrm{Sinh}\xi\mathrm{Cosh}\xi+e^{2\xi}_{o}\mathrm{Sin}2\beta\mathrm{Sin}\eta\mathrm{Cos}\eta)]/$$
$$(\mathrm{Sinh}^{2}\xi\mathrm{Cos}^{2}\eta+\mathrm{Cosh}^{2}\xi\mathrm{Sin}^{2}\eta)^{2}-$$
$$-[\{\mathrm{Cos}2\beta-\mathrm{Cosh}2\xi_{o}-2e^{2\xi}_{o}\mathrm{Sinh}(\xi-\xi_{o})\mathrm{Cosh}(\xi-\xi_{o})[(1-2\mathrm{Sin}^{2}(\eta-\beta)]\}.$$
$$.\mathrm{Sinh}\xi\mathrm{Cos}\xi]/(\mathrm{Sinh}^{2}\xi\mathrm{Cos}^{2}\eta+\mathrm{Cosh}^{2}\xi\mathrm{Sin}^{2}\eta)^{2}-$$
$$-\{2e^{2\xi}_{o}[1+2\mathrm{Sinh}^{2}(\xi-\xi_{o})]\mathrm{Sin}(\eta-\beta)\mathrm{Cos}(\eta-\beta)\mathrm{Sin}\eta\mathrm{Cos}\eta\}/$$
$$(\mathrm{Sinh}^{2}\xi\mathrm{Cos}^{2}\eta+\mathrm{Cosh}^{2}\xi\mathrm{Sin}^{2}\eta)^{2}+$$
$$+2e^{2\xi}_{o}\{2[\mathrm{Cosh}^{2}(\xi-\xi_{o})\mathrm{Cos}^{2}(\eta-\beta)-\mathrm{Sinh}^{2}(\xi-\xi_{o})\mathrm{Sin}^{2}(\eta-\beta)-1]\}/$$
$$(\mathrm{Sinh}^{2}\xi\mathrm{Cos}^{2}\eta+\mathrm{Cosh}^{2}\xi\mathrm{Sin}^{2}\eta)\}\}.$$

APPENDIX III: CALCULATION

The determination of the value of K_{tg}, the characteristic length (d_o), and the calculation of notched strength are expressed as follows:

First we know the unnotched strength (σ_o) for T300/5208 quasi-isotropic laminate is 71 Ksi, and from Table 16 we have the observed residual strength (S_n) equal to 44 Ksi at 10E3 cycles, a=0.1875", b=0.8" and K_t^∞=1.87. Now assume $K_{tg}=K_t^\infty$ at the worst state (90, -45 and +45 deg plies cracked), i.e., K_{tg} corresponds to the normalized unnotched strength at the characteristic length (d_o) as the point stress criterion stated. Here we have K_{tg}=1.67 when all 90, -45 and +45 deg plies have cracked, see column 2 in Table 16.

At the circular hole shape and with no ply cracking we can obtain a stress distribution along x-axis via FEM. After normalizing the stress distribution by applied stress, we have a normalized curve and treat it as the base curve. According to the intersection of this curve, we obtain d_o=0.09" corresponding to K_{tg}=1.67 shown in Fig. 33 and column 3 in Table 16.

We use d_o=0.09" and R=a=0.1875 to calculate ξ_1.

$\xi_1=R/(R+d_o)=0.1875/(0.1875+0.09)=0.6756767$

It is easy to find ξ_1 square, fourth, sixth and eighth power values. Plug these values into Eq. (5), we have the predicted notched strength =42.90 Ksi (column 4) with 2.5% error in comparison with the observed data.

If we have the observed data, define $K_{tg}^*=\sigma_o/S_n$,

K_{tg}*=σ_o/S_n=71/44=1.61, see column 5 in Table 16.

According to the intersection of base curve, we obtain d_o*=0.09375" (column 6) at K_{tg}*=1.61 shown in Fig. 33. We see that K_{tg}* and d_o* are close to K_{tg} and d_o. That shows that our assumption is reasonable. Other cases are listed in Table 16.

APPENDIX IV: FEM COMPUTER PROGRAM

A modified FEM computer program is listed next. The documentation of this computer program follows the implementation of the finite element method in the Appendix of Ref. [57].

```
C
C     J O I N T
C     PROGRAM FOR STRESS ANALYSIS OF TWO-DIMNENSIONAL
C     LINEAR ELASTIC QUASI-ISOTROPIC, ORTHOTROPIC AND
C     ANISOTROPIC COMPOSITE LAMINATES AND STRUCTURES
C
      COMMON /SOL/ NUMNP,NEQ,NWK,NUMEST,MIDEST,MAXEST,MK
      COMMON /DIM/ N1,N2,N3,N4,N5,N6,N7,N8,N9,N10,N11,N12,N13
      COMMON /DIM/ N14,N15
      COMMON /EL/ IND,NPAR(10), NUMEG,MTOT,NFIRST,NLAST,ITWO
      COMMON /VAR/ NG,MODEX
      COMMON /TAPES/ IELMNT,ILOAD,IIN,IOUT
C
      DIMENSION TIM(5), HED(20)
      DIMENSION IA(1)
      EQUIVALENCE (A(1),IA(1))
C
C     THE FOLLOWING TWO CARDS ARE USED TO DETERMINE THE
C     MAXIMUM HIGH SPEED STORAGE THAT CAN BE USED FOR
C     SOLUTION. TO CHANGE THE HIGH SPEED STORAGE
C     AVAILABLE FOR EXECUTION CHANGE THE VALUE OF MTOT
C     AND CORRESPONDINGLY COMMON A(MTOT)
C
      COMMON A(100000)
      MTOT = 100000
      CALL TIMEON
C
C     DOUBLE PRECISION CARD
C       ITWO = 1 SINGLE PRECISION ARITHMETIC
C       ITWO = 2 DOUBLE PRECISION ARITHMETIC
C
      ITWO=2
C
C     THE FOLLOWING SCRATCH RILES ARE USED
C       IELMNT = TAPE STORING ELEMENT DATA
C       ILOAD  = TAPE STORING LOAD VECTORS
C       IIN    = INPUT TAPE
C       IOUT   =  OUTPUT TAPE
C
      IELMNT = 1
      ILOAD  = 2
      IIN    = 5
      IOUT   = 6
C
  200 NUMEST = 0
      MAXEST = 0
C
C     I N P U T   P H A S E
C
      CALL SECOND (TIM(1))
C
```

```
C     READ CONTROL INFORMATION
C
      READ (IIN,1000)  HED,NUMNP,NUMEG,NLCASE,MODEX
      IF (NUMNP.EQ.0) STOP
      WRITE (IOUT,2000) HED,NUMNP,NUMEG,NLCASE,MODEX
C
C     READ NODAL POINT DATA
C
      N1 = 1
      N2 = N1 + 3 * NUMNP
      N3 = N2 + NUMNP * ITWO
      N4 = N3 + NUMNP * ITWO
      N5 = N4 + NUMNP * ITWO
      IF (N5.GT.MTOT) CALL ERROR (N5 - MTOT,1)
C
      CALL INPUT (A(N1),A(N2), A(N3), A(N4), NUMNP, NEQ)
C
      NEQ1 = NEQ + 1
C
C     CALCULATE AND STORE LOAD VECTORS
C
      N6 = N5 + NEQ * ITWO
      WRITE(IOUT,2005)
C
      REWIND ILOAD
C
      DO 300 L= 1, NLCASE
C
      READ(IIN,1010) LL,NLOAD
C
      WRITE(IOUT,2010) LL, NLOAD
      IF (LL.EQ.L) GO TO 310
      WRITE(IOUT,2020)
      STOP
  310 CONTINUE
C
      N7 = N6 + NLOAD
      N8 = N7 + NLOAD
      N9 = N8 + NLOAD * ITWO
C
      IF (N9.GT.MTOT) CALL ERROR (N9 - MTOT,2)
C
      CALL LOADS (A(N5),A(N6),A(N7),A(N8),A(N1),NLOAD,NEQ)
C
  300 CONTINUE
C
C     READ, GENERATE AND STORE ELEMENT DATA
C
      N6 = N5 + NEQ
      DO 10 I = N5,N6
   10 IA(I)=0
```

```
      IND=1
C
      CALL ELCAL
C
      CALL SECOND (TIM(2))
C
C     S O L U T I O N    P H A S E
C
C     ASSEMBLE STIFFNESS MATRIX
C
      CALL ADDRES (A(N2),A(N5))
C
      MM = NWK/NEQ
      N3 = N2 + NEQ +1
      N4 = N3 + NWK * ITWO
      N5 = N4 + NEQ * ITWO
      N6 = N5 + MAXEST
      IF (N6.GT.MTOT) CALL ERROR (N6 - MTOT,4)
C
C     WRITE TOTAL SYSTEM DATA
C
      WRITE(IOUT,2025) NEQ,NWK,MK,MM
C
C     IN DATA CHECK ONLY MODE WE SKIP ALL FURTHER
C     CALCULATIONS
      IF (MODEX.GT.0) GO TO 100
      CALL SECOND (TIM(3))
      CALL SECOND (TIM(4))
      CALL SECOND (TIM(5))
      GO TO 120
C
C     CLEAR STORAGE
C
  100 NNL = NWK * NEQ
      CALL CLEAR(A(N3), NNL)
C
      IND = 2
C
      CALL ASSEM (A(N5))
C
      CALL SECOND (TIM(3))
C
C     TRIANGULARIZE STIFFNESS MATRIX
C
      KTR = 1
      CALL COLSOL (A(N3),A(N4),A(N2),NEQ,NWK,NEQ1,KTR)
C
   35 CALL SECOND (TIM(4))
C
      KTR = 2
      IND = 3
```

```
C
      REWIND ILOAD
      DO 400 L=1,NLCASE
C
      CALL LOADV (A(N4),NEQ)
C
C     CALCULATION OF DISPLACEMENTS
C
      CALL COLSOL (A(N3),A(N4),A(N2),NEQ,NWK,NEQ1,KTR)
C
      WRITE(IOUT,2015) L
      CALL WRITE (A(N4),A(N1),NEQ,NUMNP)
C
C     CALCULATION OF STRESSES
C
      CALL STRESS (A(N5))
C
  400 CONTINUE
      CALL SECOND (TIM(5))
C
C     PRINT SOLUTION TIMES
C
  120 TT = 0.
      DO 500 I = 1,4
      TIM(I) = TIM(I+1) - TIM(I)
  500 TT = TT + TIM(I)
      WRITE (IOUT,2030) HED,(TIM(I),I=1,4),TT
C
C     READ NEXT ANALYSIS CASE
C
      GO TO 200
C
 1000 FORMAT (20A4/5I5)
 1010 FORMAT (2I5)
C
 2000 FORMAT (1H1,20A4///
     155H C O N T R O L  I N F O R M A T I O N          //5X,
     255HNUMBER OF NODAL POINTS . . . . . (NUMNP)  = I5//5X,
     355HNUMBER OF ELEMENT GROUPS . . . . . (NUMEG)  = I5//5X,
     455HNUMBER OF LOAD CASES . . . . . (NLCASE) = I5//5X,
     555HSOLUTION MODE . . . . . (MODEX)  = I5 /5X,
     655H   EQ.0, DATA CHECK                          /5X,
     755H   EQ.1, EXECUTION                            )
 2005 FORMAT (1H1,26H L O A D  C A S E  D A T A)
 2010 FORMAT(////4X,33H LOAD CASE NUMBER .. . . . . =,I5//5X,
     132HNUMBER OF CONCENTRATED LOADS . = ,I5)
 2015 FORMAT(1H1,9HLOAD CASE,I3)
 2020 FORMAT (1X,40H***  ERROR LOAD CASES ARE NOT IN ORDER  )
 2025 FORMAT (1H1,
     155HTOTAL SYSTEM DATA                            ///5X,
     255HNUMBER OF EQUATIONS . . . . . (NEQ) = I5//5X,
```

```
     355HNUMBER OF MATRIX ELEMENTS . . . . . . (NWK) = I5//5X,
     455HMAXIMUM HALF BANDWIDTH . . . . . . . . (MK ) = I5//5X,
     555HMEAN HALF BANDWIDTH . . . . . . . . . . (MM ) = I5)
 2030 FORMAT (1H1,52H S O L U T I O N  T I M E  L O G  I N
     1S E C O N D S,12X,11HFOR PROBLEM//1X,20A4 ////5X,
     251HTIME FOR INPUT PHASE. . . . . . . . . . = ,F12.2//5X,
     351HTIME FOR CALCULATION OF STRUCTURE STIFFNESS MATRIX
     3=,F12.2//5X,
     451HTRIANGULARIZATION OF STIFFNESS MATRIX . . =,F12.2//5X,
     551HTIME FOR LOAD CASE SOLUTIONS . . . . . =,F12.2///5X,
     651H T O T A L  S O L U T I O N  T I M E . . . = ,F12.2)
C
      END
C
      SUBROUTINE ERROR(N,I)
C
C     PROGRAM
C     TO PRINT MESSAGES WHEN HIGH-SPEED STORAGE IS EXCEEDED
C
      COMMON/TAPES/ IELMNT,ILOAD,IIN,IOUT
C
      GO TO (1,2,3,4),I
C
    1 WRITE(IOUT,2000)
      GO TO 6
    2 WRITE(IOUT,2010)
      GO TO 6
    3 WRITE(IOUT,2020)
      GO TO 6
    4 WRITE(IOUT,2030)
C
    6 WRITE (IOUT,2050) N
      STOP
 2000 FORMAT (//48H NOT ENOUGH STORAGE FOR READ-IN OF ID
     1ARRAY AND 23HNDDAL POINT COORDINATES)
 2010 FORMAT (//50H NOT ENOUGH STORAGE FOR DEFINITION OF
     1LOAD VECTORS)
 2020 FORMAT(//42H NOT ENOUGH STORAGE FOR ELEMENT DATA
     1INPUT)
 2030 FORMAT (//53H NOT ENOUGH STORAGE FOR ASSEMBLAGE OF
     1GLOBAL STRUCTUR 55HE STIFFNESS, AND DISPLACEMENT AND
     2STRESS SOLUTION PHASE)
 2050 FORMAT (// 32H *** ERROR STORAGE EXCEEDED BY, I9)
      RETURN
      END
      SUBROUTINE INPUT (ID,X,Y,Z,NUMNP,NEQ)
C
C     PROGRAM
C     TO READ, GENERATE, AND PRINT NODAL POINT INPUT DATA
C     TO CALCULATE EQUATION NUMBERS AND STORE THEM IN ID
C     ARRAY
```

```
C             N=ELEMENT NUMBER
C             ID=BOUNDARY CONDITION CODES (0=FREE,1=DELETED)
C             X,Y,Z= COORDINATES
C             KN= GENERATION CODE
C                     I.E. INCREMENT ON NODAL POINT NUMBER
C
      IMPLICIT REAL*8(A-H,O-Z)
C
C     THIS PROGRAM IS USED IN SINGLE PRECISION ARITHMETIC ON
C     CDC EQUIPMENT AND DOUBLE PRECISION ARITHMETIC ON IBM
C     OR UNIVAC MACHINES .ACTIVATE,DEACTIVATE OR ADJUST
C     ABOVE CARD FOR SINGLE OR DOUBLE PRECISION ARITHMETIC
C
      COMMON /TAPES/ IELMNT,ILOAD,IIN,IOUT
      DIMENSION X(1),Y(1),Z(1),ID(3,NUMNP)
C
C     READ AND GENERATE NODAL POINT DATA
C
      WRITE (IOUT,2000)
      WRITE (IOUT,2010)
      WRITE (IOUT,2020)
      KNOLD=0
      NOLD=0
C
   10 READ (IIN,1000) N,(ID(I,N),I=1,3),X(N),Y(N),Z(N),KN
      WRITE (IOUT,2030) N,(ID(I,N),I=1,3),X(N),Y(N),Z(N),KN
      IF (KNOLD.EQ.0) GO TO 50
      NUM=(N-NOLD) / KNOLD
      NUMN=NUM-1
      IF(NUMN.LT.1) GO TO 50
      XNUM=NUM
      DX=(X(N)-X(NOLD))/XNUM
      DY=(Y(N)-Y(NOLD))/XNUM
      DZ=(Z(N)-Z(NOLD))/XNUM
      K=NOLD
      DO 30 J=1,NUMN
      KK=K
      K=K + KNOLD
      X(K)=X(KK)+DX
      Y(K)=Y(KK)+DY
      Z(K)=Z(KK)+DZ
      DO 30 I=1,3
      ID(I,K)=ID(I,KK)
   30 CONTINUE
C
   50 NOLD=N
      KNOLD=KN
      IF(N.NE.NUMNP) GO TO 10
C
C     WRITE COMPLETE NODAL DATA
C
```

```
C     WRITE (IOUT,2015)
C     WRITE (IOUT,2020)
C
C     NUMBER UNKNOWNS
C
      NEQ=0
      DO 100 N=1,NUMNP
      DO 100 I=1,3
      IF (ID(I,N)) 110,120,110
  120 NEQ=NEQ + 1
      ID(I,N)=NEQ
      GO TO 100
  110 ID(I,N)=0
  100 CONTINUE
C
C     WRITE EQUATION NUMBERS
C
      WRITE (IOUT,2040) (N,(ID(I,N),I=1,3),N=1,NUMNP)
      RETURN
C
 1000 FORMAT (4I5,3F10.0,I5)
 2000 FORMAT(1H1,33H N O D A L  P O I N T  D A T A //)
 2010 FORMAT(18H INPUT NODAL DATA //)
 2015 FORMAT(///22H GENERATED NODAL DATA //)
 2020 FORMAT(7H NODE  9X,8HBOUNDARY,25X,11HNODAL POINT,17X,
     1 4HMESH/7H NUMBER,5X,16HCONDITION CODES·21X,
     111HCOORDINATES,14X,
     210HGENERATING/77X,4HCODE//15X,1HX,4X,1HY,4X,1HZ,
     315X,1HX,12X,1HY,12X,1HZ,10X,2HKN)
 2030 FORMAT (I5,6X,3I5,6X,3F13.3,3X,I6)
 2040 FORMAT(//17H EQUATION NUMBERS//,4X,4HNODE,9X,
     117HDEGREE OF FREEDOM/3X,6HNUMBER//,
     25X,1HN,13X,1HX,4X,1HY,4X,1HZ/(1X,I5,9X,3I5))
C
      END
C
      SUBROUTINE LOADS (R,NOD,IDIRN,FLOAD,ID,NLOAD,NEQ)
C
C     PROGRAM
C     TO READ NODAL LOAD DATA
C     TO CALCULATE THE LOAD VECTOR R FOR EACH LOAD CASE
C     AND WRITE ONTO TAPE ILOAD
C
      IMPLICIT REAL * 8(A-H,O-Z)
C
C     THIS PROGRAM IS USED IN SINGLE PRECISION ARITHMETIC ON
C     CDC EQUIPMENT AND DOUBLE PRECISION ARITHMETIC ON IBM
C     OR UNIVAC MACHINES .ACTIVATE,DEACTIVATE OR ADJUST
C     ABOVE CARD FOR SINGLE OR DOUBLE PRECISION ARITHMETIC
C
      COMMON /VAR/ NG, MODEX
```

```
      COMMON /TAPES/ IELMNT,ILOAD,IIN,IOUT
      DIMENSION R(NEQ),NOD(1),IDIRN(1),FLOAD(1)
      DIMENSION ID(3,1)
C
      WRITE (IOUT,2000)
      READ (IIN,1000) (NOD(I),IDIRN(I),FLOAD(I),I=1,NLOAD)
      WRITE(IOUT,2010) (NOD(I),IDIRN(I),FLOAD(I),I=1,NLOAD)
      IF (MODEX.EQ.0) RETURN
C
      DO 210 I=1,NEQ
  210 R(I)=0.
C
      DO 220 L=1,NLOAD
      LN=NOD(L)
      LI=IDIRN(L)
      II=ID(LI,LN)
      IF(II) 220,220,240
  240 R(II) = R(II)+ FLOAD(L)
C
  220 CONTINUE
C
      WRITE (ILOAD) R
C
  200 CONTINUE
C
 1000 FORMAT(2I5,F15.5)
 2000 FORMAT (////4X,30HNODE       DIRECTION      LOAD/
     1 3X,6HNUMBER,19X,9HMAGNITUDE)
 2010 FORMAT (1H0,I6,9X,I4,7X,E12.5)
      RETURN
      END
C
      SUBROUTINE ELCAL
C
C     PROGRAM
C     TO LOOP OVER ALL ELEMENT GROUPS FOR READING,
C     GENERATING AND STORING THE ELEMENT DATA
C
      COMMON /SOL/ NUMNP,NEQ,NWK,NUMEST,MIDEST,MAXEST,MK
      COMMON /EL/ IND,NPAR(10),NUMEG,MTOT,NFIRST,NLAST,ITWO
      COMMON /TAPES/ IELMNT,ILOAD,IIN,IOUT
      COMMON A(1)
C
      REWIND IELMNT
      WRITE (IOUT,2000)
C
C     LOOP OVER ALL ELEMENT GROUPS
C
      DO 100 N=1,NUMEG
      IF (N.NE.1) WRITE (IOUT,2010)
C
```

```
      READ (IIN,1000) NPAR
C
      CALL ELEMNT
C
      IF (MIDEST.GT.MAXEST) MAXEST=MIDEST
C
      WRITE (IELMNT) MIDEST,NPAR,(A(I),I=NFIRST,NLAST)
C
  100 CONTINUE
C
      RETURN
C
 1000 FORMAT (2015)
 2000 FORMAT (1H1,36HE L E M E N T  G R O U P  D A T A ///)
 2010 FORMAT (1H1)
C
      END
C
      SUBROUTINE ELEMNT
C
C     PROGRAM
C     TO CALL THE APPROPRIATE ELEMENT SUBROUTINE
C
      COMMON /EL/ IND,NPAR(10),NUMEG,MTOT,NFIRST,NLAST,ITWO
C
      NPAR1=NPAR(1)
C
      GO TO (1,2,3),NPAR1
C
    1 CALL TRUSS
      RETURN
C
C     OTHER ELEMENT TYPES WOULD BE CALLED HERE, IDENTIFYING
C     EACH ELEMENT TYPE BY A DIFFERENT NPAR(1) PARAMETER
C
    2 RETURN
C
    3 RETURN
C
      END
C
      SUBROUTINE COLHT (MHT,ND,LM)
C
C     PROGRAM
C     TO CALCULATE COLUMN HEIGHTS
C
      COMMON /SOL/ NUMNP,NEQ,NWK,NUMEST,MIDEST,MAXEST,MK
      DIMENSION LM(1),MHT(1)
C
      LS=100000
      DO 100 I=1,ND
```

```
      IF(LM(I)) 110,100,110
  110 IF(LM(I)-LS) 120,100,100
  120 LS=LM(I)
  100 CONTINUE
C
      DO 200 I=1,ND
      II=LM(I)
      IF(II.EQ.0) GO TO 200
      ME=II - LS
      IF(ME.GT.MHT(II)) MHT(II)=ME
  200 CONTINUE
C
      RETURN
      END
C
      SUBROUTINE ADDRES(MAXA,MHT)
C
C     PROGRAM
C     TO CALCULATE ADDRESSES OF DIAGONAL ELEMENTS IN BANDED
C     MATRIX WHOSE COLUMN HEIGHTS ARE KNOWN
C
C          MHT  = ACTIVE COLUMN HEIGHTS
C          MAXA = ADDRESSES OF DIAGONAL ELEMENTS
C
      COMMON/SOL/ NUMP,NEQ,NWK,NUMEST,MIDEST,MAXEST,MK
      DIMENSION MAXA(1),MHT(1)
C
C     CLEAR ARRAY MAXA
C
      NN=NEQ + 1
      DO 20 I=1,NN
   20 MAXA(I)=0.0
C
      MAXA(1)=1
      MAXA(2)=2
      MK=0
      IF (NEQ.EQ.1) GO TO 100
      DO 10 I=2,NEQ
      IF (MHT(I).GT.MK) MK=MHT(I)
   10 MAXA(I+1)=MAXA(I) + MHT(I) + 1
  100 MK=MK + 1
      NWK=MAXA(NEQ+1) - MAXA(1)
C
      RETURN
      END
C
      SUBROUTINE CLEAR(A,N)
C
C     PROGRAM
C     TO CLEAR ARRAY A
C
```

```
      IMPLICIT REAL*8(A-H,O-Z)
C
C     THIS PROGRAM IS USED IN SINGLE PRECISION ARITHMETIC ON
C     CDC EQUIPMENT AND DOUBLE PRECISION ARITHMETIC ON IBM
C     OR UNIVAC MACHINES .ACTIVATE,DEACTIVATE OR ADJUST
C     ABOVE CARD FOR SINGLE OR DOUBLE PRECISION ARITHMETIC
C
      DIMENSION A(1)
      DO 10 I=1,N
   10 A(I)=0.
      RETURN
      END
C
      SUBROUTINE ASSEM (AA)
C
C     PROGRAM
C     TO CALL ELEMENT SUBROUTINES FOR ASSEMBLAGE OF THE
C     STRUCTURE STIFFNESS MATRIX
C
      COMMON /EL/ IND, NPAR(10),NUMEGM,MTOT,NFIRST,NLAST,ITWO
      COMMON /TAPES/ IELMNT,ILOAD,IIN,IOUT
      DIMENSION AA(1)
C
      REWIND IELMNT
C
      DO 200 N=1,NUMEG
      READ (IELMNT)NUMEST,NPAR,(AA(I),I=1,NUMEST)
C
      CALL ELEMNT
C
  200 CONTINUE
      RETURN
C
      END
C
      SUBROUTINE ADDBAN (A,MAXA,S,LM,ND)
C
C     PROGRAM
C     TO ASSEMBLE UPPER TRIANGULAR ELEMENT STIFFNESS INTO
C     COMPACTED GLOBAL STIFFNESS
C
C          A  = GLOBAL STIFFNESS
C          S  = ELEMENT STIFFNESS
C          ND = DEGREE OF FREEDOM IN ELEMENT STIFFNESS
C                 S(1)      S(2)      S(3)      ...
C        S  =               S(ND+1)   S(ND+2)   ...
C                                     S(2*ND)   ...
C
C                 A(1)      A(3)      A(6)      ...
C        A  =               A(2)      A(5)      ...
C                                     A(4)      ...
```

```
C
      IMPLICIT REAL*8(A-H,O-Z)
C
C     THIS PROGRAM IS USED IN SINGLE PRECISION ARITHMETIC ON
C     CDC EQUIPMENT AND DOUBLE PRECISION ARITHMETIC ON IBM
C     OR UNIVAC MACHINES .ACTIVATE,DEACTIVATE OR ADJUST
C     ABOVE CARD FOR SINGLE OR DOUBLE PRECISION ARITHMETIC
C
      DIMENSION A(1),MAXA(1),S(1),LM(1)
C
      NDI=0
      DO 200 I=1,ND
      II=LM(I)
      IF(II) 200,200,100
  100 MI=MAXA(II)
      KS=I
      DO 220 J=1,ND
      JJ=LM(J)
      IF(JJ) 220,220,110
  110 IJ=II - JJ
      IF(IJ)220,210,210
  210 KK=MI + IJ
      KSS=KS
      IF(J.GE.I) KSS=J + NDI
      A(KK)=A(KK) + S(KSS)
  220 KS=KS +ND -J
  200 NDI=NDI + ND - I
C
      RETURN
      END
C
      SUBROUTINE COLSOL(A,V,MAXA,NN,NWK,NNM,KKK)
C
C     PROGRAM
C     TO SOLVE FINITE ELEMENT STATIC EQUILIBRIUM EQUATIONS IN
C     CORE, USING COMPACTED STORAGE AND COLUMN REDUCTION
C     SCHEME
C     -- INPUT VARIALES --
C        A(NWK)   = STIFFNESS MATRIX STORED IN COMPACED FORM
C        V(NN)    = RIGHT-HAND-SIDE VECTOR
C        MAXA(NNM)= VECTOR CONTAINING ADDRESSES OF DIAGONAL
C                   ELEMENTS OF STIFFNESS MATRIX IN A
C        NN       = NUMBER OF EQUATIONS
C        NWK      = NUMBER OF ELEMENTS BELOW SKYLINE OF
C                   MATRIX
C        NNM      = NN + 1
C        KKK      = INPUT FLAGE
C                   EQ. 1 TRIANGULARIZATION OF STIFFNESS MATRIX
C                   EQ. 2 REDUCTION AND BACK-SUBSTITUTION OF
C                   LOAD VECTOR
C        IOUT     = NUMBER OF OUTPUT DEVICE
```

```
C
C     -- OUTPUT VARIABLES --
C        A(NWK)   = D AND L - FACTORS OF STIFFNESS MATRIX
C        V(NN)    = DISPALCEMENT VECTORS
C
      IMPLICIT REAL*8(A-H,O-Z)
C
C     THIS PROGRAM IS USED IN SINGLE PRECISION ARITHMETIC ON
C     CDC EQUIPMENT AND DOUBLE PRECISION ARITHMETIC ON IBM
C     OR UNIVAC MACHINES .ACTIVATE,DEACTIVATE OR ADJUST
C     ABOVE CARD FOR SINGLE OR DOUBLE PRECISION ARITHMETIC
C
      COMMON /TAPES/ IELMNT,ILOAD,IIN,IOUT
      DIMENSION A(NWK),V(1),MAXA(1)
C
C     PERFORM L*D*L(T) FACTORIZATION OF STIFFNESS MATRIX
C
      IF(KKK-2)40,150,150
   40 DO 140 N=1,NN
      KN=MAXA(N)
      KL=KN+1
      KU=MAXA(N+1) -1
      KH=KU-KL
      IF(KH)110,90,50
   50 K=N-KH
      IC=0
      KLT=KU
      DO 80 J=1,KH
      IC=IC + 1
      KLT=KLT -1
      KI=MAXA(K)
      ND=MAXA(K+1) - KI - 1
      IF(ND)80,80, 60
   60 KK=MIN0(IC,ND)
      C=0.
      DO 70 L=1,KK
   70 C=C+A(KI+L)*A(KLT+L)
      A(KLT)=A(KLT)-C
   80 K=K+1
   90 K=N
      B=0.
      DO 100 KK=KL,KU
      K=K - 1
      KI=MAXA(K)
      C=A(KK)/A(KI)
      B=B +C*A(KK)
  100 A(KK)=C
      A(KN)=A(KN) -B
  110 IF(A(KN)) 120,120,140
  120 WRITE(IOUT,2000) N,A(KN)
      STOP
```

```
  140 CONTINUE
      RETURN
C
C     REDUCE RIGHT-HAND-SIDE VECTOR
C
  150 DO 180 N=1,NN
      KL=MAXA(N) + 1
      KU=MAXA(N+1) - 1
      IF(KU-KL)180,160,160
  160 K=N
      C=0.
      DO 170 KK=KL,KU
      K=K -1
  170 C=C+A(KK)*V(K)
      V(N)=V(N) -C
  180 CONTINUE
C
C     BACK-SUBSTITUTE
C
      DO 200 N=1,NN
      K=MAXA(N)
  200 V(N)=V(N)/A(K)
      IF (NN.EQ.1) RETURN
      N=NN
      DO 230 L=2,NN
      KL=MAXA(N) + 1
      KU=MAXA(N+1) - 1
      IF(KU-KL)230,210,210
  210 K=N
      DO 220 KK=KL,KU
      K=K -1
  220 V(K)=V(K)-A(KK)*V(N)
  230 N=N-1
      RETURN
 2000 FORMAT(//48H STOP - STIFFNESS MATRIX NOT POSITIVE
     1DEFINITE ,//
     1         32H NONPOSITIVE PIVOT FOR EQUATION  ,I4,//
     2         10H PIVOT =  ,E20.12 )
      END
C
      SUBROUTINE LOADV (R,NEQ)
C
C     PROGRAM
C     TO OBTAIN THE LOAD VECTOR
C
      IMPLICIT REAL*8(A-H,O-Z)
C
C     THIS PROGRAM IS USED IN SINGLE PRECISION ARITHMETIC ON
C     CDC EQUIPMENT AND DOUBLE PRECISION ARITHMETIC ON IBM
C     OR UNIVAC MACHINES .ACTIVATE,DEACTIVATE OR ADJUST
C     ABOVE CARD FOR SINGLE OR DOUBLE PRECISION ARITHMETIC
```

```
C
      COMMON /TAPES/ IELMNT,ILOAD,IIN,IOUT
      DIMENSION R(NEQ)
C
      READ (ILOAD) R
C
      RETURN
      END
C
      SUBROUTINE WRITE(DISP,ID,NEQ,NUMNP)
C
C     PROGRAM
C     TO PRINT DISPLACEMENTS
C
      IMPLICIT REAL*8(A-H,O-Z)
C
C     THIS PROGRAM IS USED IN SINGLE PRECISION ARITHMETIC ON
C     CDC EQUIPMENT AND DOUBLE PRECISION ARITHMETIC ON IBM
C     OR UNIVAC MACHINES .ACTIVATE,DEACTIVATE OR ADJUST
C     ABOVE CARD FOR SINGLE OR DOUBLE PRECISION ARITHMETIC
C
      COMMON /TAPES/IELMNT,ILOAD,IIN,IOUT
      DIMENSION DISP(NEQ),ID(3,NUMNP)
      DIMENSION D(3)
C
C     PRINT DISPLACEMENTS
C
      WRITE(IOUT,2000)
      IC=4
      DO 100 II=1,NUMNP
      IC=IC +1
      IF(IC.LT.56) GO TO 105
      WRITE(IOUT,2000)
      IC=4
  105 DO 110 I=1,3
  110 D(I)=0.
C
      DO 120 I=1,3
      KK=ID(I,II)
      IL=I
  120 IF(KK.NE.0) D(IL)=DISP(KK)
C
  100 WRITE (IOUT,2010) II,D
C
      RETURN
 2000 FORMAT(///, 26H D I S P L A C E M E N T S  // 7H NODE  ,9X
     114HX-DISPLACEMENT,4X,14HY-DISPLACEMENT,4X,14HZ-DISPLACE
     2MENT)
 2010 FORMAT(1X,I3,8X,3E18.6)
C
      END
```

```
C
      SUBROUTINE STRESS (AA)
C
C     PROGRAM
C     TO CALL THE ELEMENT SUBROUTIME FOR THE COLCULATION
C     OF STRESSES
C
      COMMON /VAR/ NG, MODEX
      COMMON /EL/ IND,NPAR(10),NUMEG,MTOT,NFIRST,NLAST,ITWO
      COMMON /TAPES/ IELMNT,ILOAD,IIN,IOUT
      DIMENSION AA(1)
C
C     LOOP OVER ALL ELEMENT GROUPS
C
      REWIND IELMNT
C
      DO 100 N=1,NUMEG
      NG=N
C
      READ (IELMNT) NUMEST,NPAR,(AA(I),I=1,NUMEST)
C
      CALL ELEMNT
C
  100 CONTINUE
C
      RETURN
      END
C
      SUBROUTINE TRUSS
C
C     PROGRAM
C     TO SET UP STORAGE AND CALL THE TRUSS ELEMENT
C     SUBROUTINE
      COMMON /SOL/ NUMNP,NEQ,NWK,NUMEST,MIDEST,MAXEST,MK
      COMMON /DIM/ N1,N2,N3,N4,N5,N6,N7,N8,N9,N10,N11,N12
      COMMON /DIM/ N13,N14,N15
      COMMON /EL/ IND,NPAR(10),NUMEG,MTOT,NFIRST,NLAST,ITWO
      COMMON /TAPES/ IELMNT,ILOAD,IIN,IOUT
      COMMON A(1)
C
      EQUIVALENCE (NPAR(2),NUME),(NPAR(3),NUMMAT)
C
      NFIRST=N6
      IF(IND.GT.1) NFIRST=N5
      N101=NFIRST
      N102=N101 + 16*NUME
      N103=N102 + 8*NUME*ITWO
      N104=N103 + 8*NUME*ITWO
      N105=N104 + NUMMAT*ITWO
      N106=N105 + NUMMAT*ITWO
      N107=N106 + NUMMAT*ITWO
```

```
      N108=N107 + NUMMAT*ITWO
      N109=N108 + NUMMAT*ITWO
      N110=N109 + NUMMAT*ITWO
      N111=N110 + NUME
      NLAST=N111
C
      IF (IND.GT.1) GO TO 100
      IF (NLAST.GT.MTOT) CALL ERROR(NLAST-MTOT,3)
      GO TO 200
  100 IF (NLAST.GT.MTOT) CALL ERROR(NLAST-MTOT,4)
C
  200 MIDEST=NLAST - NFIRST
C
      CALL RUSS (A(N1),A(N2),A(N3),A(N4),A(N4),A(N5),A(N101),
     1A(N102),A(N103),A(N104),A(N105),A(N106),A(N107),A(N108),
     2A(N109),A(N110)
C
      RETURN
C
      END
C
      SUBROUTINE RUSS (ID,X,Y,Z,U,MHT,LM,XX,YY,
     1A1,A2,A3,A4,A5,A6,MATP)
C
C     PROGRAM
C     TRUSS ELEMENT SUBROUTINE
C
      IMPLICIT REAL*8(A-H,O-Z)
C
C     THIS PROGRAM IS USED IN SINGLE PRECISION ARITHMETIC ON
C     CDC EQUIPMENT AND DOUBLE PRECISION ARITHMETIC ON IBM
C     OR UNIVAC MACHINES. ACTIVATE, DEACTIVATE OR ADJUST
C     ABOVE CARDS FOR SINGLE OR DOUBLE PRECISION ARITHMETIC
C
      COMMON /SOL/ NUMNP,NEQ,NWK,NUMEST,MIDEST,MAXEST,MK
      COMMON /DIM/ N1,N2,N3,N4,N5,N6,N7,N8,N9,N10,N11,N12
      COMMON /DIM/ N13,N14,N15
      COMMON /EL/ IND,NPAR(10),NUMEG,MTOT,NFIRST,NLAST,ITWO
      COMMON /VAR/ NG,MODEX
      COMMON /TAPES/ IELMNT,ILOAD,IIN,IOUT
      COMMON A(1)
C
      REAL A
C
      DIMENSION X(1),Y(1),Z(1),ID(3,1),LM(16,1),MATP(1),U(1),MHT(1)
      DIMENSION XX(8,1),YY(8,1),A1(1),A2(1),A3(1),A4(1),A5(1),A6(1)
      DIMENSION DR(3),IPS(1)
      DIMENSION EPSX(3,3),EPSY(3,3),GAMA(3,3)
      DIMENSION S(136),SS(16,16),UU(8),VV(8)
      DIMENSION AX(3),H(3),E(8),F(8),PNXSI(8),PNXIT(8)
      DIMENSION SIGX(3,3),SIGY(3,3),TUXY(3,3)
```

```
C
      EQUIVALENCE (NPAR(1),NPAR1),(NPAR(2),NUME),(NPAR(3),
C     1NUMMAT)
C      ND    = NUMBER DEGREE OF FREEDOM PER EACH ELEMENT
C      AX    = GAUSSIAN INTEGRATION POINTS
C      H     = GAUSSIAN INTEGRATION WEIGHTS
C      XX    = X COORDINATE OF NODE
C      YY    = Y COORDINATE OF NODE
C      MTYP  = NUMBER OF MATERIAL TYPE AT EACH ELEMENT
C      NUMMAT= TOTAL NUMBER OF MATERIAL TYPES
C      A1,A2,A3,A4,A5,A6 = A11,A12,A16,A22,A26,A66 ARE
C      EXTENSIONAL MATRIX
C      I1,I2,I3,I4,I5,I6,I7,I8 ARE NODE ORDER STARTS FROM THE
C      RIGHT-UPPER
C      CORNER OF AN ELEMENT AND COUNTED COUNTER-CLOCKWISELY
C
      ND=16
C
      AX(1)=0.774596669241483D0
      AX(2)=0.000000000000000D0
      AX(3)=-0.774596669241483D0
      H(1)=0.555555555555556D0
      H(2)=0.888888888888889D0
      H(3)=0.555555555555556D0
C
      GO TO (300,610,900),IND
C
C     READ AND GENERATE ELEMENT INFORMATION
C
  300 DO 10 I=1,NUMMAT
      READ(IIN,9000)N,A1(N),A2(N),A3(N),A4(N),A5(N),A6(N)
      WRITE(IOUT,9000)N,A1(N),A2(N),A3(N),A4(N),A5(N),A6(N)
 9000 FORMAT(I5,6F10.0)
   10 CONTINUE
C
      N=1
  100 READ (IIN,1020) M,I1,I2,I3,I4,I5,I6,I7,I8,MTYP,KG
 1020 FORMAT(11I5)
      IF (KG.EQ.0) KG=1
  120 IF(M.NE.N) GO TO 200
      MY=MTYP
      KKK=KG
C
C     SAVE COORDINATE SYSTEM
C
  200 XX(1,N)=X(I1)
      YY(1,N)=Y(I1)
      XX(2,N)=X(I2)
      YY(2,N)=Y(I2)
      XX(3,N)=X(I3)
      YY(3,N)=Y(I3)
```

```
      XX(4,N)=X(I4)
      YY(4,N)=Y(I4)
      XX(5,N)=X(I5)
      YY(5,N)=Y(I5)
      XX(6,N)=X(I6)
      YY(6,N)=Y(I6)
      XX(7,N)=X(I7)
      YY(7,N)=Y(I7)
      XX(8,N)=X(I8)
      YY(8,N)=Y(I8)
C
      MATP(N)=MY
C
C     LM = DEGREE OF FREEDOM IN X,Y DIRECTIONS PER EACH NODE
C
      DO 390 L=1,16
  390 LM(L,N)=0
      DO 391 LK=1,2
      LM(LK,N)=ID(LK,I1)
      LM(LK+2,N)=ID(LK,I2)
      LM(LK+4,N)=ID(LK,I3)
      LM(LK+6,N)=ID(LK,I4)
      LM(LK+8,N)=ID(LK,I5)
      LM(LK+10,N)=ID(LK,I6)
      LM(LK+12,N)=ID(LK,I7)
      LM(LK+14,N)=ID(LK,I8)
  391 CONTINUE
C
      CALL COLHT (MHT,ND,LM(1,N))
C
      WRITE(IOUT,2050) N,I1,I2,I3,I4,I5,I6,I7,I8,MY
 2050 FORMAT(10I5)
      IF (N.EQ.NUME) RETURN
      N=N+1
      I1=I1+KKK
      I2=I2+KKK
      I3=I3+KKK
      I4=I4+KKK
      I5=I5+KKK
      I6=I6+KKK
      I7=I7+KKK
      I8=I8+KKK
C
      IF (N.GT.M) GO TO 100
      GO TO 120
C
C     DEVELOP STIFFNESS MATRIX OF EIGHT-NODED ELEMENT
C
  610 DO 611 N=1,NUME
      MY=MATP(N)
      A11=A1(MY)
```

```
      A12=A2(MY)
      A16=A3(MY)
      A22=A4(MY)
      A26=A5(MY)
      A66=A6(MY)
      DO 612 I=1,16
      DO 612 J=1,16
      SS(I,J)=0.D0
  612 CONTINUE
C
      DO 102 L=1,3
      XA=AX(L)
      DO 102 K=1,3
      YA=AX(K)
C
      XJ11=0.D0
      XJ12=0.D0
      XJ21=0.D0
      XJ22=0.D0
C
C     PARTIAL PHI OVER PARTIAL XSI
C
      PNXSI(1)=(2.D0*XA+YA+2.D0*XA*YA+YA*YA)/4.D0
      PNXSI(2)=(-2.D0*XA-2.D0*XA*YA)/2.D0
      PNXSI(3)=(2.D0*XA-YA+2.D0*XA*YA-YA*YA)/4.D0
      PNXSI(4)=(-1.D0+YA*YA)/2.D0
      PNXSI(5)=(2.D0*XA+YA-2.D0*XA*YA-YA*YA)/4.D0
      PNXSI(6)=(-2.D0*XA+2.D0*XA*YA)/2.D0
      PNXSI(7)=(2.D0*XA-YA-2.D0*XA*YA+YA*YA)/4.D0
      PNXSI(8)=(1.D0-YA*YA)/2.D0
C
C     PARTIAL PHI OVER PARTIAL ETA
C
      PNXIT(1)=(2.D0*YA+XA+XA*XA+2.D0*XA*YA)/4.D0
      PNXIT(2)=(1.D0-XA*XA)/2.D0
      PNXIT(3)=(2.D0*YA-XA+XA*XA-2.D0*XA*YA)/4.D0
      PNXIT(4)=(-2.D0*YA+2.D0*XA*YA)/2.D0
      PNXIT(5)=(2.D0*YA+XA-XA*XA-2.D0*XA*YA)/4.D0
      PNXIT(6)=(-1.D0+XA*XA)/2.D0
      PNXIT(7)=(2.D0*YA-XA-XA*XA+2.D0*XA*YA)/4.D0
      PNXIT(8)=(-2.D0*YA-2.D0*XA*YA)/2.D0
C
C     ELEMENTS OF JACOBIAN
C
      DO 52 KK=1,8
      XJ11=XJ11+PNXSI(KK)*XX(KK,N)
      XJ12=XJ12+PNXSI(KK)*YY(KK,N)
      XJ21=XJ21+PNXIT(KK)*XX(KK,N)
      XJ22=XJ22+PNXIT(KK)*YY(KK,N)
   52 CONTINUE
C
```

```
C     DETERMINANT OF JACOBIAN
C
      AVXJ=(XJ11*XJ22)-(XJ12*XJ21)
C
C     INVERSE OF JACOBIAN
C
      STJ11=XJ22/AVXJ
      STJ12=-XJ12/AVXJ
      STJ21=-XJ21/AVXJ
      STJ22=XJ11/AVXJ
C
C     E(I): PARTIAL PHI OVER PARTIAL X
C
      DO 12 I=1,8
      E(I)=STJ11*PNXSI(I)+STJ12*PNXIT(I)
   12 CONTINUE
C
C     F(I): PARTIAL PHI OVER PARTIAL Y
C
      DO 13 I=1,8
      F(I)=STJ21*PNXSI(I)+STJ22*PNXIT(I)
   13 CONTINUE
C
C     STIFFNESS MATRIX OF EIGHT-NODED ELEMENT: 16 BY 16
C
      DO 90 I=1,8
      DO 90 J=1,8
      KI=I*2-1
      KJ=J*2-1
      SS(KI,KJ)=SS(KI,KJ)+(A11*E(I)*E(J)+A16*F(I)*E(J)+
     *A16*E(I)*F(J)+A66*F(I)*F(J))*AVXJ*H(L)*H(K)
      SS(KI+1,KJ)=SS(KI+1,KJ)+(A12*F(I)*E(J)+A16*E(I)*E(J)+
     *A26*F(I)*F(J)+A66*E(I)*F(J))*AVXJ*H(L)*H(K)
      SS(KI,KJ+1)=SS(KI,KJ+1)+(A16*E(I)*E(J)+A66*F(I)*E(J)+
     *A12*E(I)*F(J)+A26*F(I)*F(J))*AVXJ*H(L)*H(K)
      SS(KI+1,KJ+1)=SS(KI+1,KJ+1)+(A26*F(I)*E(J)+A66*E(I)*E(J)+
     *A22*F(I)*F(J)+A26*E(I)*F(J))*AVXJ*H(L)*H(K)
   90 CONTINUE
  102 CONTINUE
C
C     TRANSFORM SS(I,J) INTO S(IJ)
C
      IJ=0
      DO 95 I=1,16
      DO 95 J=I,16
      IJ=IJ+1
      S(IJ)=SS(I,J)
   95 CONTINUE
C     WRITE(IOUT,9070)
C     WRITE(IOUT,9075)(S(IJ),IJ=1,136)
C9070 FORMAT(/)
```

```
C9075 FORMAT(8E10.3)
C
      CALL ADDBAN (A(N3),A(N2),S,LM(1,N),ND)
C
  611 CONTINUE
      RETURN
C
C     STRESS CALCULATION
C
C     EPSX    = EPSILON X
C     EPSY    = EPSILON Y
C     GAMA    = GAMA XY
C     SIGX    = SIGMA X
C     SIGY    = SIGMA Y
C     TUXY    = TAU XY
C
  900 WRITE(IOUT,9090)
      DO 663 N=1,NUME
C
      DO 664 I=1,8
      UU(I)=0.D0
      VV(I)=0.D0
  664 CONTINUE
C
      DO 666 I=1,3
      DO 666 J=1,3
      EPSX(I,J)=0.D0
      EPSY(I,J)=0.D0
      GAMA(I,J)=0.D0
  666 CONTINUE
C
      MY=MATP(N)
      A11=A1(MY)
      A12=A2(MY)
      A16=A3(MY)
      A22=A4(MY)
      A26=A5(MY)
      A66=A6(MY)
C
      DO 655 L=1,3
      XA=AX(L)
      DO 655 K=1,3
      YA=AX(K)
C
      XJ11=0.D0
      XJ12=0.D0
      XJ21=0.D0
      XJ22=0.D0
C
C     PARTIAL PHI OVER PARTIAL XSI
C
```

```
      PNXSI(1)=(2.D0*XA+YA+2.D0*XA*YA+YA*YA)/4.D0
      PNXSI(2)=(-2.D0*XA-2.D0*XA*YA)/2.D0
      PNXSI(3)=(2.D0*XA-YA+2.D0*XA*YA-YA*YA)/4.D0
      PNXSI(4)=(-1.D0+YA*YA)/2.D0
      PNXSI(5)=(2.D0*XA+YA-2.D0*XA*YA-YA*YA)/4.D0
      PNXSI(6)=(-2.D0*XA+2.D0*XA*YA)/2.D0
      PNXSI(7)=(2.D0*XA-YA-2.D0*XA*YA+YA*YA)/4.D0
      PNXSI(8)=(1.D0-YA*YA)/2.D0
C
C     PARTIAL PHI OVER PARTIAL ETA
C
      PNXIT(1)=(2.D0*YA+XA+XA*XA+2.D0*XA*YA)/4.D0
      PNXIT(2)=(1.D0-XA*XA)/2.D0
      PNXIT(3)=(2.D0*YA-XA+XA*XA-2.D0*XA*YA)/4.D0
      PNXIT(4)=(-2.D0*YA+2.D0*XA*YA)/2.D0
      PNXIT(5)=(2.D0*YA+XA-XA*XA-2.D0*XA*YA)/4.D0
      PNXIT(6)=(-1.D0+XA*XA)/2.D0
      PNXIT(7)=(2.D0*YA-XA-XA*XA+2.D0*XA*YA)/4.D0
      PNXIT(8)=(-2.D0*YA-2.D0*XA*YA)/2.D0
C
C     ELEMENTS OF JACOBIAN
C
      DO 53 KK=1,8
      XJ11=XJ11+PNXSI(KK)*XX(KK,N)
      XJ12=XJ12+PNXSI(KK)*YY(KK,N)
      XJ21=XJ21+PNXIT(KK)*XX(KK,N)
      XJ22=XJ22+PNXIT(KK)*YY(KK,N)
   53 CONTINUE
C
C     DETERMINANT OF JACOBIAN
C
      AVXJ=(XJ11*XJ22)-(XJ12*XJ21)
C
      STJ11=XJ22/AVXJ
      STJ12=-XJ12/AVXJ
      STJ21=-XJ21/AVXJ
      STJ22=XJ11/AVXJ
C
C     E(I): PARTIAL PHI OVER PARTIAL X
C
      DO 771 I=1,8
      E(I)=STJ11*PNXSI(I)+STJ12*PNXIT(I)
  771 CONTINUE
C
C     F(I): PARTIAL PHI OVER PARTIAL Y
C
      DO 772 I=1,8
      F(I)=STJ21*PNXSI(I)+STJ22*PNXIT(I)
  772 CONTINUE
C
C     CALCULATION OF STRAIN
```

```
C
      KK=LM(1,N)
      IF (KK.EQ.0) GO TO 801
      UU(1)=U(KK)
C
  801 KK=LM(2,N)
      IF (KK.EQ.0) GO TO 802
      VV(1)=U(KK)
C
  802 KK=LM(3,N)
      IF (KK.EQ.0) GO TO 803
      UU(2)=U(KK)
C
  803 KK=LM(4,N)
      IF (KK.EQ.0) GO TO 804
      VV(2)=U(KK)
C
  804 KK=LM(5,N)
      IF (KK.EQ.0) GO TO 805
      UU(3)=U(KK)
C
  805 KK=LM(6,N)
      IF (KK.EQ.0) GO TO 806
      VV(3)=U(KK)
C
  806 KK=LM(7,N)
      IF (KK.EQ.0) GO TO 807
      UU(4)=U(KK)
C
  807 KK=LM(8,N)
      IF (KK.EQ.0) GO TO 808
      VV(4)=U(KK)
C
  808 KK=LM(9,N)
      IF (KK.EQ.0) GO TO 809
      UU(5)=U(KK)
C
  809 KK=LM(10,N)
      IF (KK.EQ.0) GO TO 810
      VV(5)=U(KK)
C
  810 KK=LM(11,N)
      IF (KK.EQ.0) GO TO 811
      UU(6)=U(KK)
C
  811 KK=LM(12,N)
      IF (KK.EQ.0) GO TO 812
      VV(6)=U(KK)
C
  812 KK=LM(13,N)
      IF (KK.EQ.0) GO TO 813
```

```
      UU(7)=U(KK)
C
  813 KK=LM(14,N)
      IF (KK.EQ.0) GO TO 814
      VV(7)=U(KK)
C
  814 KK=LM(15,N)
      IF (KK.EQ.0) GO TO 815
      UU(8)=U(KK)
C
  815 KK=LM(16,N)
      IF (KK.EQ.0) GO TO 816
      VV(8)=U(KK)
C
  816 DO 655 LK=1,8
      EPSX(L,K)=EPSX(L,K)+UU(LK)*E(LK)
      EPSY(L,K)=EPSY(L,K)+VV(LK)*F(LK)
      GAMA(L,K)=GAMA(L,K)+(UU(LK)*F(LK)+VV(LK)*E(LK))
  655 CONTINUE
C
C     STRESS-STRAIN RELATIONSHIP
C
      DO 667 L=1,3
      DO 667 K=1,3
      SIGX(L,K)=A11*EPSX(L,K)+A12*EPSY(L,K)+A16*GAMA(L,K)
      SIGY(L,K)=A12*EPSX(L,K)+A22*EPSY(L,K)+A26*GAMA(L,K)
      TUXY(L,K)=A16*EPSX(L,K)+A26*EPSY(L,K)+A66*GAMA(L,K)
  667 CONTINUE
C
      LK=0
      DO 668 L=1,3
      DO 668 K=1,3
      LK=LK+1
      WRITE(IOUT,9095)N,LK,SIGX(L,K),SIGY(L,K),TUXY(L,K)
 9095 FORMAT(1X,I5,1X,I5,3E18.6)
  668 CONTINUE
      WRITE(IOUT,9085)
 9085 FORMAT(/)
C
  663 CONTINUE
 9090 FORMAT(///, 26H   STRESSES //6HELEMNT,1X,5H NODE,
     15X,14H SIGMA - X ,4X,14H SIGMA - Y ,4X,14H TAU - XY)
      RETURN
      END
C
      SUBROUTINE SECOND(TIM)
C
C     SUBROUTINE TO OBTINE TIME
C
      CALL TIMECK(II)
      TIM=FLOAT(II)/100.
```

```
RETURN
END
```

The vita has been removed from the scanned document